Ε Θ Ν Ι Κ Ο Μ Ε Τ Σ Ο Β Ι Ο Π Ο Λ Υ Τ Ε Χ Ν Ε Ι Ο
ΣΧΟΛΗ ΠΟΛΙΤΙΚΩΝ ΜΗΧΑΝΙΚΩΝ - ΤΟΜΕΑΣ ΓΕΩΤΕΧΝΙΚΗΣ
Ηρώων Πολυτεχνείου 9, Πολυτεχνειούπολη Ζωγράφου 157 80
Τηλ: 210 772 3780, Fax: 210 772 3428,
e-mail: gbouck@central.ntua.gr *www.georgebouckovalas.com*

ΠΡΑΞΗ:

«ΘΑΛΗΣ- ΕΜΠ: ΠΡΩΤΟΤΥΠΟΣ ΣΧΕΔΙΑΣΜΟΣ ΒΑΘΡΩΝ ΓΕΦΥΡΩΝ ΣΕ ΡΕΥΣΤΟΠΟΙΗΣΙΜΟ ΕΔΑΦΟΣ ΜΕ ΧΡΗΣΗ ΦΥΣΙΚΗΣ ΣΕΙΣΜΙΚΗΣ ΜΟΝΩΣΗΣ»

MIS 380043

Επιστημονικός Υπεύθυνος: Καθ. Γ. ΜΠΟΥΚΟΒΑΛΑΣ

ΔΡΑΣΗ 8

Εφαρμογή σε Χαλύβδινη Καλωδιωτή Γέφυρα

ΠΑΡΑΔΟΤΕΑ:

Πρότυπη Μελέτη για Χαλύβδινη Καλωδιωτή Γέφυρα

Συγκριτική αξιολόγηση έναντι συμβατικής μεθολογίας σχεδιασμού (Π8β)

Ιούνιος 2015

Ευρωπαϊκή Ένωση
Ευρωπαϊκό Κοινωνικό Ταμείο

ΕΠΙΧΕΙΡΗΣΙΑΚΟ ΠΡΟΓΡΑΜΜΑ
ΕΚΠΑΙΔΕΥΣΗ ΚΑΙ ΔΙΑ ΒΙΟΥ ΜΑΘΗΣΗ
επένδυση στην κοινωνία της γνώσης
ΥΠΟΥΡΓΕΙΟ ΠΑΙΔΕΙΑΣ & ΘΡΗΣΚΕΥΜΑΤΩΝ, ΠΟΛΙΤΙΣΜΟΥ & ΑΘΛΗΤΙΣΜΟΥ
ΕΙΔΙΚΗ ΥΠΗΡΕΣΙΑ ΔΙΑΧΕΙΡΙΣΗΣ

ΕΣΠΑ 2007-2013
πρόγραμμα για την ανάπτυξη
ΕΥΡΩΠΑΪΚΟ ΚΟΙΝΩΝΙΚΟ ΤΑΜΕΙΟ

Με τη συγχρηματοδότηση της Ελλάδας και της Ευρωπαϊκής Ένωσης

ΕΚΤΕΝΗΣ ΠΕΡΙΛΗΨΗ

ΕΙΣΑΓΩΓΗ

Η παρούσα Τεχνική Έκθεση αποτελεί το Παραδοτέο Π8β της Δράσης (Επιμέρους Εργασίας) Δ8 του Ερευνητικού Προγράμματος με τίτλο:

ΘΑΛΗΣ-ΕΜΠ (MIS 380043)

Πρωτότυπος Σχεδιασμός Βάθρων Γεφυρών σε Ρευστοποιήσιμο Έδαφος με Φυσική Σεισμική Μόνωση

με Συντονιστή (Ερευνητικό Υπεύθυνο) τον Γεώργιο Μπουκοβάλα Καθηγητή ΕΜΠ, και με Επιστημονικό Υπεύθυνο της Δράσης Δ8 τον Χάρη Γαντέ, Καθηγητή ΕΜΠ.

Συγκεκριμένα, η εν λόγω Δράση Δ8, με τίτλο:

"Εφαρμογή σε Χαλύβδινη (Καλωδιωτή) Γέφυρα"

αφορά στην εφαρμογή και συγκριτική αξιολόγηση της προτεινόμενης νέας μεθοδολογίας σχεδισμού σε χαλύβδινη γέφυρα, ενώ το αντικείμενο του εν λόγω παραδοτέου περιγράφεται στην εγκεκριμένη ερευνητική πρόταση ως ακολούθως:

"Ο σκοπός της Ερευνητικής Ομάδας είναι να διερευνήσει τη δυνατότητα εφαρμογής της προτεινόμενης μεθοδολογίας σχεδιασμού και τα προτερήματα έναντι συμβατικών μεθόδων σχεδιασμού για την περίπτωση μιας καλωδιωτής γέφυρας, με χαλύβδινους πυλώνες και σύμμικτο κατάστρωμα. Αυτός ο τύπος γέφυρας, αν και είναι λιγότερο διαδεδομένος στην Ελλάδα, μπορεί να αποτελέσει μία τεχνικά και οικονομικά καλύτερη λύση σε περιπτώσεις γεφυρών μεσαίων-μεγάλων ανοιγμάτων ανάμεσα στα μεσόβαθρα (π.χ. μεγαλύτερα από 80m). Παράλληλα, παρουσιάζει συγκεκριμένες ιδιαιτερότητες σε σχέση με τις γέφυρες από σκυρόδεμα των Δράσεων 6 και 7, λόγω των διαφορετικών υλικών κατασκευής αλλά και λόγω της πιο εύκαμπτης απόκρισης, η οποία μπορεί να οδηγήσει σε: (α) λιγότερο αυστηρά κριτήρια επιτελεστικότητας βάσει των επιτρεπόμενων μετακινήσεων της θεμελίωσης, αλλά επίσης (β) αυξανόμενο κίνδυνο συντονισμού του φορέα της ανωδομής κατά τη λειτουργία του ρευστοποιημένου εδάφους ως «φυσικού» συστήματος σεισμικής μόνωσης.

Οι κύριες δραστηριότητες που θα πρέπει να πραγματοποιηθούν για την ολοκλήρωση αυτής της Δράσης είναι οι ακόλουθες:

(α) *Αρχικώς, θα πρέπει να εκτιμηθούν οι επιτρεπόμενες μετακινήσεις στη θεμελίωση (καθιζήσεις και στροφές) για διάφορους τύπους καλωδιωτών γεφυρών, και συγκεκριμένα για τύπο «άρπας» (harp) και ακτινωτό (fan), με μονόπλευρο ή αμφίπλευρους πυλώνες, καθώς και για ανηρτημένες γέφυρες με κύριο καλώδιο μεταξύ των κορυφών των πυλώνων και κατακόρυφους αναρτήρες. Θα ληφθούν υπόψη τα επιτρεπόμενα επίπεδα βλάβης και*

λειτουργικότητας (π.χ. όχληση στην οδήγηση, επισκευάσιμες βλάβες, μή επισκευάσιμες βλάβες) καθώς και το αναμενόμενο επίπεδο σεισμικότητας (π.χ. σεισμική διέγερση με 90, 450 ή 900 χρόνια περίοδο επαναφοράς) και θα καθοριστούν μετά από μία συλλογική αξιολόγηση των παρακάτω:

- *μία εκτεταμένη βιβλιογραφική έρευνας των συναφών κανονιστικών διατάξεων και οδηγιών (π.χ. Ευρωκώδικας 2 – Μέρος 2, Ευρωκώδικας 8 – Μέρος 2, Ευρωκώδικας 7, MCEER & FHA – κεφάλαιο 11.4),*

- *παραδείγματα απόκρισης από ήδη κατασκευασμένες γέφυρες κατά τη διάρκεια πρόσφατων σεισμών, και*

- *παραμετρικές αναλύσεις διαφόρων δομικών στοιχείων της γέφυρας (π.χ. μεσόβαθρα, καλώδια, κατάστρωμα) υπό στατικές και ανακυκλιζόμενες δυναμικές φορτίσεις.*

(β) *Στη συνέχεια, τα βάθρα μιας τυπικής καλωδιωτής γέφυρας, τύπου «άρπας» ή ακτινωτού, με μεσαίο άνοιγμα 80-120m μεταξύ των πυλώνων, θα σχεδιαστούν με βάση την συμβατική μεθοδολογία θεμελίωσης, με χρήση ομάδας πασσάλων και καθολική βελτίωση του εδάφους στην περιοχή της θεμελίωσης. Πρόθεσή μας είναι να επιλέξουμε μία υπαρκτή γέφυρα ή μία μελετημένη γέφυρα σε στάδιο οριστικής μελέτης σε περιοχή ποταμού, όπου οι συνθήκες του υπεδάφους είναι καθορισμένες από πλήρεις γεωτεχνικές μελέτες, ενώ προβλέπεται εκτεταμένη ρευστοποίηση κάτω από ένα ή περισσότερα βάθρα της γέφυρας.*

(γ) *Τέλος, η διαστασιολόγηση της γέφυρας σε στατικούς και σεισμικούς συνδυασμούς φορτίσεων θα επαναληφθεί για τη νέα μεθοδολογία της «φυσικής» σεισμικής μόνωσης, εφαρμόζοντας επιφανειακή θεμελίωση και μερική βελτίωση του ρευστοποιήσιμου εδάφους με δημιουργία επιφανειακής μόνον κρούστας, σε συνδυασμό με τις επιτρεπόμενες μετακινήσεις στη θεμελίωσης που θα καθοριστούν στο βήμα (α) που περιγράφηκε παραπάνω. Τα πλεονεκτήματα αλλά και οι περιορισμοί της νέας μεθοδολογίας θα συγκριθούν με τα αντίστοιχα της συμβατικής λύσης και θα αξιολογηθούν με βάση τόσο τεχνικών όσο και οικονομικών κριτηρίων.*

Η παρούσα Ερευνητική Έκθεση - παραδοτέο, αφορά στις Επιμέρους Εργασίες (β) και (γ) ανωτέρω, ενώ η Επιμέρους Εργασία (α) περιγράφεται στην Ερευνητική Έκθεση - Παραδοτέο (Π8α).

Επισημαίνεται ότι, κατά τα πρώτα βήματα αυτής της διερεύνησης, διαπιστώθηκε ότι οι τάσεις εδάφους λόγω μονίμων φορτίων στις θέσεις των βάθρων κοινών καλωδιωτών ή κρεμαστών γεφυρών ήταν μεγαλύτερες από τα όρια που θεωρήθηκαν ως αποδεκτά για την προτεινόμενη καινοτόμο λύση, για βάθρα που θεμελιώνονται σε ρευστοποιήσιμα εδάφη. Γι' αυτό αποφασίστηκε να μελετηθεί η περίπτωση μιας τοξωτής μεταλλικής γέφυρας με ανηρτημένο σύμμικτο κατάστρωμα, που είναι μία συνήθης λύση γέφυρας με καλώδια για μικρότερα ανοίγματα και επομένως οδηγεί σε μικρότερες τάσεις εδάφους λόγω μονίμων φορτίων. Πέραν τούτου, ο εν λόγω τύπος γέφυρας διατηρεί πολλά από τα χαρακτηριστικά των καλωδιωτών γεφυρών (π.χ. μεγαλύτερη ανοχή σε μετακινήσεις της θεμελίωσης) και έτσι ικανοποιεί πλήρως τις απαιτήσεις του ερευνητικού προγράμματος.

ΜΕΘΟΔΟΛΟΓΙΑ ΚΑΙ ΑΠΟΤΕΛΕΣΜΑΤΑ

Όπως προαναφέρθηκε, μελετάται μία οδική τοξωτή μεταλλική γέφυρα με ανηρτημένο σύμμικτο κατάστρωμα δύο αμφιέρειστων τμημάτων. Η γέφυρα θεωρείται πως θεμελιώνεται επιφανειακά σε έδαφος ρευστοποιήσιμο σε μεγάλο βάθος. Το γεωτεχνικό προφίλ του εδάφους έχει επιλεγεί από μία υπαρκτή γέφυρα στην περιοχή του ποταμού Στρυμώνα, όπου οι συνθήκες του υπεδάφους είναι καθορισμένες από πλήρεις γεωτεχνικές μελέτες, ενώ προβλέπεται εκτεταμένη ρευστοποίηση κάτω από το μεσόβαθρα της γέφυρας.

Η γέφυρα αποτελείται από δύο αμφιέρειστα ανοίγματα θεωρητικού μήκους 42.00m το καθένα, τα οποία συνδέονται μεταξύ τους με πλάκα συνέχειας. Το θεωρητικό πλάτος του

καταστρώματος ισούται με 14.70m. Το κατάστρωμα της γέφυρας είναι σύμμικτο και το κάθε άνοιγμα αποτελείται από δύο κύριες δοκούς και δεκαεφτά διαδοκίδες. Κάθε κύρια δοκός αναρτάται από ένα τόξο με τη χρήση αναρτήρων ενώ τα δύο τόξα του κάθε ανοίγματος συνδέονται μεταξύ τους με εγκάρσιους και διαγώνιους συνδέσμους δυσκαμψίας. Το ύψος των τόξων είναι ίσο με 10.00m. Οι δοκοί, οι διαδοκίδες, τα τόξα και οι σύνδεσμοι δυσκαμψίας έχουν κατασκευαστεί από δομικό χάλυβα. Το μεσόβαθρο αποτελείται από τη δοκό έδρασης και τρεις στύλους κυκλικής συμπαγούς διατομής από οπλισμένο σκυρόδεμα μορφώνοντας έτσι ένα πλαίσιο στην εγκάρσια έννοια της γέφυρας, έχει δε ύψος 10m συμπεριλαμβανομένης της δοκού έδρασης. Τα ακρόβαθρα θεωρούνται πολύ δύσκαμπτα σε σχέση με τη γέφυρα και γι' αυτό λαμβάνονται υπόψη ως ακλόνητα.

Αρχικώς μελετάται η συμβατική λύση θεμελίωσης, σύμφωνα με την οποία το μεσόβαθρο θεμελιώνεται σε μία ομάδα πασσάλων που συνδέονται με τους στύλους του μεσοβάθρου μέσω δύσκαμπτου κεφαλοδέσμου. Το έδαφος γύρω και ανάμεσα από τους πασσάλους θεωρείται ότι βελτιώνεται με χαλικοπασσάλους. Μορφώνεται προσομοίωμα της γέφυρας που περιλαμβάνει την ανωδομή, το μεσόβαθρο, τον κεφαλόδεσμο και τους πασσάλους, ενώ η αλληλεπίδραση εδάφους – κατασκευής λαμβάνεται υπόψη με οριζόντια και κατακόρυφα ελατήρια. Ο σχεδιασμός της γέφυρας πραγματοποιείται σε Οριακή Κατάσταση Αστοχίας (ΟΚΑ) καθώς και σε Οριακή Κατάσταση Λειτουργικότητας (ΟΚΛ), εφαρμόζοντας τους συνδυασμούς φορτίσεων σύμφωνα με τους ισχύοντες κανονισμούς (Ευρωκώδικες) και γίνεται έλεγχος επάρκειας όλων των στοιχείων της γέφυρας (μεταλλικά στοιχεία, πλάκα ανωδομής από οπλισμένο σκυρόδεμα, στύλοι μεσοβάθρου, πάσσαλοι και κεφαλόδεσμος από οπλισμένο σκυρόδεμα, εφέδρανα, αρμοί).

Στη συνέχεια μελετάται η καινοτόμος λύση θεμελίωσης και επαναλαμβάνεται η ανάλυση της γέφυρας σε ΟΚΑ και σε ΟΚΛ. Η καινοτόμος λύση θεμελίωσης έχει στόχο την εκμετάλλευση της «φυσικής σεισμικής μόνωσης» που προκαλείται από το φαινόμενο της ρευστοποίησης. Σε αυτήν την περίπτωση η θεμελίωση της γέφυρας είναι επιφανειακή, ενώ πραγματοποιείται μερική βελτίωση του ρευστοποιήσιμου εδάφους με χαλικοπασσάλους, δημιουργώντας έτσι μία επιφανειακή κρούστα. Μορφώνεται και πάλι προσομοίωμα της γέφυρας που περιλαμβάνει την ανωδομή και το μεσόβαθρο, ενώ το θεμέλιο του μεσοβάθρου καθώς και η αλληλεπίδραση εδάφους – κατασκευής λαμβάνονται υπόψη με μεταφορικά και στροφικά ελατήρια. Θεωρούνται στατικά και σεισμικά ελατήρια για τα στατικά και σεισμικά φορτία, αντίστοιχα. Επίσης, στη δυναμική ανάλυση ενεργοποιούνται αποσβεστήρες που έχουν εφαρμοστεί στη βάση του θεμελίου.

Για την καινοτόμο λύση θεωρούνται δύο Σεισμικά Σενάρια που καθορίζονται στη γεωτεχνική μελέτη. Στο πρώτο Σεισμικό Σενάριο, λαμβάνεται υπόψη ένας σεισμός με περίοδο επαναφοράς T_{ret} = 225 χρόνια, ο οποίος δεν προκαλεί ρευστοποίηση, ενώ στο δεύτερο Σεισμικό Σενάριο ο σεισμός έχει περίοδο επαναφοράς T_{ret} = 1000 χρόνια και προκαλεί ρευστοποίηση. Τα δυναμικά ελατήρια και οι αποσβεστήρες στη βάση του μεσοβάθρου έχουν διαφορετικές τιμές για τα δύο Σεισμικά Σενάρια, με αυτά του Σεναρίου 1, σύμφωνα με το οποίο δεν πραγματοποιείται ρευστοποίηση, να έχουν μεγαλύτερες τιμές. Παράλληλα, το πρώτο Σεισμικό Σενάριο, οδηγεί σε μεγαλύτερη φασματική επιτάχυνση, εφόσον το δεύτερο Σεισμικό Σενάριο εκμεταλλεύεται τη «φυσική σεισμική μόνωση» κατά τη διάρκεια της ρευστοποίησης. Ωστόσο, το δεύτερο Σεισμικό Σενάριο προϋποθέτει την εξέλιξη μεγάλων παροδικών οριζόντιων μετακινήσεων στη βάση του μεσοβάθρου κατά τη διάρκεια του σεισμού και υποδηλώνει την ανάπτυξη σημαντικών παραμενουσών καθιζήσεων και στροφών μετά το σεισμικό γεγονός, καταναγκασμοί που συμπεριλαμβάνονται στους στατικούς συνδυασμούς. Σκοπός του σχεδιασμού είναι η στατική επάρκεια της γέφυρας με την επιφανειακή θεμελίωση και για τα δύο Σεισμικά Σενάρια. Και σε αυτή τη λύση ο σχεδιασμός της γέφυρας πραγματοποιείται σε ΟΚΑ και ΟΚΛ, εφαρμόζοντας τους συνδυασμούς φορτίσεων σύμφωνα με τους ισχύοντες κανονισμούς (Ευρωκώδικες) και γίνεται έλεγχος επάρκειας όλων των στοιχείων της γέφυρας (μεταλλικά στοιχεία, στύλοι μεσοβάθρου από οπλισμένο σκυρόδεμα, εφέδρανα, αρμοί).

Από τις αναλύσεις προέκυψε πως για την καινοτόμο λύση πράγματι η ρευστοποίηση λειτουργεί ως σεισμική μόνωση για την ανωδομή της γέφυρας, με αποτέλεσμα οι σεισμικοί συνδυασμοί του δεύτερου Σεισμικού Σεναρίου να οδηγούν σε σχετικά χαμηλές καταπονήσεις και να μην

είναι κρίσιμοι για τη διαστασιολόγηση, παρά το γεγονός ότι λαμβάνονται υπόψη σε αυτούς τους συνδυασμούς ταυτόχρονες σημαντικές παροδικές οριζόντιες μετακινήσεις στη βάση του μεσοβάθρου. Το τίμημα όμως που πρέπει να καταβληθεί στα πλαίσια αυτής της λύσης είναι ότι κρίσιμοι πλέον γίνονται οι στατικοί συνδυασμοί που αφορούν την κατάσταση λειτουργίας της γέφυρας μετά το σεισμό που προκαλεί ρευστοποίηση και συμπεριλαμβάνουν τις μόνιμες καθιζήσεις και στροφές που οφείλονται στη ρευστοποίηση. Το αποτέλεσμα είναι τα μεταλλικά στοιχεία της ανωδομής να έχουν για την περίπτωση αυτή ελαφρώς μεγαλύτερους συντελεστές εκμετάλλευσης από αυτούς που προκύπτουν από την ανάλυση της συμβατικής λύσης, χωρίς πάντως να απαιτείται αύξηση της διατομής τους, με εξαίρεση τους διαγώνιους συνδέσμους δυσκαμψίας μεταξύ των τόξων, τα εφέδρανα και τους αρμούς.

Παράλληλα, για το μεσόβαθρο, η ευμενής δράση της ρευστοποίησης ως φυσικής σεισμικής μόνωσης και η ευκαμψία της θεμελίωσης σε σχέση με τη βαθιά θεμελίωση των πασσάλων, δεν προκαλεί διαφορά στη διατομή των στύλων ή και στον οπλισμό τους σε σχέση με την συμβατική λύση, καθ' ό,τι δυσμενέστερο για το μεσόβαθρο αποδεικνύεται το Σεισμικό Σενάριο 1 που οδηγεί σε μεγαλύτερο σεισμό, ενώ ο απαιτούμενος οπλισμός για το Σεισμικό Σενάριο 1 είναι παρόμοιος με αυτόν που προκύπτει από τη συμβατική λύση. Έτσι, αν και το κόστος της αισθητά απλούστερης καινοτόμου λύσης θεμελίωσης του μεσοβάθρου ανέρχεται σε περίπου 36% του αντίστοιχου κόστους της συμβατικής λύσης, το συνολικό οικονομικό όφελος της καινοτόμου λύσης σε σύγκριση με τη συμβατική για ολόκληρη την εξεταζόμενη γέφυρα ανέρχεται σε 9%÷13%. Το ποσοστό αυτό θα είναι υψηλότερο σε γέφυρες πολλών ανοιγμάτων, με μεγαλύτερο αριθμό μεσοβάθρων, όπου εκτιμάται ότι θα προσεγγίζει το 20%, ανάλογα βέβαια και με το πλήθος των μεσοβάθρων.

Επισημαίνεται επίσης ότι ο ακριβής υπολογισμός των παροδικών μετακινήσεων του εδάφους κατά τη διάρκεια του σεισμού, αλλά και των μόνιμων καθιζήσεων και στροφών μετά από ένα σεισμό που προκαλεί ρευστοποίηση, κρίνεται πολύ σημαντικός, καθ' ό,τι τα μεγέθη αυτά είναι κρίσιμα στο σχεδιασμό της γέφυρας με την καινοτόμο λύσης θεμελίωσης. Με δεδομένη τη δυσκολία αξιόπιστου υπολογισμού αυτών των μεγεθών, αυτό είναι ένα θέμα που πρέπει να επιλυθεί, προκειμένου να διευκολυνθεί η διάδοση εφαρμογής αυτής της λύσης. Εναλλακτικά αλλά και συμπληρωματικά, είναι αυτονόητο ότι η καινοτόμος λύση θεμελίωσης προσφέρεται περισσότερο για στατικά συστήματα ανωδομής τα οποία είναι λιγότερο ευαίσθητα σε καθιζήσεις και στροφές της θεμελίωσης.

Συμπληρωματικά των παραπάνω τονίζεται ότι για τη συγκεκριμένη γέφυρα τα στοιχεία της ανωδομής που απαιτούν αύξηση λόγω των στατικών συνδυασμών δράσεων μετά τη ρευστοποίηση (διαγώνιοι σύνδεσμοι δυσκαμψίας μεταξύ των τόξων, εφέδρανα και αρμοί) είναι δευτερεύοντα και εύκολα αντικαταστάσιμα. Είναι συνεπώς δυνατόν να υιοθετηθεί στον σχεδιασμό η στρατηγική διατήρησης αυτών των στοιχείων στα αρχικά τους μεγέθη, αφαίρεσή τους (εφόσον απαιτηθεί) μετά από ενδεχόμενο σεισμικό γεγονός που θα έχει προκαλέσει ρευστοποίηση, με αποτέλεσμα την ανάταξη των υπόλοιπων δομικών στοιχείων της ανωδομής της κατά τα άλλα ισοστατικής γέφυρας, και αντικατάστασή τους. Τότε, για τον έλεγχο της ανωδομής, δεν θα χρειάζεται να ληφθούν υπόψη στους στατικούς συνδυασμούς μετά τη ρευστοποίηση οι παραμένουσες βυθίσεις και στροφές, δεδομένου ότι αφετηρία θα είναι ένας απαραμόρφωτος φορέας, με εξαίρεση μόνον τα ίδια βάρη. Κύριο πλεονέκτημα αυτής της θεώρησης δεν είναι τόσο η – έτσι και αλλιώς αμελητέα - οικονομία του αρχικού σχεδιασμού, όσο η υποβάθμιση της σημασίας της πρόβλεψης των οφειλόμενων σε ρευστοποίηση παραμενουσών βυθίσεων και στροφών.

Επισημαίνεται όμως ότι, σε κάθε περίπτωση, η καινοτόμος λύση προσφέρει το επιπλέον πλεονέκτημα μιας ασφαλιστικής δικλείδας έναντι ατυχηματικών πολύ υψηλών σεισμικών δράσεων που θα μπορούσαν να εκδηλωθούν, μεγαλύτερων ακόμη και των δράσεων που χρησιμοποιούνται στο Σεισμικό Σενάριο 2, δεδομένου ότι τότε θα συμβεί ρευστοποίηση και θα ενεργοποιηθεί η προστασία της γέφυρας μέσω της αναπτυσσόμενης φυσικής σεισμικής μόνωσης. Αυτονόητο είναι ότι η συμβατική λύση δεν προσφέρει τέτοια προστασία και θα κινδυνεύει από πολύ σοβαρές βλάβες και ενδεχόμενη κατάρρευση σε τέτοιες περιπτώσεις.

ΟΜΑΔΑ ΕΡΓΑΣΙΑΣ

Η εργασία που παρουσιάζεται στο παρόν Παραδοτέο Π8β ολοκληρώθηκε με την συμβολή των παρακάτω μελών της Ερευνητικής Ομάδας του Εθνικού Μετσόβιου Πολυτεχνείου (Εργαστήριο Μεταλλικών Κατασκευών Σχολής Πολιτικών Μηχανικών):

- **Χάρης Ι. Γαντές**, Καθηγητής, Σχολή Πολιτικών Μηχανικών, ΕΜΠ
- **Ισαβέλλα Βασιλοπούλου,** Δρ. Πολιτικός Μηχανικός

NATIONAL TECHNICAL UNIVERSITY OF ATHENS
SCHOOL OF CIVIL ENGINEERING – GEOTECHNICAL DEPARTMENT
9 Iroon Polytechniou str., 15780, Zografou Campus, Greece
Tel: 210 772 3780, Fax: 210 772 3428,
e-mail: gbouck@central.ntua.gr *www.georgebouckovalas.com*

PROJECT:

«THALIS-NTUA: INNOVATIVE DESIGN OF BRIDGE PIERS ON LIQUEFIABLE SOILS WITH THE USE OF NATURAL SEISMIC ISOLATION»

MIS 380043

Coordinator: Prof. G. BOUCKOVALAS

WORK PACKAGE 8

Application to Steel Cable Bridge

DELIVERABLES:

Pilot Study for Steel Cable Bridge

Comparative evaluation against conventional design method (D8b)

June 2015

European Union
European Social Fund

OPERATIONAL PROGRAMME
EDUCATION AND LIFELONG LEARNING
investing in knowledge society
MINISTRY OF EDUCATION & RELIGIOUS AFFAIRS, CULTURE & SPORTS
MANAGING AUTHORITY

NSRF 2007-2013
programme for development
EUROPEAN SOCIAL FUND

Co-financed by Greece and the European Union

TABLE OF CONTENTS

Chapter 1

INTRODUCTION

This Technical Report constitutes part of Deliverable 8 of the Research Project entitled:

THALIS-NTUA (MIS 380043)

Innovative Design of Bridge Piers on Liquefiable Soils with the use of Natural Seismic Isolation

performed under the general coordination of Professor George Bouckovalas (Principal Investigator) and Professor Charis Gantes (Scientific Responsible for WP8).

Namely, it presents the actions taken and the associated results of Work Package WP8, entitled:

"Application to large span, cable-stayed bridges"

The Scope of **Work Package WP8**, has been described in the approved Research Proposal as follows:

"The aim of this WP is to explore the feasibility of the proposed new design methodology, and the resulting advantages over conventional design methods, in the case of a cable-stayed bridge, with steel piers and composite deck system. This bridge type, although less common in Greece, may provide a technically and economically optimum solution for cases of medium-large spans between the piers (e.g. larger than 80 m). In parallel, it presents specific peculiarities as compared to the RC bridges of WP 6 and WP 7, due to the different construction materials, as well as due to the more flexible response which may lead to: (a) less strict performance criteria with regard to the allowable foundation movements, but also (b) increased risk of structure-to-excitation resonance when part of the liquefied ground will act as a "natural" base isolation system.

The main work tasks required to achieve the aim of this WP are the following:

(a) *Initially, the allowable foundation movements (settlements and rotations) will have to be established for different types of cable-stayed bridges, namely "harp" and "fan" types, with one or two pylons, as well as cable suspended bridges with a main suspension cable between the pylon tops and vertical hangers. The relevant criteria will take into account the permissible damage and serviceability levels (e.g. driving discomfort, repairable damage, non-repairable damage), as well as the anticipated seismicity level (e.g. seismic excitation with 90, 450 or 900 years return period), and will be established after a joint evaluation of:*

- *an extensive literature survey of relevant codes and guidelines (e.g. Eurocode 2-Part 2, Eurocode 8-Part 2, Eurocode 7, MCEER & FHA-chapter 11.4),*

- *examples of actual bridge performance during recent earthquakes, and*

- *parametric analyses of various bridge components (e.g. pylons, cables, deck) under static and cyclic dynamic loading.*

(b) *Next, the pylons of a typical "harp" or "fan" type cable-stayed bridge, with a midspan of 80-120m, will be designed using the conventional foundation approach, i.e. pile groups with ground improvement between and around the piles. It is our intention to select an actual (existing or in the design stage) river bridge site, where the subsoil conditions are well established by geotechnical surveys, while extensive liquefaction is expected underneath one or more of the bridge piers.*

(c) *Finally, the static and seismic design of this bridge will be repeated with the new methodology of "natural" seismic isolation (i.e. shallow foundation and partial improvement, of the top part only of the liquefiable soil), in connection with the allowable foundation movements which were established in work task (a) above. The comparative advantages and limitations of the new design methodology, relative to the conventional ones, will be consequently evaluated on the basis of technical, as well as cost criteria.*

The present Research Report -Deliverable (D8b) refers to work tasks (b) and (c) above, while the work task (a) is described in a separate Research Report - Deliverable (D8a).

It should be clarified in advance that, during the initial phases of this investigation it was established that the soil stresses due to permanent loads developing under the piers of common cable-stayed and cable suspended bridges exceeded the values which are considered as acceptable for the proposed innovative solution of piers seated on liquefiable soil. It was therefore decided to address in this WP the case of an arch steel bridge with suspended deck, which is a solution adopted for smaller spans and therefore leads to smaller soil stresses under permanent loads. Furthermore, this bridge type maintains a number of basic characteristics of cable suspended bridges (i.e. the capacity to sustain relatively large foundation displacements) and consequently satisfies all relevant project requirements.

The work described herein constitutes the study of the arch steel bridge with conventional pile foundation. It has been performed with the contribution of the following members of our **Research Team**, from the Institute of Steel Structures, School of Civil Engineering, National Technical University of Athens:

- **Charis J. Gantes**, Professor, School of Civil Engineering, NTUA

- **Isabella Vassilopoulou,** Civil Engineer, Ph.D.

Chapter 2

APPLIED CODES

The codes that are used for the design of the bridge are the following:

- Eurocode 0: Basis of structural design;
- Eurocode 1-1.4: Actions on structures – General actions, Wind actions;
- Eurocode 1-1.5: Actions on structures – General actions, Thermal actions;
- Eurocode 1-2: Actions on structures – Traffic loads on bridges;
- Eurocode 2-1.1: Design of concrete structures – General rules and rules for buildings;
- Eurocode 2-2: Design of concrete structures – Concrete Bridges – Design and detailing rules;
- Eurocode 3-1: Design of steel structures – General rules and rules for buildings;
- Eurocode 3-1.8: Design of steel structures – Design of joints;
- Eurocode 3-2: Design of steel structures – Steel Bridges;
- Eurocode 4-1.1: Design of composite steel and concrete structures – General rules and rules for buildings;
- Eurocode 4-2: Design of composite steel and concrete structures – General rules and rules for bridges;
- Eurocode 8-1: Design of structures for earthquake resistance – General rules, seismic actions and rules for buildings;
- Eurocode 8-2: Design of structures for earthquake resistance – Bridges;
- DIN 4141-14: Structural bearings, laminated elastomeric bearings – design and construction;
- EN1337-1: Structural bearings – General design rules;
- EN1337-3: Structural bearings – Elastomeric bearings;
- DIN 4014: Bored Cast-in-place Piles - Formation, Design and Bearing Capacity.

PART I: CONVENTIONAL SOLUTION

Chapter 3

BRIDGE DESCRIPTION

3.1 Geometry and cross sections

The bridge under investigation is situated over a riverbank and it is a steel arch road bridge with two simply supported spans, with total length 87.60m. The total width of the deck is equal to 15.00m, while at the supports it becomes 15.55m. The steel members of each span include two (2) main beams, seventeen (17) transverse beams, two (2) arches connected with transverse and diagonal bracing members. Each main beam is suspended by each arch with seven (7) hangers. The distance of the transverse steel beams is 2.625m. A composite deck is formed using trapezoidal profiles of type SYMDECK 150 and a concrete slab. The total thickness of the composite slab is 35cm. The concrete slab is connected with the transverse and main beams through steel shear connectors in order to ensure composite action. The characteristics of the bridge's steel members are listed in Table 3.1. The elevation view of a single span is illustrated in Figure 3.1, the arrangement in plan view of the main and transverse beams is shown in Figure 3.2, the plane view of the bridge in Figure 3.3 and the section of the bridge at mid span in Figure 3.4.

Table 3.1: Characteristics of the bridge's steel members

Πίνακας 3.1: Χαρακτηριστικά των μεταλλικών στοιχείων της γέφυρας

Type	Total number	Cross section	Length of each member	Theoretical span/rise
Main beams	4	HEB900	43.30m	42.00m
Transverse beams	34	HEB900	14.30m	14.70m
Arches	4	CHS750/20	47.70m	42.00m / 10.00m
Transverse bracing members	10	CHS244.5/8	13.95m	14.70m
Diagonal bracing members	16	CHS139.7/8	8.45m	9.13m
Hangers	28	CHS168.3/8	3.90m – 9.625m	4.375m – 10.00m

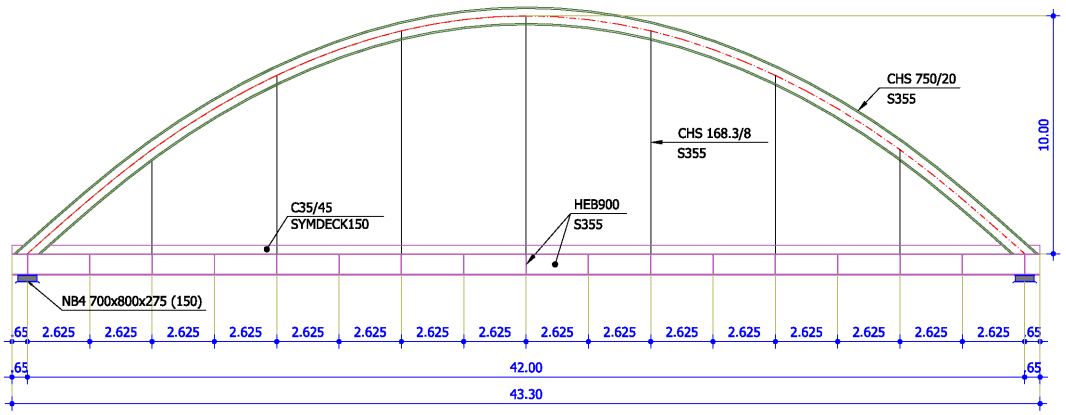

Figure 3.1: Elevation view of a single span

Σχήμα 3.1: Όψη εντός ανοίγματος γέφυρας

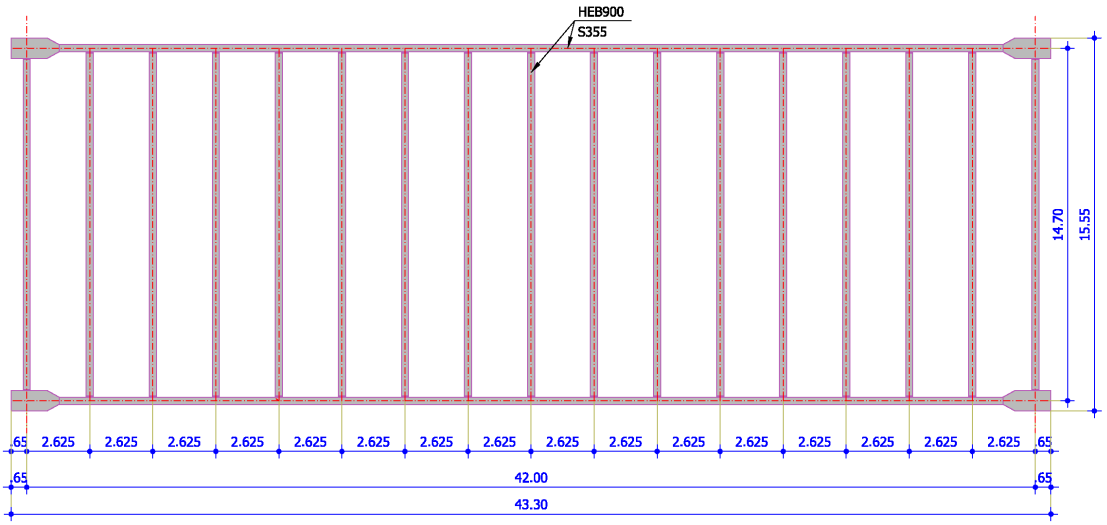

Figure 3.2: Arrangement in plan view of the deck's beams of a single span

Σχήμα 3.2: Διάταξη δοκών καταστρώματος εντός ανοίγματος γέφυρας

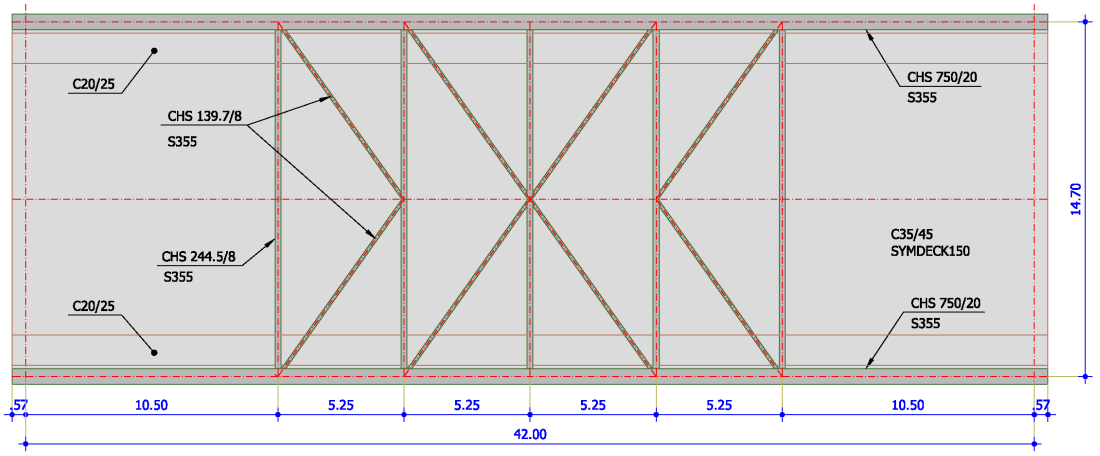

Figure 3.3: Plan view of a single span

Σχήμα 3.3: Κάτοψη εντός ανοίγματος γέφυρας

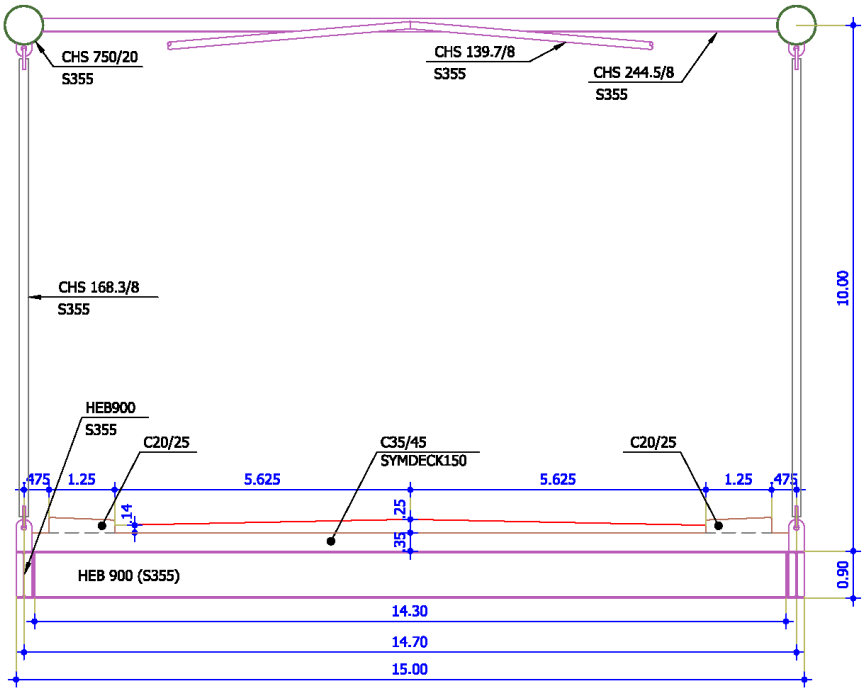

Figure 3.4: Section of the bridge at midspan

Σχήμα 3.4: Εγκάρσια τομή γέφυρας στο μέσον του ανοίγματος

The pier consists of three circular reinforced concrete columns, 8.00m tall, having a circular cross section of 1.50m diameter. The distance between the three columns is equal to 7.35m. They are connected at the top with a 17.00m long concrete beam, having the cross – section of Figure 3.5a. The pier's foundation consists of eight piles Φ120 and L=25.00m, arranged in a grid of orthogonal distances X × Y = 4.00m × 4.90m. The pilecap's dimensions are 17.70m × 6.00m and its thickness is 2.00m (Figure 3.5b). The section of the bridge at the pier is given in Figure 3.6. The elevation view of the bridge is illustrated in Figure 3.7.

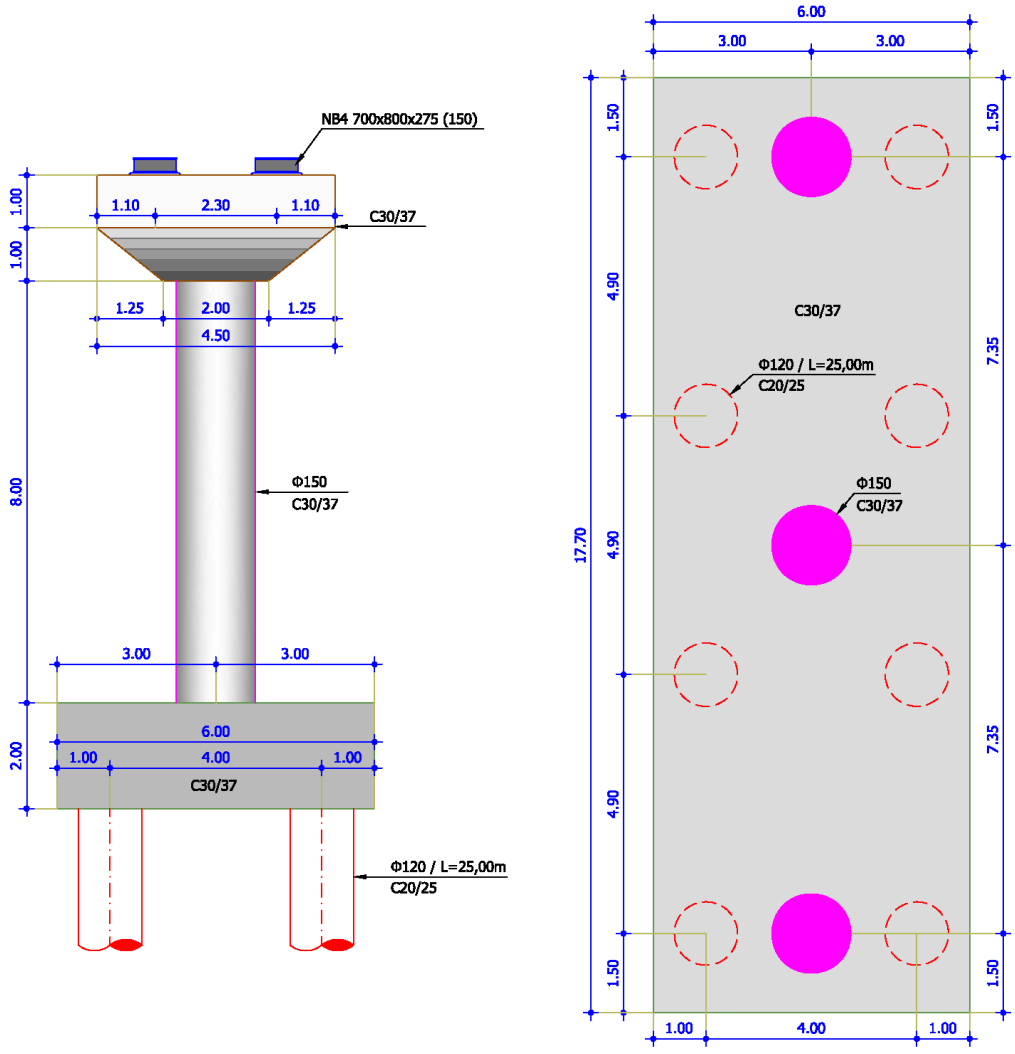

(a) (b)

Figure 3.5: (a) Geometry of the pier in longitudinal section, (b) Geometry of the pier's pilecap

Σχήμα 3.5: (a) Γεωμετρία μεσοβάθρου στη διαμήκη έννοια, (b) Γεωμετρία κεφαλοδέσμου μεσοβάθρου

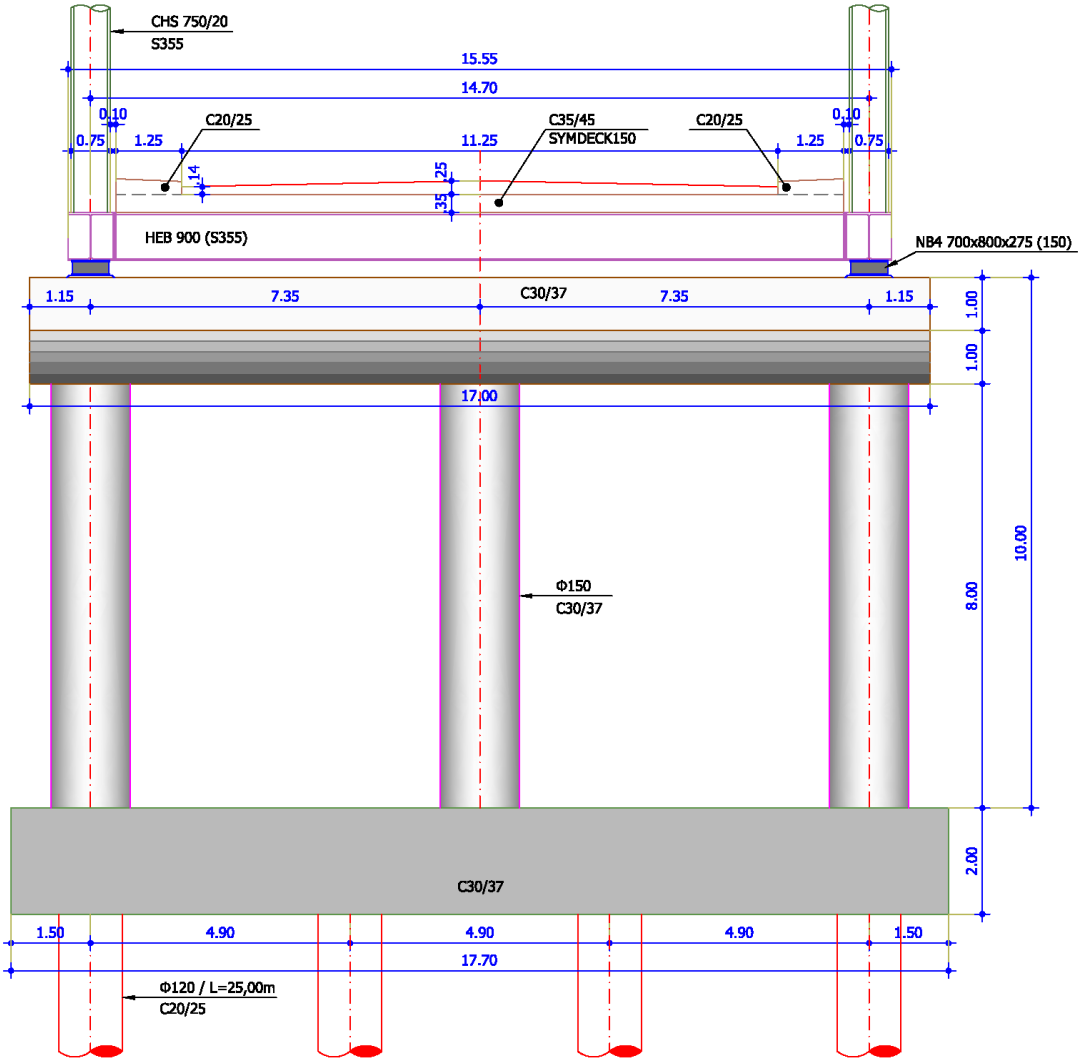

Figure 3.6: Section of the bridge at the pier

Σχήμα 3.6: Εγκάρσια τομή γέφυρας στη θέση μεσοβάθρου

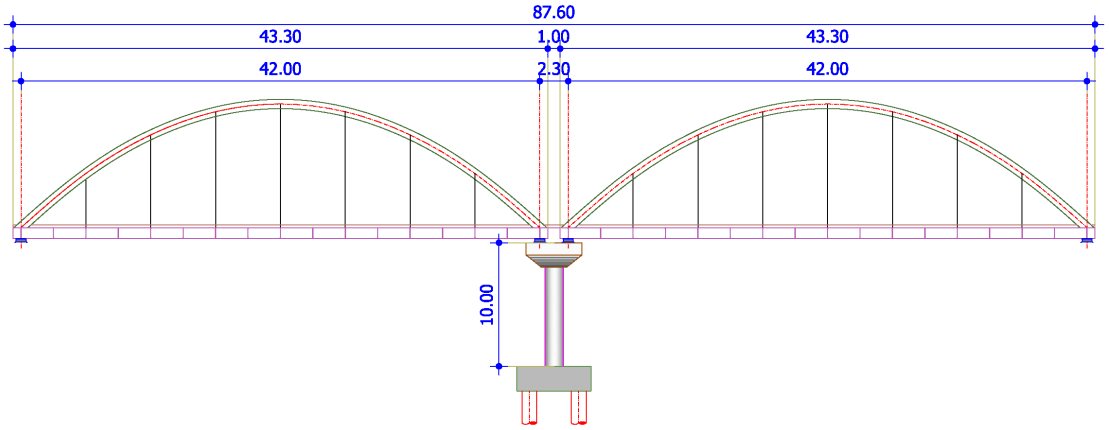

Figure 3.7: Elevation view of the bridge

Σχήμα 3.7: Όψη γέφυρας

The connection of the deck and the pier and the abutments is realized with anchored elastomeric bearings type NB4 700x800x275 (150). The bearings consist of ten (10) layers of elastomer, with thickness t_e=0.015m. The total thickness of the elastomer is t=0.150m. Details of the bearings are shown in Figure 3.8.

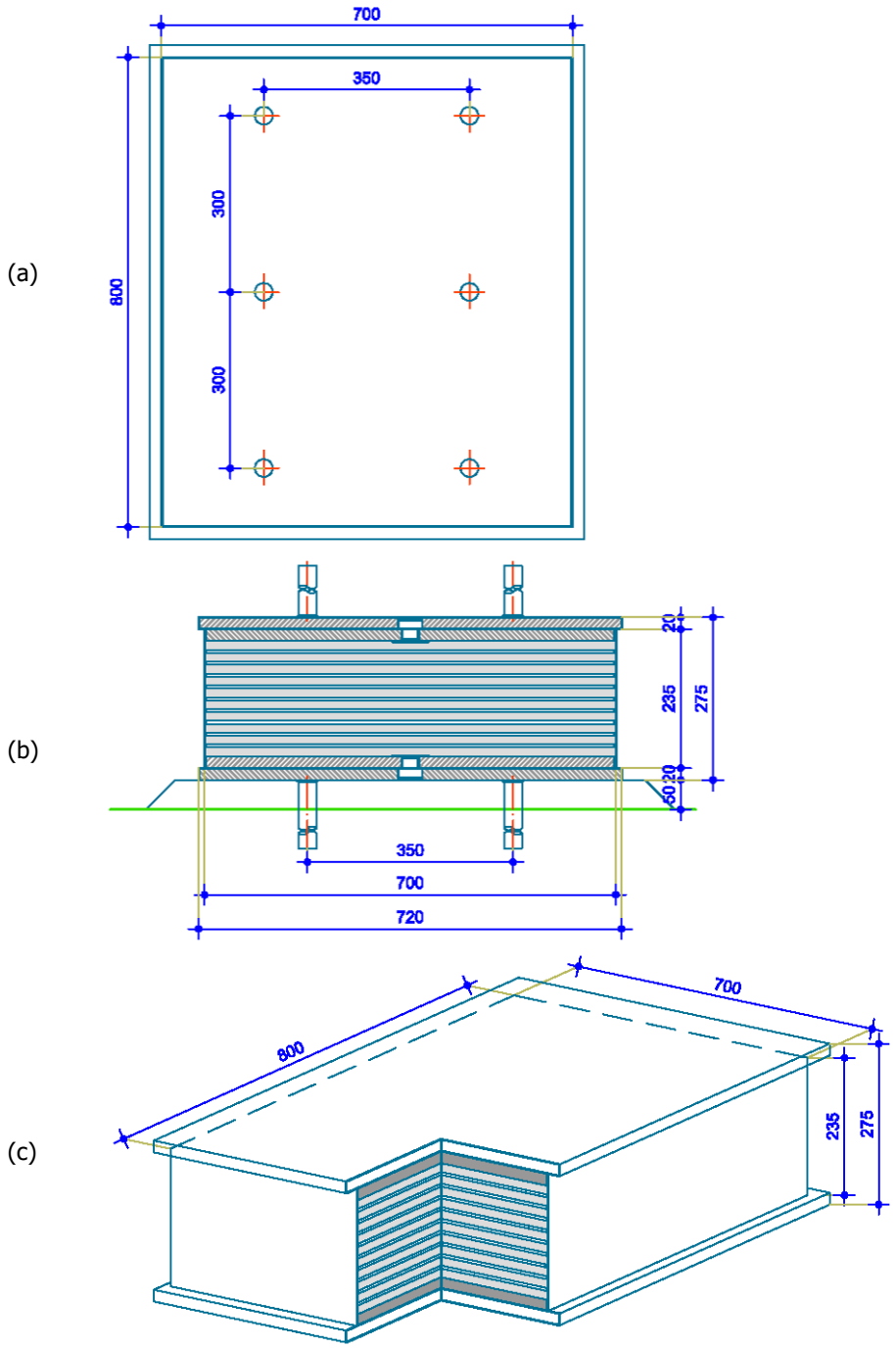

Figure 3.8: Details of the elastomeric bearings: (a) plan view, (b) vertical section, (c) perspective view

Σχήμα 3.8: Λεπτομέρειες ελαστομερικών εφεδράνων: (a) κάτοψη (β) κατακόρυφη τομή (γ) προοπτικό

3.2 Materials

All steel members are made of S355 structural steel. For the composite deck reinforced concrete C35/45 is used, for the sidewalks C20/25, for the pilecap, the columns and the beam of the pier C30/37, and for the piles C20/25. The reinforcement steel is B500C.

3.3 Soil profile

The selected site is located within the riverbed of Strymonas river in Serres, Greece, and has been the subject of geotechnical investigation due to the foundation of the middle pier of "Strymonas river" bridge of "Egnatia Odos" Highway. The soil profile at the site has been created from river deposits and consists of loose liquefiable silty sands and soft clays, while the ground water table is located on the ground surface, a fact that is further enhancing the liquefaction susceptibility. More specifically, the following soil layers were identified:

Layer 1 (0-28m): Silty sand (SM) and locally non-plastic silt (ML)

Layer 2 (28-31m): Low plasticity clay (CL)

Layer 3 (31-34m): Silty sand (SM) and locally low plasticity clayey sand (SM-SC)

Layer 4 (34-43m): Low plasticity clay (CL)

Layer 5 (43-50m): Non-plastic silt (ML) and locally well graded silty sand (SW-SM).

In more detail, the soil profile that will be used for the numerical analyses is plotted in Figure 3.9, along with the factor of safety against liquefaction (from Appendix C of Deliverable D4: Elastic Response Spectra for Liquefiable soils).

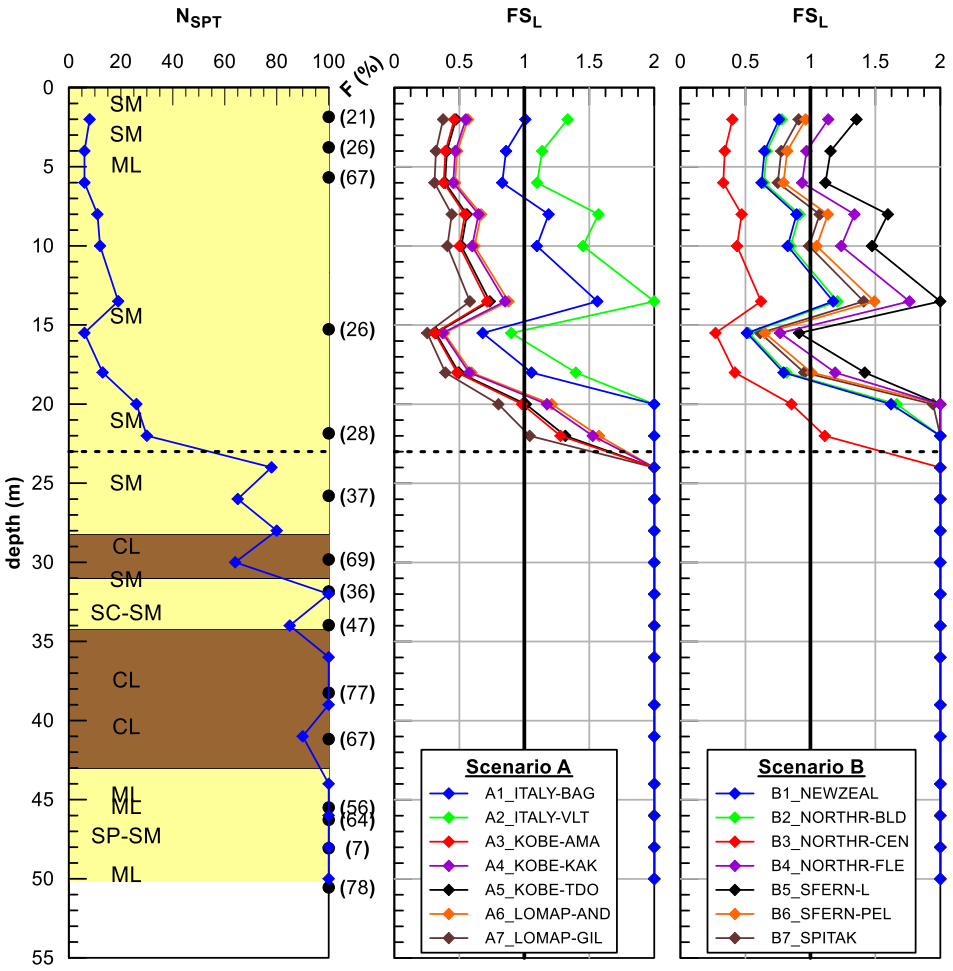

Figure 3.9: Examined soil profile and factor of safety against liquefaction with depth

Σχήμα 3.9: Εδαφικό προφίλ και έλεγχος ρευστοποίησης

The Young Modulus of the soil's layers is given in Table 3.2, as well as the constant of the horizontal springs for a single pile, which is equal to K_h=E/D, where D is the pile's diameter

(for D>1.0m, it is taken equal to 1.00m). These constants have to be reduced according to the methodology described in DIN4014. In Table 3.3, instead, the vertical springs for pile's diameter D=1.20m are provided with depth. These have to be reduced due to group of piles according to Poulos and Davis (1974), with a reduction factor calculated according to Table 3.4, where pile's stiffness coefficient K can be taken equal to 2000.

Table 3.2: Young Modulus E of the soil's layers and horizontal springs for pile's diameter D=1.20m

Πίνακας 3.2: Μέτρο ελαστικότητας Ε του εδάφους και οριζόντια ελατήρια για πάσσαλο διαμέτρου D=1.20m

Depth (m)	**E (MPa)**	**K_h (MN/m³)**
0 – 24	20	20
24 – 28	25	25
28 – 31	30	30
31 – 34	30	30
34 – 43	55	55
43 - 50	38	38

Table 3.3: Vertical spring's constant for pile's diameter D=1.20m

Πίνακας 3.3: Κατακόρυφα ελατήρια για πάσσαλο διαμέτρου D=1.20m

L (m)	**K_v (MN/m) for D=120m**
15	132
20	160
25	191
30	224
35	271

Table 3.4: Reduction factor R_s for the vertical springs of a group of piles

Πίνακας 3.4: Μειωτικός συντελεστής R_s για τα κατακόρυφα ελατήρια ομάδας πασσάλων αιχμής

		Number of piles in the group															
Length / Diameter	Distance / Diameter	4				9				16				25			
(L/B)	(e/B)	Pile's Stiffness K															
		10	100	1000	∞	10	100	1000	∞	10	100	1000	∞	10	100	1000	∞
	2	1.52	1.14	1.00	2.02	1.31	1.31	1.00	1.00	2.39	1.49	1.00	1.00	2.70	1.63	1.00	1.00
10	5	1.15	1.08	1.00	1.23	1.23	1.12	1.02	1.00	1.30	1.14	1.02	1.00	1.33	1.15	1.03	1.00
	10	1.02	1.01	1.00	1.04	1.04	1.02	1.00	1.00	1.04	1.02	1.00	1.00	1.03	1.02	1.00	1.00
	2	1.88	1.62	1.05	1.00	2.84	2.57	1.16	1.00	3.70	3.28	1.33	1.00	4.48	4.13	1.50	1.00
25	5	1.36	1.36	1.08	1.00	1.67	1.70	1.16	1.00	1.94	2.00	1.23	1.00	2.15	2.23	1.28	1.00
	10	1.14	1.15	1.04	1.00	1.23	1.26	1.06	1.00	1.30	1.33	1.07	1.00	1.33	1.38	1.08	1.00
	2	2.54	2.26	1.81	1.00	4.40	3.95	3.04	1.00	6.24	5.89	4.61	1.00	8.18	7.93	6.40	1.00
100	5	1.85	1.84	1.67	1.00	2.71	2.77	2.52	1.00	3.54	3.74	3.47	1.00	4.33	4.68	4.45	1.00
	10	1.44	1.49	1.46	1.00	1.84	1.99	1.98	1.00	2.21	2.48	2.53	1.00	2.53	2.98	3.10	1.00

Chapter 4

SEISMIC CONDITIONS

4.1 Seismic response spectra

In order to define seismic actions the design spectrum of Eurocode 8 is taken into consideration, for soil type D, soil factor S=0.80 and peak ground acceleration PGA_b=0.32g, accounting for the Seismic Scenario 2, with the following characteristics:

- return period T_{ret} = 1000 years
- earthquake magnitude Mw = 7.0
- peak ground acceleration at outcropping bedrock PGA_b = 0.32g

Additionally, the following parameters are considered:

- Behavior factor q_h=1.50, q_v=1.00
- Damping ratio ζ=3%
- Damping correction factor $\eta = \sqrt{\frac{10}{5+3}} = 1.118$
- Peak ground acceleration $PGA_{b,h}$=0.32g, $PGA_{b,v}$=0.90×0.32g=0.288g
- Periods for horizontal component (T_B=0.20s, T_C=0.80s, T_D=2.00s, S=0.80)
- Periods for vertical component (T_B=0.05s, T_C=0.15s, T_D=1.00s)

The horizontal elastic response spectrum is illustrated in Figure 4.1a, while Figure 4.1b shows the vertical one.

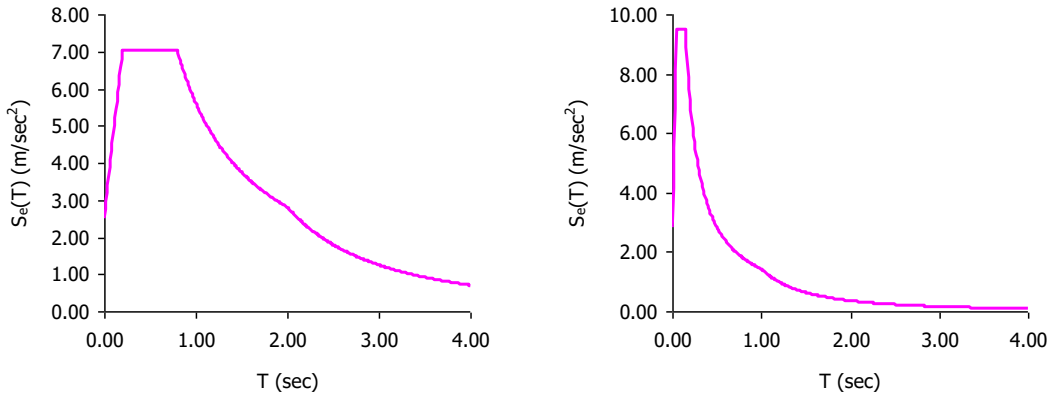

(a) (b)

Figure 4.1: (a) Horizontal elastic response spectrum, (b) Vertical elastic response spectrum

Σχήμα 4.1: (a) Οριζόντιο ελαστικό φάσμα απόκρισης, (b) Κατακόρυφο ελαστικό φάσμα απόκρισης

4.2 Modal response spectrum analysis

A modal analysis is performed to calculate the natural frequencies and vibration modes of the bridge. The inertial effects of the design seismic action are evaluated by taking into account the presence of the masses associated with all gravity loads appearing in the following combination of actions:

$\sum_{j\geq 1} G_{kj} "+" \sum_{i\geq 1} \psi_E \cdot Q_{ki}$ where ψ_E=0.20 for road traffic loads.

It is ensured that the sum of the effective modal masses for the modes taken into account is at least 90% of the total mass of the structure. The total mass does not include the piles' mass. The maximum displacements, internal loads and stresses are superimposed according to CQC (Complete Quadratic Combination) method.

Chapter 5

ANALYSIS OF THE BRIDGE

5.1 Model of the bridge

The main and transverse beams, the horizontal bracing members of the arches and the arches are modeled with beam elements. Moment releases are applied at the ends of the transverse beams. The hangers and the diagonal bracing members of the arches are modeled with truss elements. The concrete slab is simulated using shell elements with a thickness of 25cm, accounting for the mean value of the slab's thickness. The bearings at the abutments and the pier are modeled with equivalent elastic springs, with different stiffness for static and seismic combinations. Thus, for the horizontal springs the stiffness of the bearings for static load combinations is:

$$K_{h,st} = \frac{G_g \times A}{t} = \frac{900\text{kN/m}^2 \times 0.7\text{m} \times 0.8\text{m}}{0.150\text{m}} = 3360\text{kN/m} \tag{5.1}$$

while for displacements under seismic load combinations the stiffness of the horizontal springs is given as:

$$K_{h,se} = \frac{1.25 \times G_g \times A}{t} = 1.25 \times 3360\text{kN/m} = 4200\text{kN/m} \tag{5.2}$$

and for the calculation of the internal forces under seismic load combinations, the corresponding stiffness of the horizontal springs is:

$$K_{h,se,In} = \frac{1.20 \times 1.25 \times G_g \times A}{t} = 1.20 \times 4200\text{kN/m} = 5040\text{kN/m} \tag{5.3}$$

with G_g=900kN/m^2 the conventional shear modulus, A the overall plan area of the bearing and t the total thickness of the elastomer layers. The vertical springs have a stiffness constant equal to:

$$K_v = \frac{A}{\sum t_i \times \left(\frac{1}{5 \times G \times S^2} + \frac{1}{E_b} \right)} =$$

$$= \frac{0.70\text{m} \times 0.80\text{m}}{0.150\text{m} \times \left(\frac{1}{5 \times 1.25 \times 900\text{kN/m}^2 \times 12.44^2} + \frac{1}{2000000\,\text{kN/m}^2} \right)} = 2.26 \times 10^6\text{kN/m} \tag{5.4}$$

where S is the shape factor of the elastomeric bearing equal to:

$$S = \frac{A}{L \times t_e} = \frac{0.70m \times 0.80m}{2 \times (0.70m + 0.80m) \times 0.015m} = 12.44 \quad (5.5)$$

with L the perimeter of the bearing and t_e the effective thickness of an individual elastomer layer and the bulk modulus is taken equal to E_b=2000MPa.

The soil-structure interaction is taken into account with equivalent springs acting on the piles. More specifically, the calculated spring constant of a single pile is based on the values of Table 3.2, as also shown in Figure 5.1.

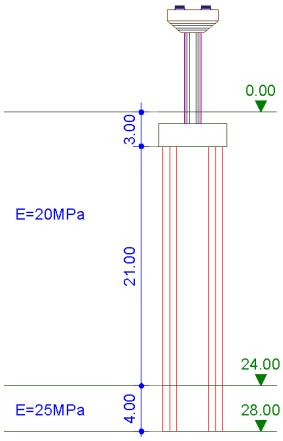

Figure 5.1: Young modulus E of soil with respect to the piles' length

Σχήμα 5.1: Μέτρο ελαστικότητας εδάφους E σε σχέση με το μήκος πασσάλων

The values of the springs' stiffness are:

$k_s = E_s / D$ ➔ k_s = 20000 kN/m^3 for the upper 21.00m of the pile (5.6)

$k_s = E_s / D$ ➔ k_s = 25000 kN/m^3 for the remaining 4.00m of the pile (5.7)

where D is the pile diameter (considered equal to 1.00m if the pile diameter is larger than 1.00m).

The elastic length of the pile L is:

$$L = \left(\frac{EI}{k_s D}\right)^{0.25} = \left(\frac{30 \cdot 10^6 \cdot \pi \cdot 1.20^4 / 64}{20000 \cdot 1.20}\right)^{0.25} \Rightarrow L = 3.36m \quad (5.8)$$

Thus, l/L =25.00 / 3.36 = 7.44 > 4.00 (where l is the pile's length that corresponds to the E taken into account).

For the reduction factors of the springs, the distances of the piles are taken into account (a_L in the direction of the force and a_Q perpendicular to the force) and the factors α_L and α_{QZ} are calculated according to DIN4014. In the longitudinal direction the reduced values of the springs are (Figure 5.2):

$$k_{si} = (\bar{\alpha}_{QZ} * \bar{\alpha}_L)^{1.33} \cdot k_s = (0.67 \times 1.00)^{1.33} \times 20000 kN/m^3 = \\ = (0.58 \times 20000) kN/m^3 \text{ for the upper } 21.00m \quad (5.9)$$

$$k_{si} = (\bar{a}_{QZ} * \bar{a}_L)^{1.33} \cdot k_s = (0.67 \times 1.00)^{1.33} \times 25000\ kN/m^3 = \\ =(0.58 \times 20000)kN/m^3 \text{ for the remaining } 3.00m \quad (5.10)$$

In the transverse direction the reduced values of the springs are (Figure 5.3):

$$k_{si} = (\bar{a}_{QZ} * \bar{a}_L)^{1.33} \cdot k_s = (0.76 \times 1.00)^{1.33} \times 20000\ kN/m^3 = \\ =(0.69 \times 20000)kN/m^3 \text{ for the upper } 21.00m \quad (5.11)$$

$$k_{si} = (\bar{a}_{QZ} * \bar{a}_L)^{1.33} \cdot k_s = (0.76 \times 1.00)^{1.33} \times 25000\ kN/m^3 = \\ =(0.69 \times 25000)kN/m^3 \text{ for the remaining } 3.00m \quad (5.12)$$

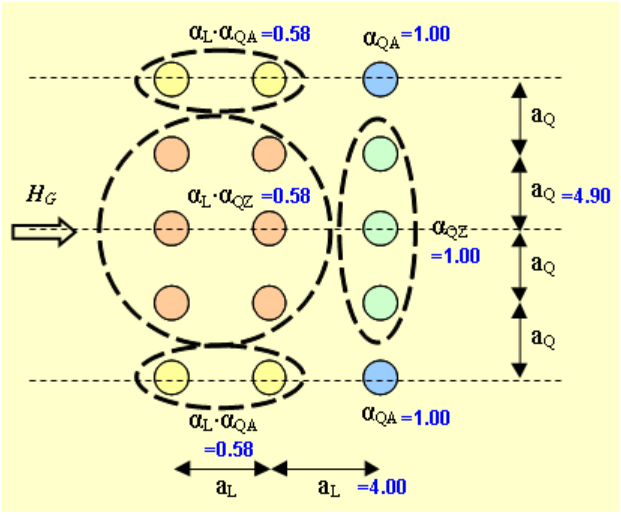

Figure 5.2: Reduced factors for pile's horizontal springs in the longitudinal direction

Σχήμα 5.2: Μειωτικοί συντελεστές οριζόντιων ελατηρίων πασσάλων, κατά τη διαμήκη έννοια

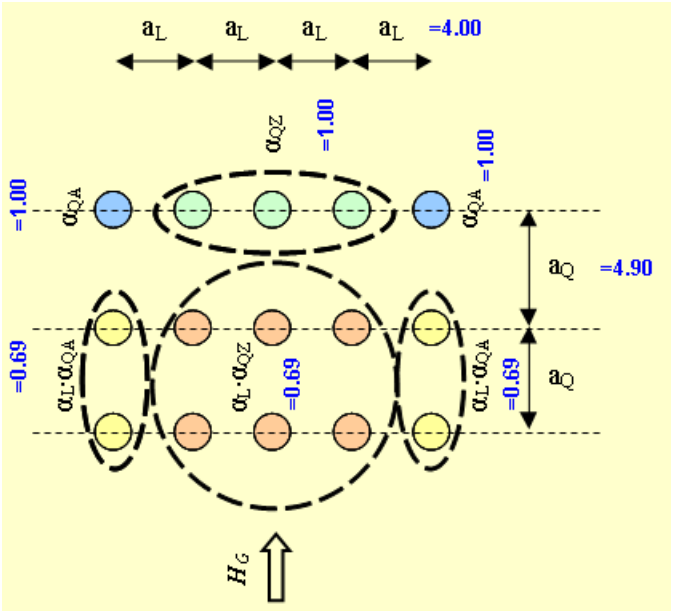

Figure 5.3: Reduced factors for pile's horizontal springs in the transverse direction

Σχήμα 5.3: Μειωτικοί συντελεστές οριζόντιων ελατηρίων πασσάλων, κατά την εγκάρσια έννοια

Regarding the vertical springs of the piles, the constant for a pile of L=24.00m is given in Table 3.3 and it is equal to k_v=191MN/m, while the reduction factor R_s according to Table 3.4 is equal to 1.15, considering L/B=20, e/B=4.08 and K=2000. Thus, the vertical spring's constant for the piles of diameter 1.20m are:

$$k_v = 191000kN/m/1.15 = 166000kN/m \quad (5.13)$$

The numerical model of the bridge is shown in Figure 5.4. The finite element analysis software that is used is Sofistik.

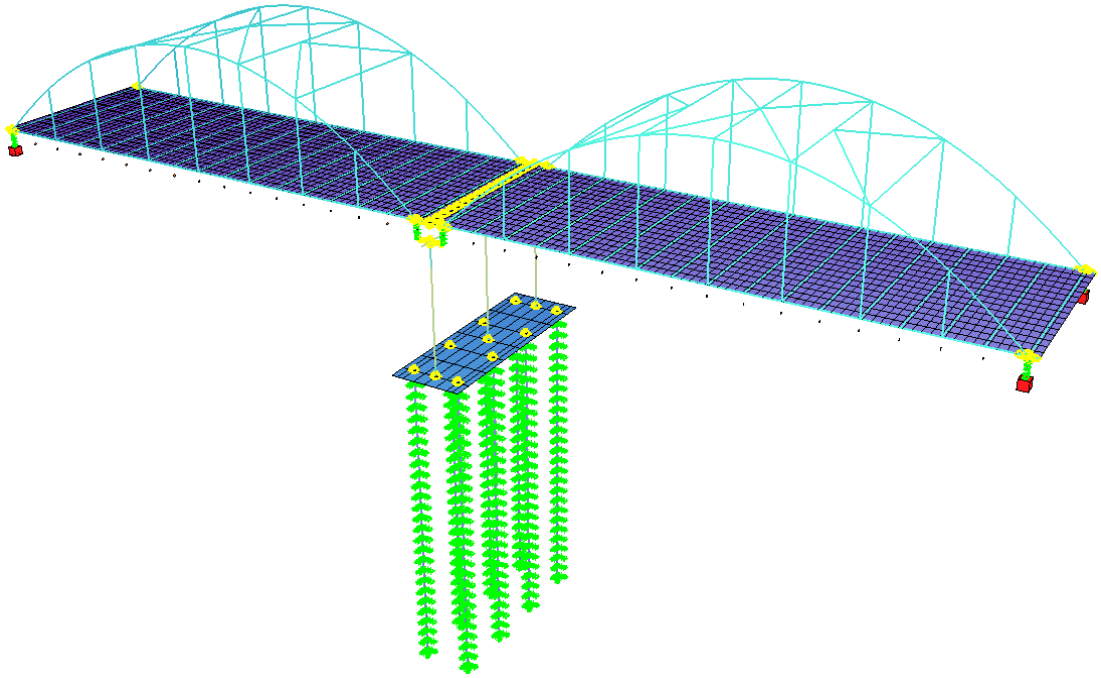

Figure 5.4: Model of the bridge
Σχήμα 5.4: Προσομοίωμα γέφυρας

5.2 Vibration modes and natural frequencies

The natural frequencies and periods of the first six vibration modes are listed in Table 5.1, while Figure 5.5 shows the corresponding modal shapes.

Table 5.1: Eigenfrequencies and eigenperiods of the bridge
Πίνακας 5.1: Ιδιοσυχνότητες και ιδιοπερίοδοι της γέφυρας

Mode number	Eigenfrequency (rad/sec)	Eigenfrequency (Hz)	Period (sec)
1	3.733	0.594	1.683
2	4.000	0.637	1.571
3	5.069	0.807	1.239
4	11.265	1.793	0.558
5	13.317	2.119	0.472
6	13.877	2.209	0.453

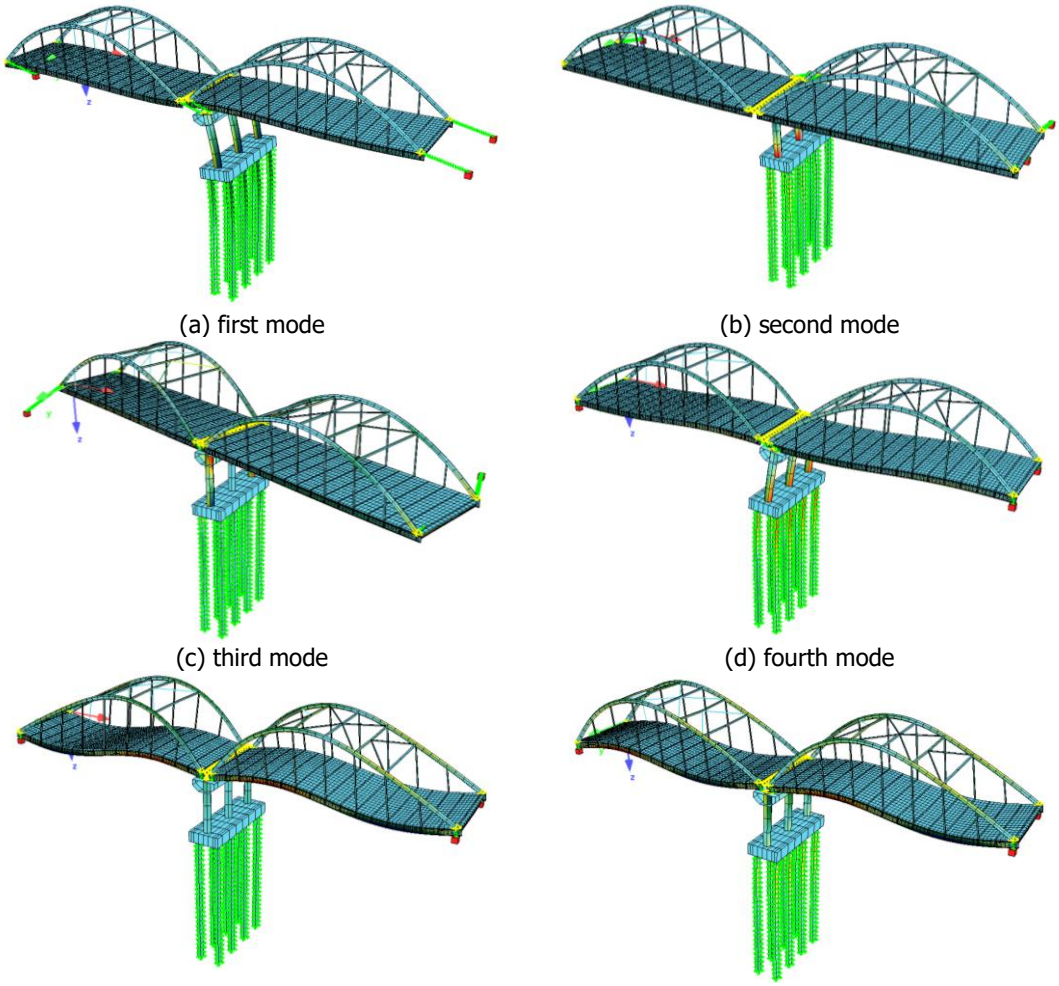

(a) first mode (b) second mode

(c) third mode (d) fourth mode

(e) fifth mode (f) sixth mode

Figure 5.5: Eigenmodes of the bridge

Σχήμα 5.5: Ιδιομορφές γέφυρας

5.3 Load Cases

The load cases considered are the following:

LC 1: Self weight

LC 2: Superimposed

Pavement and future layer: $g=0.20m\times24kN/m^3+0.50kN/m^2=5.30kN/m^2$

Each sidewalk with parapets: $g=(0.33m^2\times25kN/m^3 + 0.95kN/m) / 1.25m = 7.36kN/m^2$

Earth weight on the pilecap $g=0.50m \times 20\ kN/m^3= 10kN/m^2$.

LC 3: Shrinkage and creep

An equivalent uniform decrease of temperature is used to simulate the shrinkage of the concrete slab, equal to -13°.

LC 4: Braking load

The total braking load is:

$Q_{ik}=0.6\alpha_{Ql}(2Q_{lk})+0.10\alpha_{ql}\ q_{lk}\ w_1\ L=0.6\times0.9\times2\times300+0.10\times1.0\times9\times3\times87.60=560.52kN$

It is: $180\times\alpha_{Ql}<=Q_{ik}<=900 => 180\times0.9<=Q_{ik}<=900 => 162<=Q_{ik}<=900$.

The distributed uniform horizontal load over the bridge's deck is:

$Q_{ik}/(14.70m \times 87.60m)=0.43\ kN/m^2$

LC 5-6: Uniform difference of temperature for check of elastomeric bearings and expansion joints.

For the check of bearings and expansion joints the uniform difference of temperature is calculated as:

$\Delta T_{N,con}$-20ºC=-41ºC, $\Delta T_{N,exp}+20_oC=59ºC$.

As in LC 15 and 16, the temperature variations are applied on the steel members of the superstructure and the slab of the deck.

LC 7: Wind action y

Considering a wind velocity V_b=30m/sec, a uniform load is applied at the members of the bridge towards +y (depending on their exposed dimension):

Piers: 0.0238kN/m

Deck: $0.415kN/m^2$

Hangers: 0.11-0.13kN/m

Arches: 0.56kN/m

Diagonal bracing members: 0.09kN/m

LC 8: Wind action x

Similarly, considering a wind velocity V_b=30m/sec, a uniform load is applied at the members of the bridge towards +x:

Piers: 0.0323kN/m

Deck: $0.104kN/m^2$

Hangers: 0.11-0.13kN/m

Arches: 0.56kN/m

Diagonal bracing members: 0.07kN/m

Horizontal bracing members:: 0.19kN/m

LC 9: Wind action z

Considering a wind velocity V_b=30m/sec, a uniform load is applied at the members of the bridge towards +z:

Half Deck: $1.01kN/m^2$

Arches: 0.56kN/m

Diagonal bracing members: 0.11kN/m

Horizontal bracing members: 0.19kN/m

LC 10, 11, 12: Settlement of 1cm at the pier and 1cm at the abutments.

LC 15-16: Uniform difference of temperature on deck.

Considering an initial temperature T_0=+10ºC, a minimum shade air temperature T_{min}=-15ºC and a maximum one T_{max}=+45ºC, the uniform temperature components are determined by EC1. Part.1-5 for a composite bridge (Type 2) and are equal to $T_{e,min}$=-11ºC and $T_{e,max}$=+49ºC. Thus:

$\Delta T_{N,con}=T_0-T_{e,min}$=-21ºC, $\Delta T_{N,exp}= T_{e,max} - T_0$ =+39ºC.

The temperature variations are applied on the steel members of the superstructure and the slab of the deck.

LC 20-99: Tandem System of Traffic Load Model 1

The carriageway width is 11.25m, thus, three lanes are considered with width 3.00m and a tandem system is applied at varied positions of the bridge, as:

Lane 1: 0.9×150kN=135kN/wheel (four wheels)

Lane 2: 0.9×100kN=90kN/wheel (four wheels)

Lane 3: 0.9×50kN=45kN/wheel (four wheels)

LC 101-103: UDL System of Traffic Load Model 1

A distributed load is applied on the deck equal to 2.5kN/m^2

LC 121-123, 141-143: UDL System of Traffic Load Model 1

At Lane 1 an additional distributed load is applied, equal to 6.5kN/m^2.

LC 201-260: Tandem System of Traffic Load Model 2

A single axle load is applied at different positions of the bridge with value: 0.9×200kN=180kN/wheel (two wheels)

LC 320-399: Tandem System of Traffic Load Model 1 with cracked deck concrete

LC 401-403: UDL System of Traffic Load Model 1 with cracked deck concrete

LC 421-423, 441-443: UDL System of Traffic Load Model 1 with cracked deck concrete

LC 501-560: Tandem System of Traffic Load Model 2 with cracked deck concrete

LC600: Uniform road traffic loads

This load case is used for the seismic combinations, taking into account Load Model 1. The loads considered for this LC are listed in Table 5.2. A uniform load is applied to the shell elements equal to 4.67kN/m^2.

Table 5.2: Live Load of the road bridge
Πίνακας 5.2: Κινητό φορτίο οδογέφυρας

	Load	Width	Length	Sum of Loads
TS	Lane 1: 0.9×600kN=540kN Lane 2: 0.9×400kN=360kN Lane 3: 0.9×200kN=180kN			1080.00kN
UDL	9.00kN/m^2	3.00m	87.60m	2365.20kN
UDL	2.50kN/m^2	14.70m-3.00m	87.60m	2562.30kN
Total Load				6007.50kN
Distributed Load		14.70m	87.60m	**4.67kN/m^2**

LC2010: Earthquake x-x

LC2011: Earthquake y-y

LC2012: Earthquake z-z

5.4 Load Combinations at Ultimate Limit State (ULS)

The load combination at ULS is described as:

$$\sum_{j\geq 1} \gamma_{Gj} \cdot G_{kj} "+" \gamma_{Q1} \cdot Q_{k1} "+" \sum_{i\geq 1} \gamma_{Qi} \cdot \psi_{0i} \cdot Q_{ki} \qquad (5.14)$$

where the partial factors γ_G and γ_Q are listed in Table 5.3, while factor ψ_0 can be found in Table 5.4:

Table 5.3: Partial factors for actions in ULS
Πίνακας 5.3: Επιμέρους συντελεστές για δράσεις σε ΟΚΑ

Action	Contribution	Factor	Persistent / Transient	Accidental
Permanent actions	unfavourable	γ_{Gsup}	1.35	1.00
	favourable	γ_{Ginf}	1.00	1.00
Traffic loads	unfavourable	γ_Q	1.35	1.00
	favourable	γ_Q	0.00	0.00
Settlements	unfavourable	γ_{Gset}	1.20	0.00
	favourable	γ_{Gset}	0.00	0.00
Other variable actions	unfavourable	γ_Q	1.50	1.00
	favourable	γ_Q	0.00	0.00
Accidental actions	unfavourable	γ_A	---	1.00

The following ULS load combinations are considered:

LC 1100 and 1200: This combination includes the following load cases:

LC1	Self weight
+LC2	Superimposed
+LC3	Shrinkage
+LC4	Braking load
+LC7 or LC8	Wind action ±x or ± y
+LC9	Wind action ±z

+LC10, 11, 12	Settlements at the pier and the abutments (only for the design of superstructure)
+LC15, 16	Thermal loads
+LC20-99	Tandem System (LM1)
+LC101-103	UDL 2.5kN/m^2 (LM1)
+LC121-123 or 141-143	UDL 6.50kN/m^2 (LM1)

LC 1300: This combination includes the following load cases:

LC1	Self weight
+LC2	Superimposed
+LC3	Shrinkage
+LC4	Braking load
+LC7 or LC8	Wind action ±x or ± y
+LC9	Wind action ±z
+LC10, 11, 12	Settlements at the pier and the abutments (only for the design of superstructure)
+LC15, 16	Thermal loads
+LC201-260	Traffic load (LM2)

5.5 Load Combinations at Serviceability Limit State (SLS)

The load combinations at the SLS are:

$$\text{Characteristic combination: } \sum_{j\geq 1} G_{kj} "+" Q_{k1} "+" \sum_{i\geq 1} \psi_0 \cdot\cdot Q_{ki} \tag{5.15}$$

$$\text{Frequent combination: } \sum_{j\geq 1} G_{kj} "+" \psi_{1,1} \cdot Q_{k1} "+" \sum_{i\geq 1} \psi_{2i} \cdot\cdot Q_{ki} \tag{5.16}$$

where the ψ factors for road bridges are given in Table 5.4:

Table 5.4: Factors ψ for road bridges
Πίνακας 5.4: Συντελεστές ψ για οδογέφυρες

Actions	Symbol		ψ_0	ψ_1	ψ_2
Traffic load	Gr1 (LM1)	TS	0.75	0.75	0.00
		UDL	0.40	0.40	0.00
	Gr2 (LM2)		0.00	0.75	0.00
Thermal actions			0.60	0.60	0.50
Horizontal forces			0.00	0.00	0.00
Wind forces			1.00	0.00	0.00
Settlements			1.00	1.00	1.00

The SLS load combinations are:

LC 1600: Characteristic Load Combination

For this combination the tensile strength in the concrete reinforcement should not exceed $0.80f_{yk}$, otherwise the reinforcement is increased. Additionally, the compressive stress in the concrete slab should be less or equal to $0.60f_{ck}$.

LC1	Self weight
+LC2	Superimposed
+LC3	Shrinkage
+LC4	Braking load
+LC7 or LC8	Wind action ±x or ± y
+LC9	Wind action ±z
+LC15, 16	Thermal loads
+LC20-99	Tandem System (LM1)
+LC101-103	UDL 2.5kN/m^2 (LM1)
+LC121-123 or 141-143	UDL 6.50kN/m^2 (LM1)

LC 1700: Characteristic Load Combination

For this combination the tensile strength in the reinforcement should not exceed $0.80f_{yk}$, otherwise the reinforcement is increased. Additionally, the compressive stress in the slab concrete should be less or equal to $0.60f_{ck}$.

LC1	Self weight
+LC2	Superimposed
+LC3	Shrinkage
+LC4	Braking load
+LC7 or LC8	Wind action ±x or ± y
+LC9	Wind action ±z
+LC15, 16	Thermal loads
+LC201-260	Traffic load (LM2)

LC 1800: Frequent Load Combination (Calculation of deformations taking into account cracked deck concrete)

LC1	Self weight
+LC2	Superimposed
+LC3	Shrinkage
+LC15, 16	Thermal loads

+LC320-399	Tandem System (LM1)
+LC401-403	UDL 2.5kN/m^2 (LM1)
+LC421-423 or 441-443	UDL 6.50kN/m^2 (LM1)

5.6 Seismic Load Combinations

The seismic load combination is described as:

$$\sum_{j\geq 1} G_{kj} "+" \sum_{i\geq 1} \psi_{Ei} \cdot Q_{ki} "+" E \qquad (5.17)$$

where Q are the variable loads, including traffic and thermal loads, while E represents the following earthquake combinations:

E_{Edx} "+" 0.30 E_{Edy} "+" 0.30 E_{Edz}

0.30 E_{Edx} "+" E_{Edy} "+" 0.30 E_{Edz}

0.30 E_{Edx} "+" 0.30 E_{Edy} "+" E_{Edz}

The ψ_E factors for the variable loads are listed in Table 5.5:

Table 5.5: Factors ψ_E for seismic load combinations
Πίνακας 5.5: Συντελεστές ψ_E για σεισμικούς συνδυασμούς

Actions	Symbol		ψ_E
Traffic load	Gr1 (LM1)	TS	0.20
		UDL	0.20
	Gr2 (LM2)		0.00
Thermal actions			0.50
Horizontal forces			0.00
Wind forces			0.00

The load cases included in the seismic load combinations are:

LC 4000: This combination concerns the pier's columns and the superstructure. It includes the following load cases:

LC1	Self weight
+LC2	Superimposed
+LC3	Shrinkage
+LC600	Uniform traffic load
+LC15, 16	Thermal loads
+LC2010 (±1.0 or ±0.3)/1.50	Earthquake X
+LC2011 (±1.0 or ±0.3)/1.50	Earthquake Y
+LC2012 (±1.0 or ±0.3)	Earthquake Z

LC 4100: This combination concerns the pier's piles and pilecap. It includes the following load cases:

LC1	Self weight
+LC2	Superimposed
+LC3	Shrinkage
+LC600	Uniform traffic load
+LC15, 16	Thermal loads
+LC2010 ($\pm$1.0 or $\pm$0.3)	Earthquake X
+LC2011 ($\pm$1.0 or $\pm$0.3)	Earthquake Y
+LC2012 ($\pm$1.0 or $\pm$0.3)	Earthquake Z

Chapter 6

DESIGN OF CONCRETE MEMBERS

6.1 Evaluation of the results

The results of the concrete components of the bridge are summarizing in Table 6.1.

Table 6.1: Analyses' results/requirements for concrete members

Πίνακας 6.1: Αποτελέσματα/απαιτήσεις αναλύσεων για στοιχεία από οπλισμένο σκυρόδεμα

Members	Results / Requirement	Conventional Solution
Piles	Longitudinal Reinforcement	90.4cm^2
	Stirrups	8.45cm^2
	Max compressive force	4574kN (static)
		5085kN (seismic)
Pilecap	Longitudinal Reinforcement	49.70cm^2
	Transverse Reinforcemnt	33.6cm^2
Pier	Longitudinal Reinforcement	186.70cm^2
	Stirrups	16.60cm^2
	Max compressive force	9673kN
Deck slab	Longitudinal Reinforcement	47.9cm^2
	Transverse Reinforcemnt	33.6cm^2

6.2 Reinforcement of the piles

The required reinforcement of the piles is equal to 90.4cm^2 (Figure 6.1). A minimum percentage of 1% is considered and 25Φ25 (122.75m^2) are used for the piles.

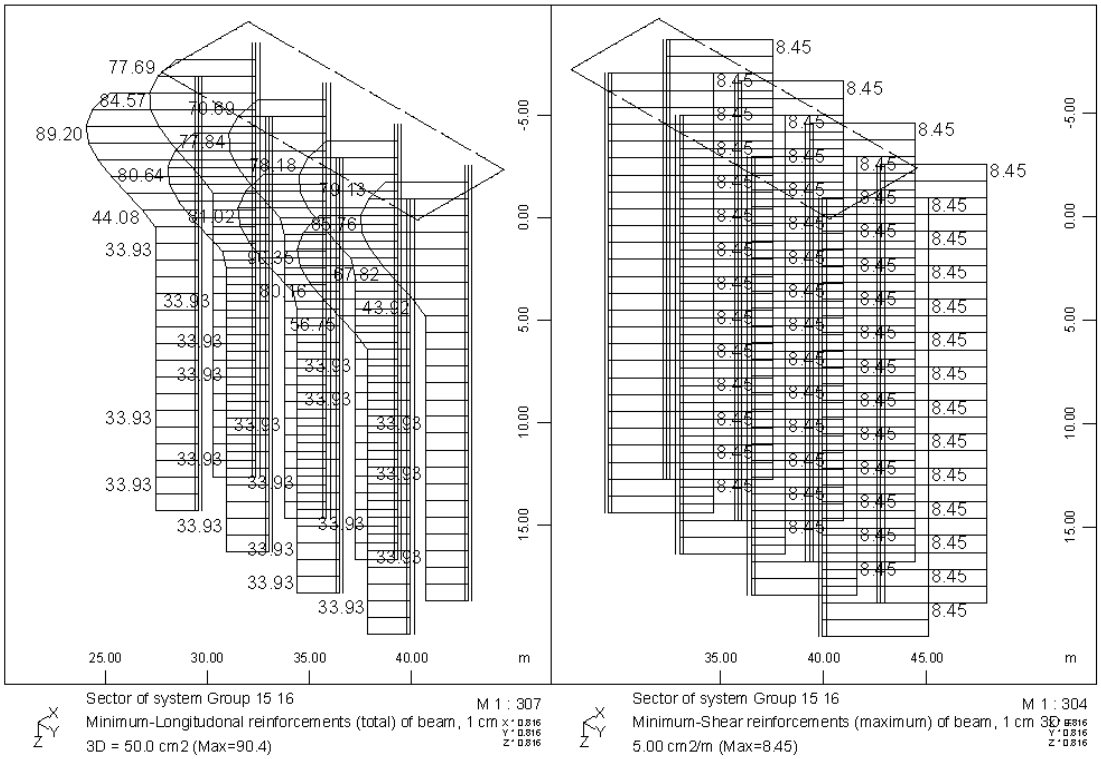

Figure 6.1: Required reinforcement of the piles

Σχήμα 6.1: Απαιτούμενος οπλισμός πασσάλων

6.3 Bearing capacity of the piles

Given the soil profile of Figure 3.9, the bearing capacity of the piles is calculated according to the Appendix C of Deliverable D4: Elastic Response Spectra for Liquefiable soils, for three pile diameters, Φ100, Φ120 and Φ150 (Figure 6.2). For the calculation of the piles' bearing capacity, safety factors 2.00 and 1.30 are taken into account, referring to the static combinations and seismic ones, respectively. Thus, the bearing capacity of a pile with a diameter 1.20m and length 25.00m is 9.50MN /2.00=4.75MN for static loads and 9.50MN/1.30=7.30MN for seismic loads. The maximum values of the load at the top of the pier's piles are:

Static combinations: minN = 4553 kN (LC 1100) <4750kN (Figure 6.3) √

Seismic combinations: minN = 5092 kN (LC 4100) <7300kN (Figure 6.4) √

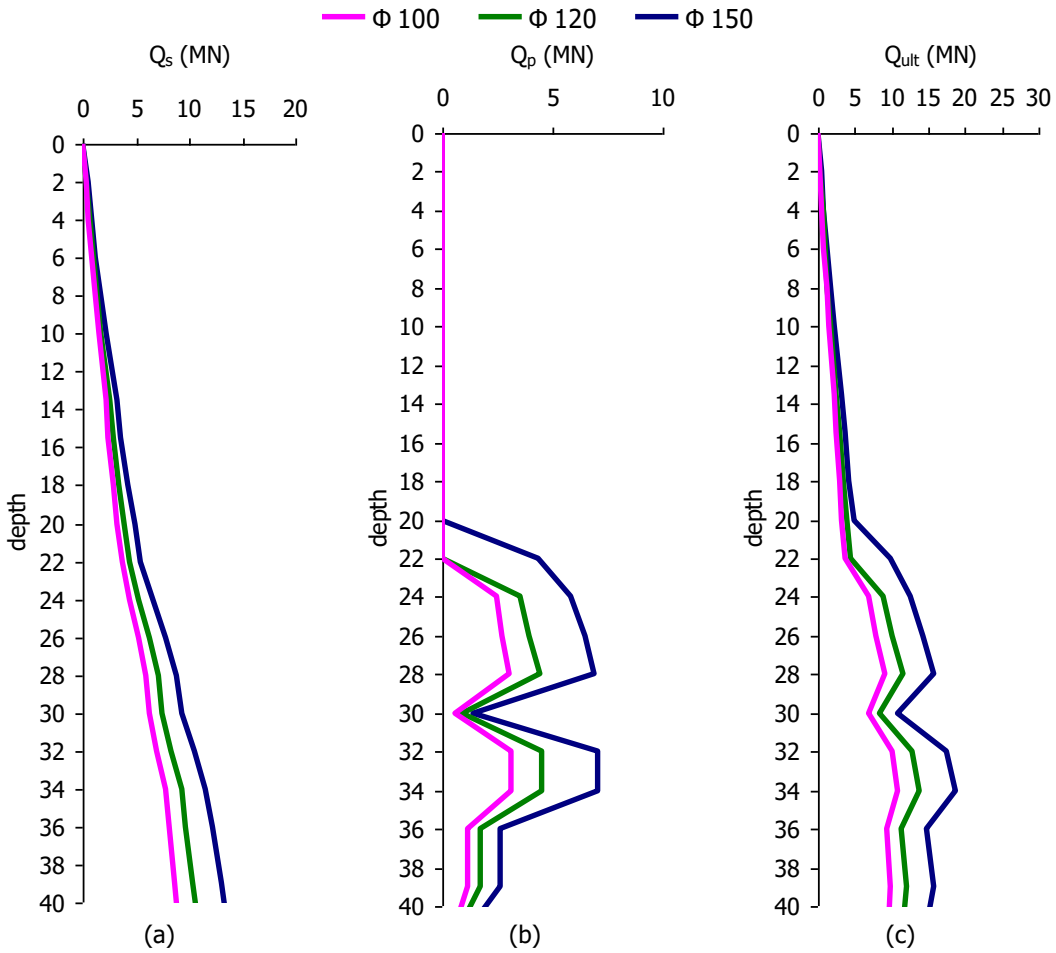

Figure 6.2: (a) Friction (b) Tip (c) Ultimate bearing capacities of piles

Σχήμα 6.2: Φέρουσα ικανότητα πασσάλων (a) Οριακό φορτίο τριβής (b) Οριακό φορτίο αιχμής (c) Επιτρεπόμενο οριακό φορτίο πασσάλων

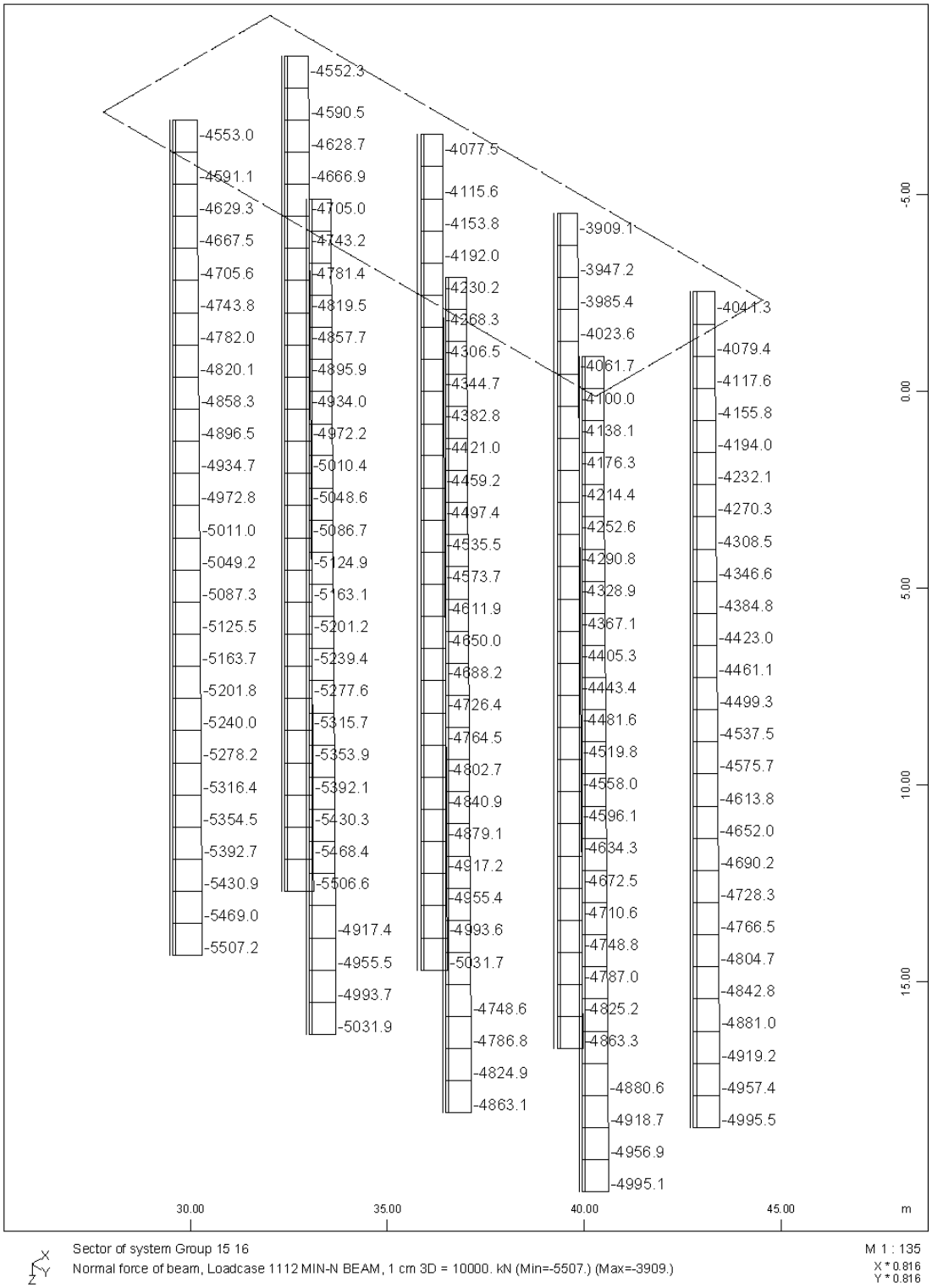

Figure 6.3: Maximum axial force at the piles for static load combinations

Σχήμα 6.3: Μέγιστο αξονικό φορτίο στους πασσάλους για στατικούς συνδυασμούς φορτίσεων

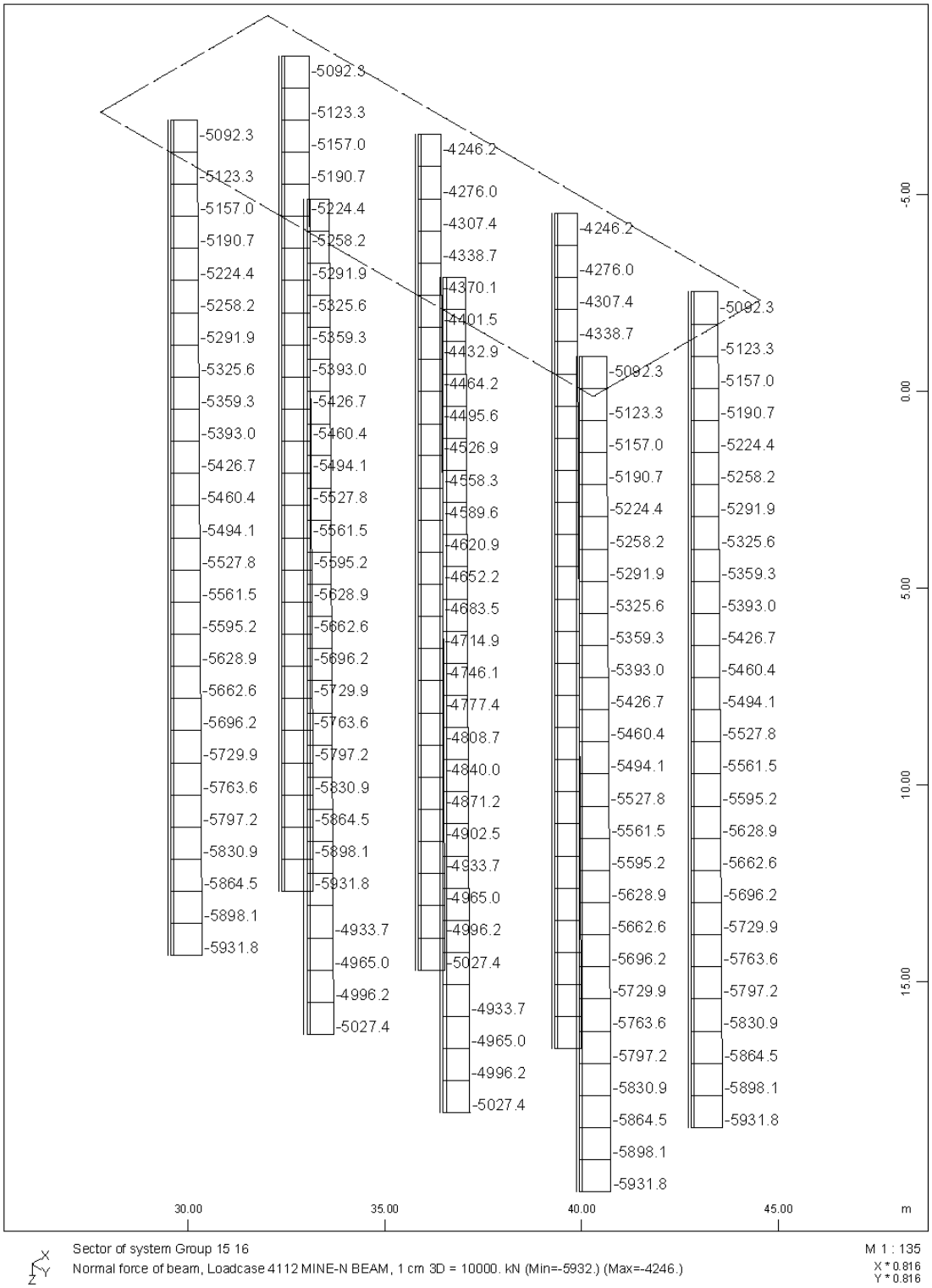

Figure 6.4: Maximum axial force at the piles for seismic load combinations

Σχήμα 6.4: Μέγιστο αξονικό φορτίο στους πασσάλους για σεισμικούς συνδυασμούς φορτίσεων

6.4 Piles' Confinement

The maximum compressive load of the piles is N_c=5092kN.

Since the normalized axial force n_k exceeds the limit of 0.08, as:

$$n_k = \frac{N_c}{f_{ck} A_c} = 5092 / (20000 \times 3.14 \times 1.20^2/4) = 0.23 > 0.08$$

confinement should be provided. The minimum amount of confining reinforcement for a spiral is:

$$\omega_{min} = 1.40 \cdot \frac{A_c}{A_{cc}} \cdot \lambda \cdot n_k \geq 0.18 = 1.40 \times 1.20^2 / 1.04^2 \times 0.37 \times 0.23 = 0.16 < 0.18 \rightarrow \omega = 0.18$$

The quantity of the confining reinforcement is defined by the mechanical reinforcement ratio which is:

$$\min \rho_w = \omega_{min} \frac{f_{cd}}{f_{yd}} \Rightarrow \min \rho_w = 0.18 \times \frac{\frac{20 \times 10^3}{1.5}}{\frac{500 \times 10^3}{1.15}} \Rightarrow \min \rho_w = 0.00552$$

A spiral Φ14/10 is used accounting for a volumetric ratio equal to:

$$\rho_w = \frac{4 A_{sp}}{D_{sp} s_L} = 4 \times 1.54 cm^2 / (104 cm \times 10 cm) \Rightarrow \rho_w = 0.006 > \min \rho_w$$

The spacing of the spiral satisfies the limits of:

$s_L = 10cm < 6 d_{bL} = 6 \times 2.2cm = 13.2cm$ where d_{bL} is the longitudinal bar diameter and

$s_L = 10cm < D_{cc}/5 = 104cm/5 = 20.8cm$ where D_{cc} is the diameter of the confined concrete core.

6.5 Reinforcement of pilecap

The required reinforcement of the pilecap is illustrated in Figure 6.5, where the principal direction is parallel to x-axis, while the cross one is parallel to y-axis. A reinforcement grid of Φ22/10 is used for the upper and lower reinforcement of the pilecap.

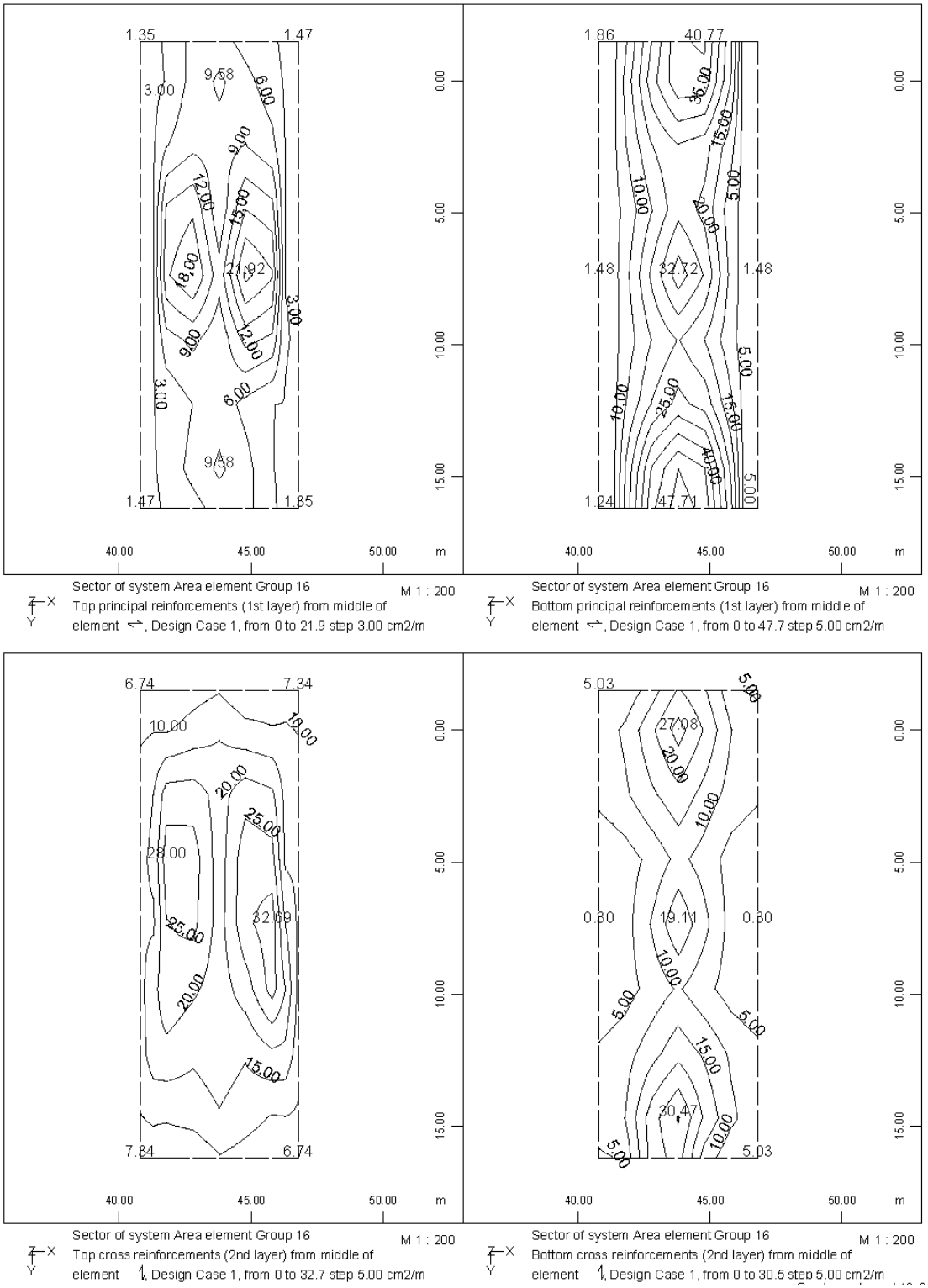

Figure 6.5: Required reinforcement of the pilecap

Σχήμα 6.5: Απαιτούμενος οπλισμός κεφαλοδέσμου πασσάλων

6.6 Reinforcement of the pier

The required reinforcement of the pier's columns is equal to 186.7cm^2 (Figure 6.6). A minimum percentage of 1% is considered and 45Φ25 (220.95cm^2) are used for the columns of the pier.

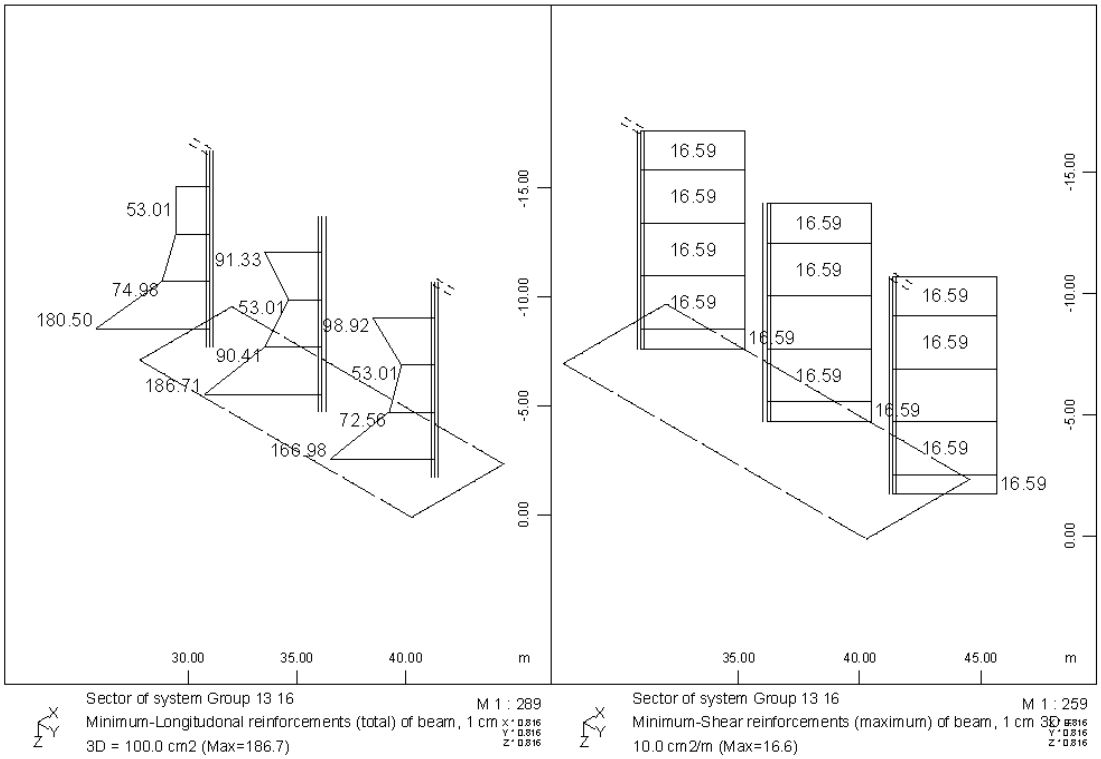

Figure 6.6: Required reinforcement of the pier

Σχήμα 6.6: Απαιτούμενος οπλισμός στύλων μεσοβάθρου

6.7 Pier's Confinement

The maximum compressive load of the piers is for Load Combination 1200 and it is equal to N_c=9673kN (Figure 6.7).

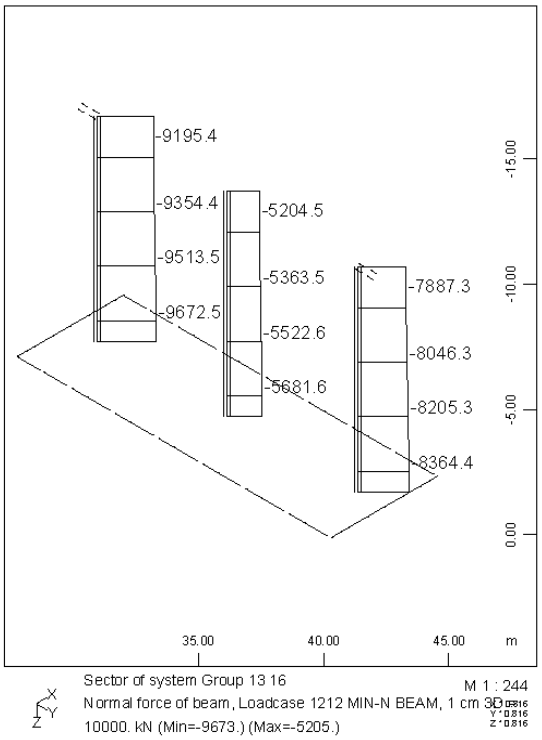

Figure 6.7: Maximum axial force at the pier

Σχήμα 6.7: Μέγιστο αξονικό φορτίο στους στύλους μεσοβάθρου

Since the normalized axial force n_k exceeds the limit of 0.08, as:

$$n_k = \frac{N_c}{f_{ck} A_c} = 9673 / (30000 \times 3.14 \times 1.50^2/4) = 0.18 > 0.08$$

confinement should be provided. The minimum amount of confining reinforcement for a spiral is:

$$\omega_{min} = 1.40 \cdot \frac{A_c}{A_{cc}} \cdot \lambda \cdot n_k \geq 0.18 = 1.40 \times 1.50^2 / 1.34^2 \times 0.37 \times 0.18 = 0.12 < 0.18 \rightarrow \omega = 0.18$$

The mechanical reinforcement ratio is:

$$\min \rho_w = \omega_{min} \frac{f_{cd}}{f_{yd}} \Rightarrow \min \rho_w = 0.18 \times \frac{\frac{30 \times 10^3}{1.5}}{\frac{500 \times 10^3}{1.15}} \Rightarrow \min \rho_w = 0.008$$

Stirrups 2Φ16/15 are used with a volumetric ratio:

$$\rho_w = \frac{4 A_{sp}}{D_{sp} s_L} = 2 \times 4 \times 2.00 cm^2 / (134 cm \times 15 cm) \Rightarrow \rho_w = 0.008 = \min \rho_w$$

The spacing of the stirrups satisfies the limits of:

$s_L = 15cm = 6 d_{bL} = 6 \times 2.5cm = 15cm$ where d_{bL} is the longitudinal bar diameter and

$s_L = 15cm < D_{cc}/5 = 134cm/5 = 26.8cm$ where D_{cc} is the diameter of the confined concrete core.

6.8 Reinforcement of deck slab

The required reinforcement of the deck slab is shown in Figure 6.8, where the principal direction is parallel to x-axis, while the cross one is parallel to y-axis. In the longitudinal direction Φ14/10 is used for the upper and lower reinforcement, while in the transverse direction Φ12/10 is chosen.

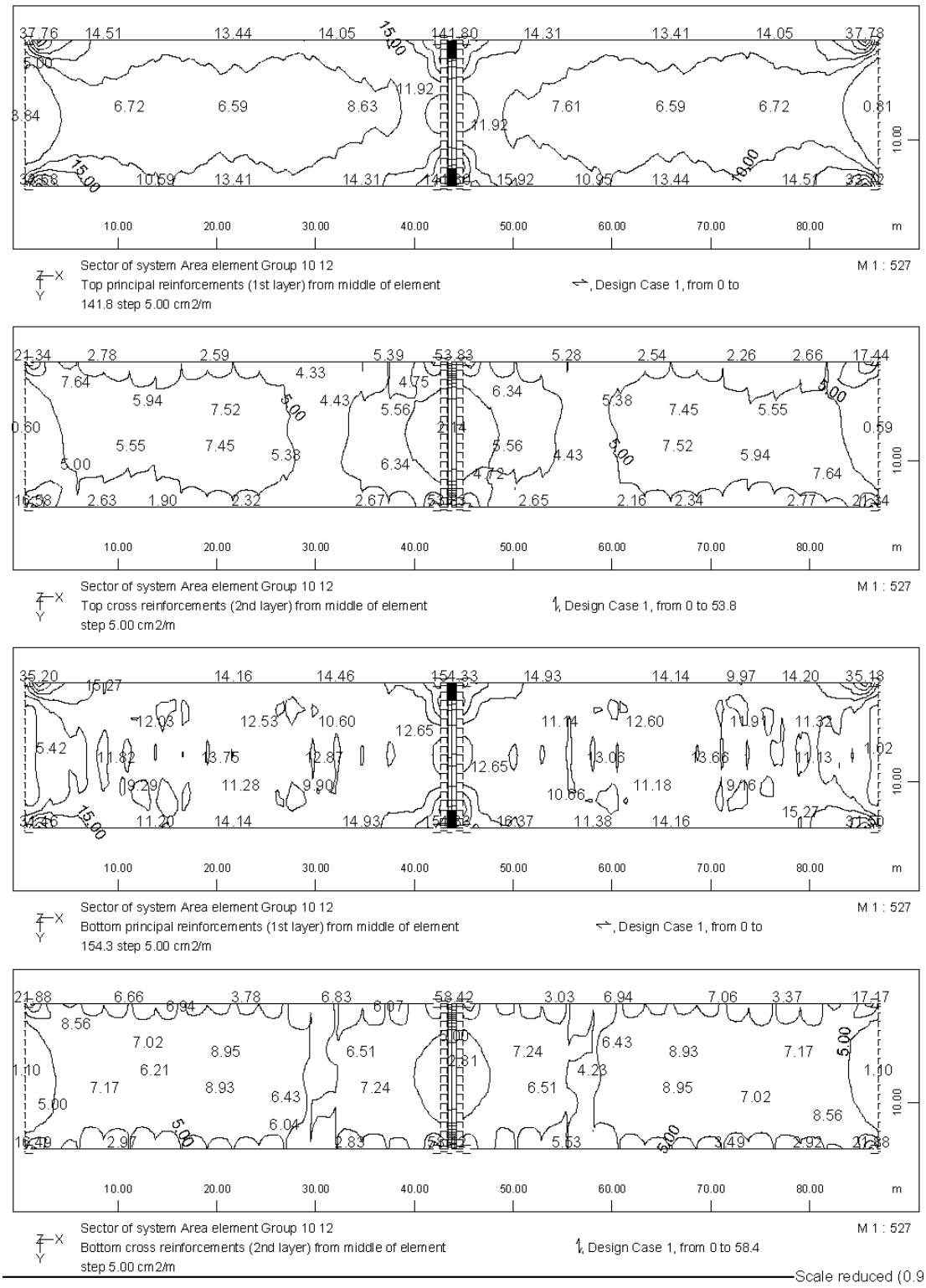

Figure 6.8: Required reinforcement of the concrete deck slab

Σχήμα 6.8: Απαιτούμενος οπλισμός πλάκας καταστρώματος

Chapter 7

DESIGN OF STEEL MEMBERS

7.1 Evaluation of the results

The maximum internal forces for the steel members are listed in Table 7.1.

Table 7.1: Analyses' results for the steel members
Πίνακας 7.1: Αποτελέσματα αναλύσεων για τα μεταλλικά στοιχεία

Members	Results	Conventional Solution	Max. Exploitation Factor (EF)
Arches	minN (LC1100)	-6242kN	0.82
	maxM_y (LC1100)	1033kNm	
	maxM_z (LC4100)	971.4kNm	
Transverse bracing	maxN (LC4100)	202.1kN	0.46
	minN (LC1100)	-125.9kN	
	maxM_y (LC4100)	31.8kNm	
	maxM_z (LC4100)	13.3kNm	
Diagonal bracing	minN (LC4000)	-137.2kN	0.99
Hangers	maxN (LC1100)	1211kN	0.85
Transverse beams	maxN (LC1100)	3327kN	0.94
	minN (LC4100)	-1651kN	
	maxM_y (LC1100)	2032kNm	
	maxM_z (LC1100)	111.4kNm	
Main beams	maxN (LC1100)	5239kN	0.52
	minN (LC4100)	-1481kN	
	maxM_y (LC1100)	2057kNm	
	maxM_z (LC1100)	121.1kNm	

7.2 Arches

For the design of the arches, first a buckling analysis is conducted with a model that includes one main beam, one arch and the hangers (Figure 7.1). The supports at the ends of the main beam are considered as pinned. For a distributed vertical load equal to 100kN, applied at the main beam, the normal force of the arch is presented in Figure 7.2. The mean value of the normal force along the arch is N=2516kN. The first buckling mode of the arch is the in plane one and it is shown in Figure 7.3. The second one, illustrated in Figure 7.4, concerns the out of plane buckling. For the first mode the buckling factor is equal to 14.34, while for the second one is 24.25. Thus the critical force of force N_{cr} in the arch for in plane buckling is $N_{cr,y}$=14.34 × 2516kN=36073kN, while for out of plane buckling $N_{cr,z}$=24.25 × 2516kN = 61013kN.

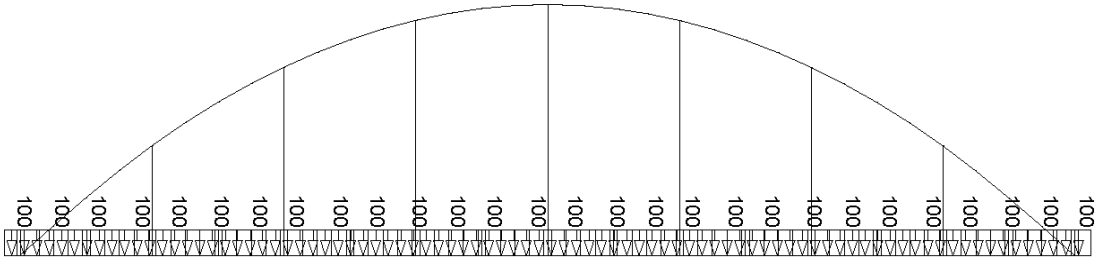

Figure 7.1: Model and load for buckling analysis of the arch

Σχήμα 7.1: Προσομοίωμα και φορτίο για ανάλυση λυγισμού τόξου

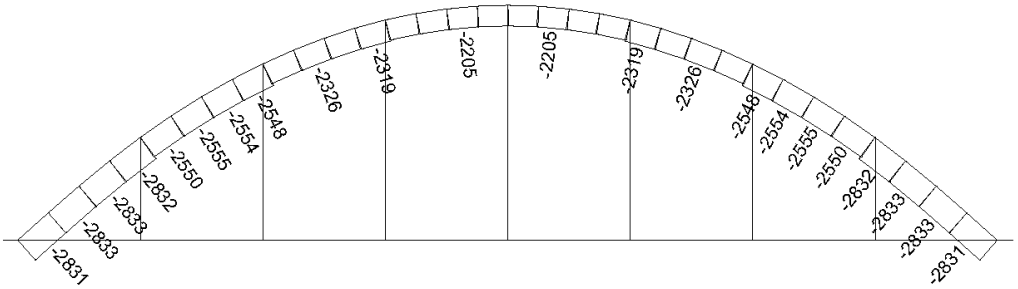

Figure 7.2: Normal force of the arch due to distributed vertical load applied at the main beam

Σχήμα 7.2: Αξονική δύναμη τόξου λόγω κατανεμημένου κατακόρυφου φορτίου στην κύρια δοκό

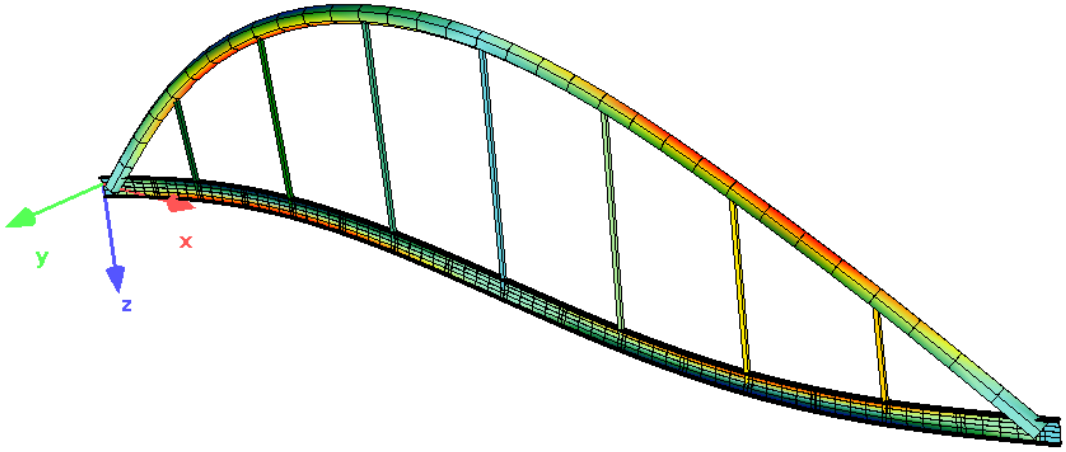

Figure 7.3: The first buckling mode of the arch

Σχήμα 7.3: Η πρώτη μορφή λυγισμού τόξου

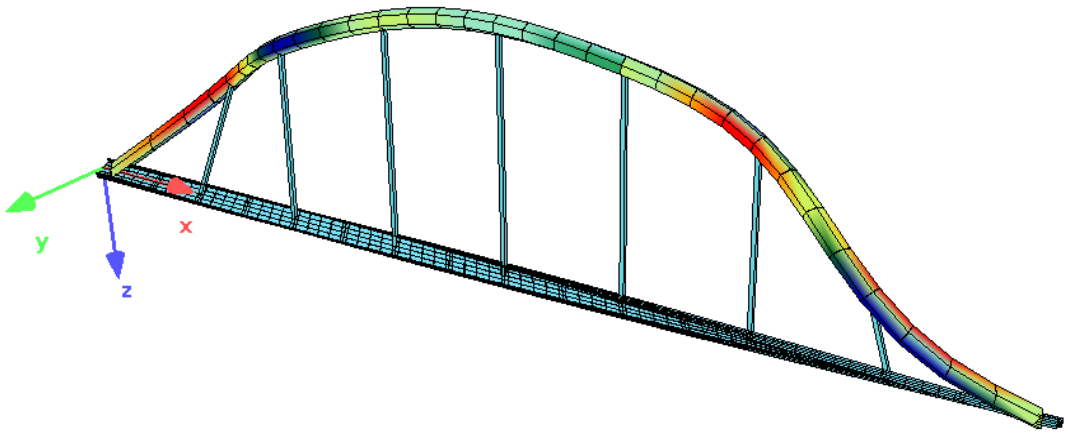

Figure 7.4: The second buckling mode of the arch

Σχήμα 7.4: Η δεύτερη μορφή λυγισμού τόξου

Alternatively, according to Annex D, §D.3 of EC3, Part.2, the buckling length factor β can be estimated by Figure 7.5. Thus, for f=10.00m, l=42.00, f/l=0.24 and m=7, factor β is equal to 0.55 and the critical force of force N_{cr} in the arch for in plane buckling is expressed as:

$$N_{cr} = \left(\frac{\pi}{\beta s}\right)^2 EI = \left(\frac{\pi}{0.55 \cdot 23.85m}\right)^2 \cdot 210.000.000kN/m^2 \cdot 0.00306m^4 = 36859kN$$

where s=23.85m is the half length of the arch and EI is the in plane flexural stiffness of the arch, with:

$$I = \frac{\pi \cdot \left[(0.75m)^4 - (0.71m)^4\right]}{64} = 0.00306m^4$$

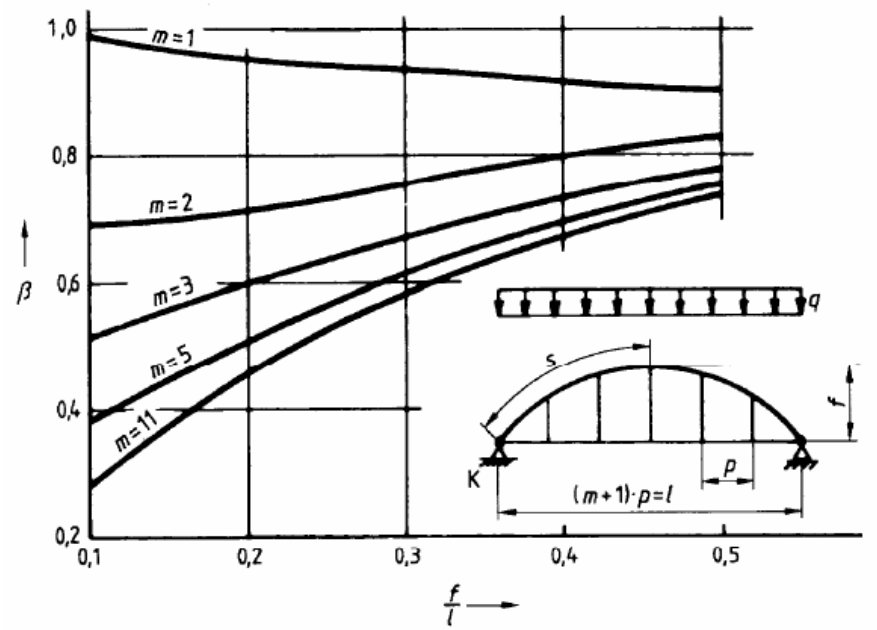

Figure 7.5: Buckling length factor β of arches with a tension tie and hangers

Σχήμα 7.5: Συντελεστής λυγισμού β τόξου με ελκυστήρα και αναρτήρες

The critical force estimated by this procedure approaches the results of the buckling analysis. Thus, for the check of the arches the critical force in the arches will be considered equal to N_{cr}=36073kN. The non-dimensional slenderness is calculated as:

$$\bar{\lambda} = \sqrt{\frac{Af_y}{N_{cr}}} = \sqrt{\frac{458.67cm^2 \cdot 35.5kN/cm^2}{36073kN}} = 0.67$$

The reduction factor χ for buckling curve c (cold formed hollow sections) is equal to χ=0.742 and the design buckling resistance of the arches is:

$$N_{b,Rd} = \frac{\chi A f_y}{\gamma_{M1}} = \frac{0.74 \cdot 458.67cm^2 \cdot 35.5kN/cm^2}{1.1} = 10953.87kN$$

Since circular hollow sections are not susceptible to lateral torsional buckling, χ_{LT}=1.00. Considering also conservatively $k_{yy}=k_{yz}$=1.0, all elements of the arches should satisfy:

$$EF = \frac{N_{Ed}}{N_{b,Rd}} + \frac{M_{y,Ed} + M_{z,Ed}}{M_{b,Rd}} \le 1.00$$

where

$$M_{b,Rd} = \frac{W_{pl} f_y}{\gamma_{M1}} = \frac{10660.67 cm^3 \cdot 35.5 kN/cm^2}{1.1} = 344049 kNcm$$

The maximum compression force and the maximum bending moment $M_{Ed,y}$ are observed for Load Combination 1100. Figure 7.6 illustrates the diagrams of the maximum axial force and the corresponding bending moments, while in Figure 7.7 the maximum bending moment $M_{Ed,y}$ and the corresponding axial force and bending moment $M_{Ed,z}$ are plotted. Similarly, the diagrams of internal forces for the combination with the maximum bending moment $M_{Ed,z}$ is shown in Figure 7.8. The maximum exploitation factor for the arches is EF=0.82<1.00.

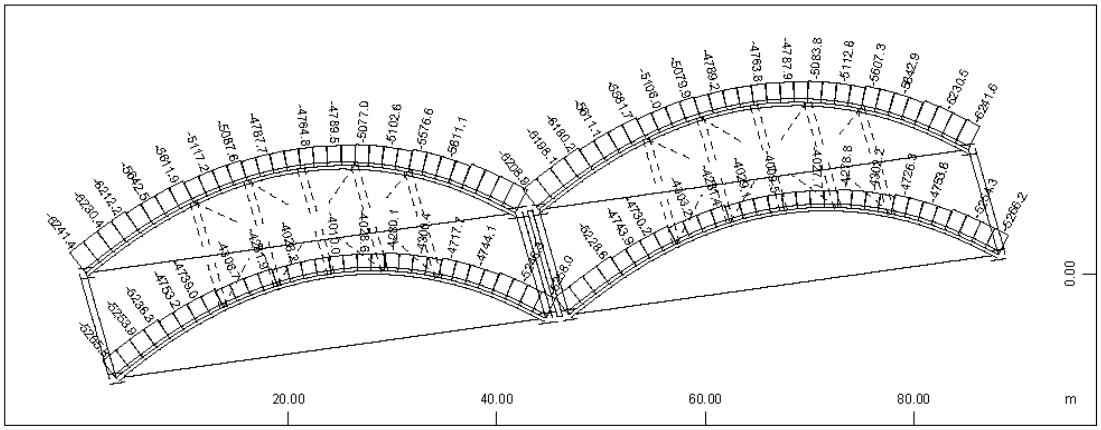

Sector of system Group 3 10...12
Normal force of beam, Loadcase 1112 MIN-N BEAM, 1 cm 3D = 15000. kN (Min=-6242.) (Max=-4009.)

M 1 : 602
X * 0.990
Y * 0.714
Z * 0.714

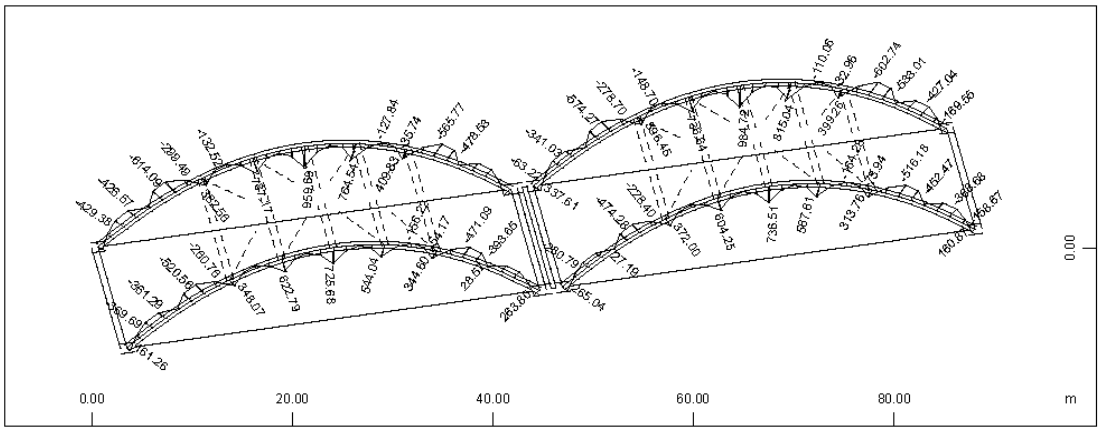

Sector of system Group 3 10...12
Bending moment My of beam, Loadcase 1112 MIN-N BEAM, 1 cm 3D = 2000. kNm (Min=-614.1)
(Max=984.7)

M 1 : 626
X * 0.990
Y * 0.714
Z * 0.714

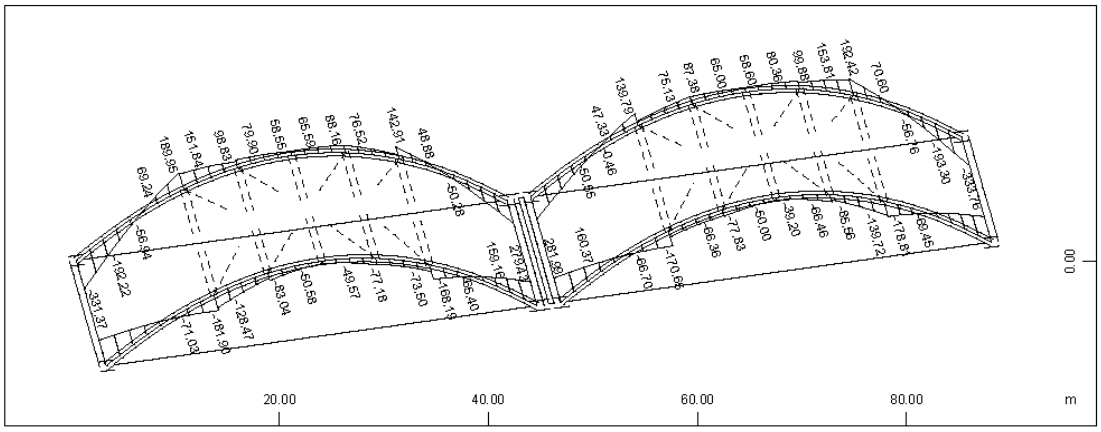

Sector of system Group 3 10...12
Bending moment Mz of beam, Loadcase 1112 MIN-N BEAM, 1 cm 3D = 500.0 kNm (Min=-333.8)
(Max=298.7)

M 1 : 600
X * 0.990
Y * 0.714

Scale reduced (0.9

Figure 7.6: Internal forces for the load combination with the maximum axial force at the arches

Σχήμα 7.6: Εντατικά μεγέθη για τον συνδυασμό φορτίσεων με τη μέγιστη αξονική δύναμη στα τόξα

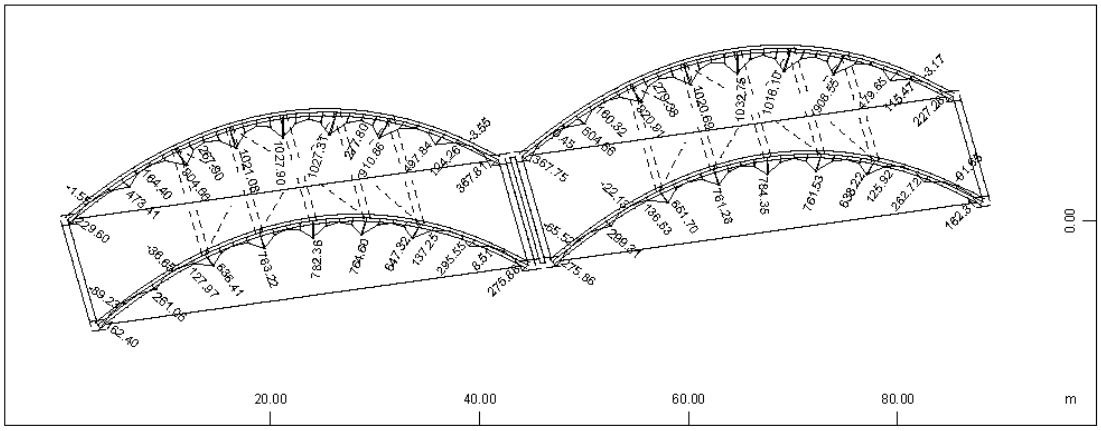

Sector of system Group 3 10...12
Bending moment My of beam, Loadcase 1101 MAX-MY BEAM, 1 cm 3D = 2000. kNm (Min=-91.7)
(Max=1033.)

M 1 : 600
X * 0.990
Y * 0.714
Z * 0.714

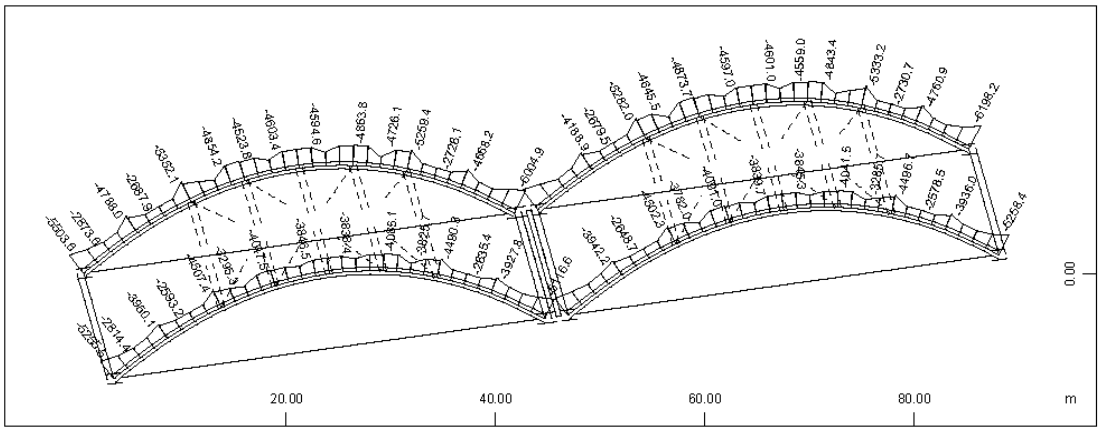

Sector of system Group 3 10...12
Normal force of beam, Loadcase 1101 MAX-MY BEAM, 1 cm 3D = 15000. kN (Min=-6198.) (Max=-2377.)

M 1 : 600
X * 0.990
Y * 0.714
Z * 0.714

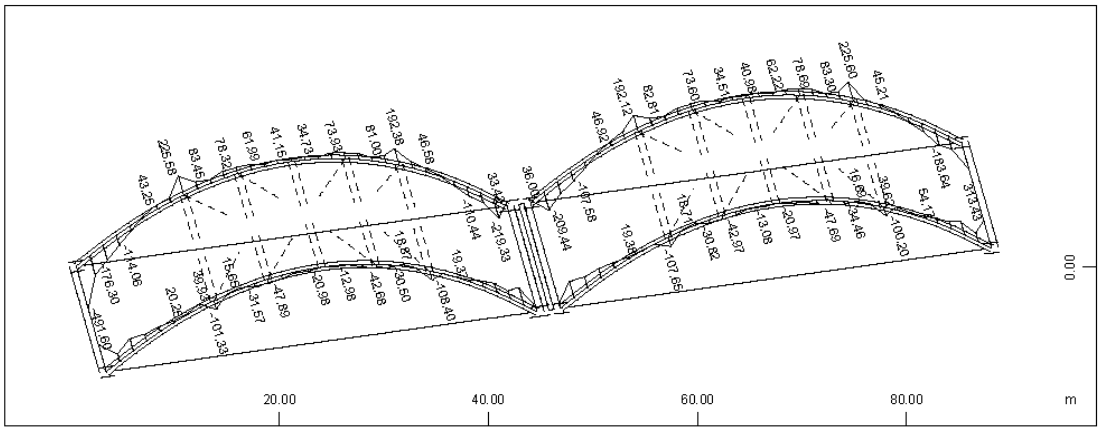

Sector of system Group 3 10...12
Bending moment Mz of beam, Loadcase 1101 MAX-MY BEAM, 1 cm 3D = 500.0 kNm (Min=-491.6)
(Max=316.6)

M 1 : 600
X * 0.990
Y * 0.714

Scale reduced (0.9

Figure 7.7: Internal forces for the load combination with the maximum bending moment $M_{Ed,y}$ at the arches

Σχήμα 7.7: Εντατικά μεγέθη για τον συνδυασμό φορτίσεων με τη μέγιστη καμπτική ροπή $M_{Ed,y}$ στα τόξα

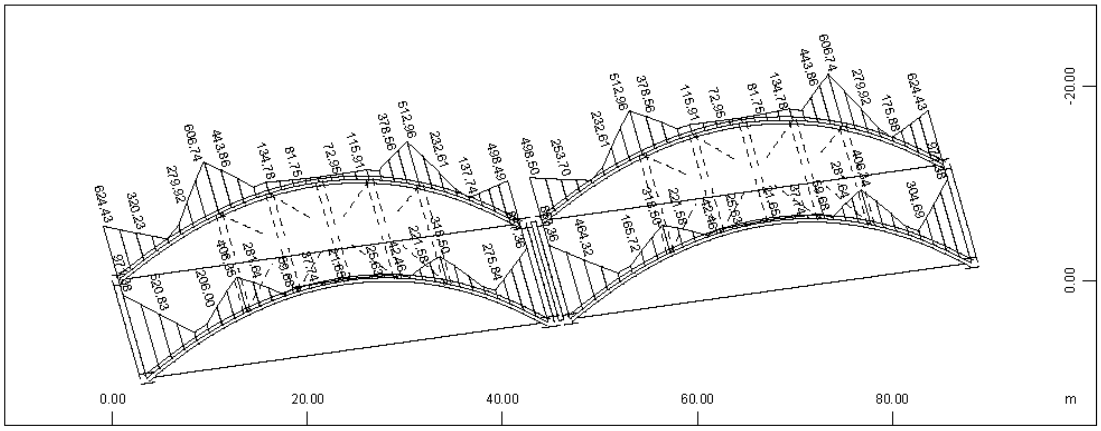

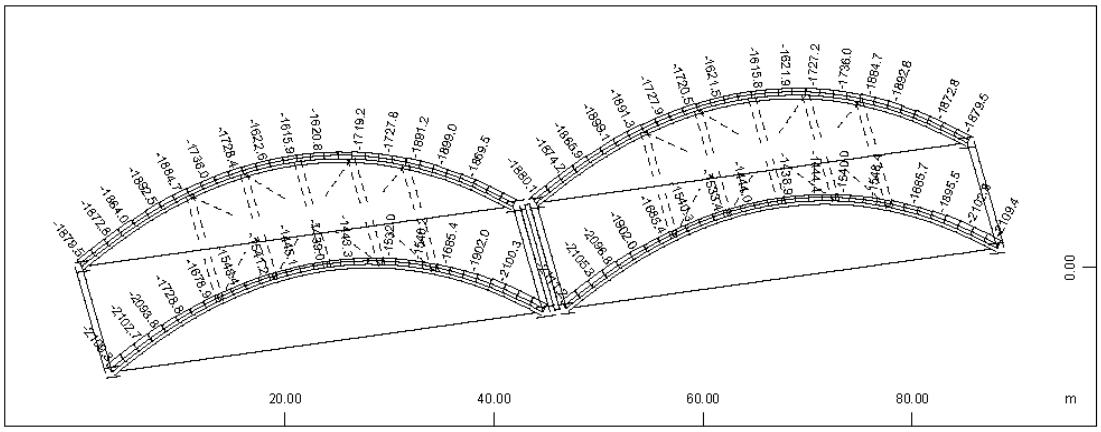

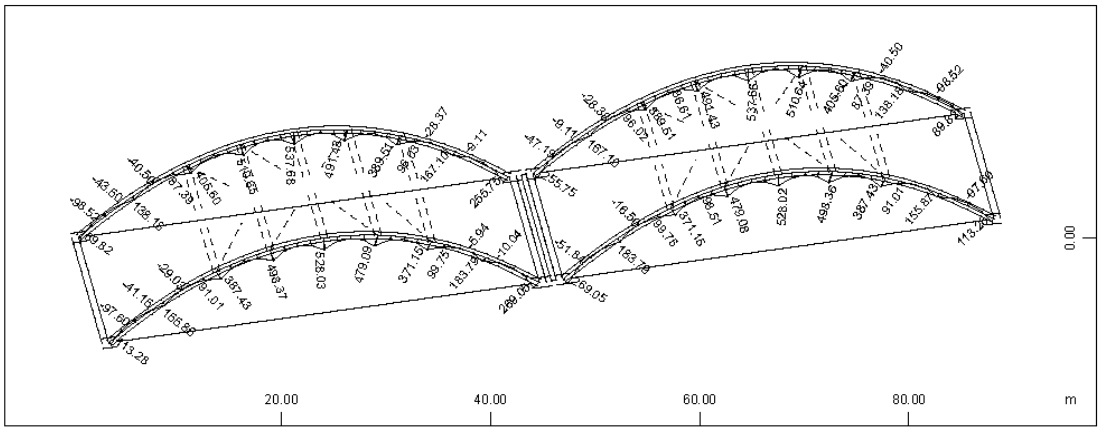

Figure 7.8: Internal forces for the load combination with the maximum bending moment $M_{Ed,z}$ at the arches

Σχήμα 7.8: Εντατικά μεγέθη για τον συνδυασμό φορτίσεων με τη μέγιστη καμπτική ροπή $M_{Ed,z}$ στα τόξα

7.3 Transverse bracing members

The non-dimensional slenderness for the transverse bracing members is calculated as:

$$\bar{\lambda} = \frac{L}{\pi}\sqrt{\frac{Af_y}{EI}} = \frac{1470cm}{\pi}\sqrt{\frac{59.44cm^2 \cdot 35.5kN/cm^2}{21000kN/cm^2 \cdot 4160cm^4}} = 2.30$$

and the reduction factor χ for buckling curve c is χ=0.15. Thus, the design buckling resistance of the transverse bracing members is:

$$N_{b,Rd} = \frac{\chi A f_y}{\gamma_{M1}} = \frac{0.15 \cdot 59.44cm^2 \cdot 35.5kN/cm^2}{1.1} = 287.74kN$$

The maximum compression force at the transverse bracing members is developed for the Load Combination 1100 and it is equal to N_{Ed}=125.9kN<$N_{b,Rd}$. For this combination the bending moment is negligible (Figure 7.9). The maximum bending moment appears for the seismic Load Combination 4100. For this combination, the internal forces are N_{Ed}=42.3kN (compressive force), $M_{y,Ed}$=31.8kNm, $M_{z,Ed}$=12.90kNm (Figure 7.10). Since the following criterion is satisfied:

N_{Ed}=42.3kN<0.25 × $N_{pl,Rd}$=0.25 × 2110.12kN=527.53kN

where

$N_{pl,Rd}=Af_y$=59.44cm^2 × 35.5kN/cm^2=2110.12kN

no effect of the axial force is taken into account. Hence:

$$\left[\frac{M_{y,Ed}}{M_{Rd}}\right]^2 + \left[\frac{M_{z,Ed}}{M_{Rd}}\right]^2 = \left[\frac{3180kNcm}{14446.24kNcm}\right]^2 + \left[\frac{1290kNcm}{14446.24kNcm}\right]^2 = 0.06 < 1.00$$

where

$$M_{Rd} = \frac{W_{pl} f_y}{\gamma_{M1}} = \frac{447.63cm^3 \cdot 35.5kN/cm^2}{1.1} = 14446.24kNcm$$

Since circular hollow sections are not susceptible to lateral torsional buckling, χ_{LT}=1.00. Considering also conservatively $k_{yy}=k_{yz}$=1.0, the transverse bracing members should satisfy:

$$EF = \frac{N_{Ed}}{N_{b,Rd}} + \frac{M_{y,Ed} + M_{z,Ed}}{M_{b,Rd}} \le 1.00 \Rightarrow EF = \frac{42.30kN}{287.74kN} + \frac{3180kNcm + 1290kNcm}{14446.24kNcm} = 0.46 < 1.00$$

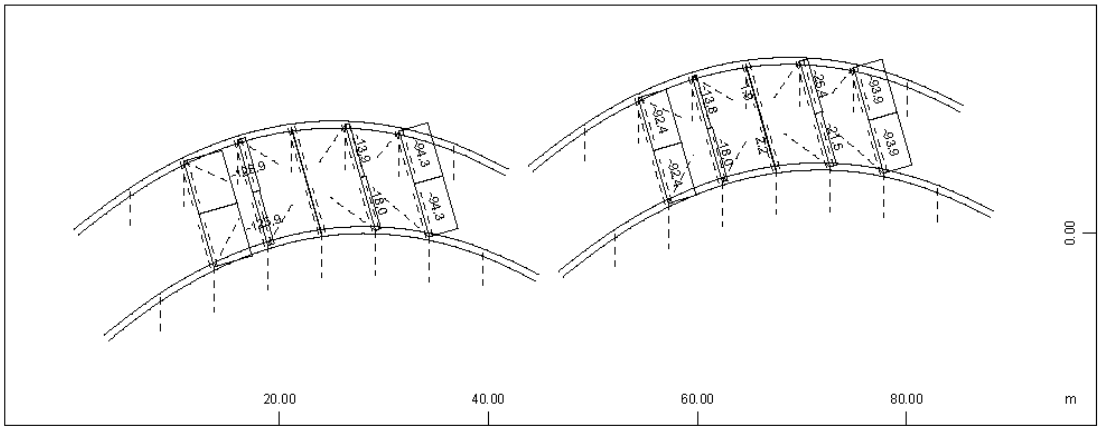

Sector of system Beam Group 3
Structure
Normal force of beam, Loadcase 1162 MIN-N BEAM, 1 cm 3D = 200.0 kN (Min=-125.9) (Max=2.20)

M 1 : 600
X * 0.990
Y * 0.714
Z * 0.714

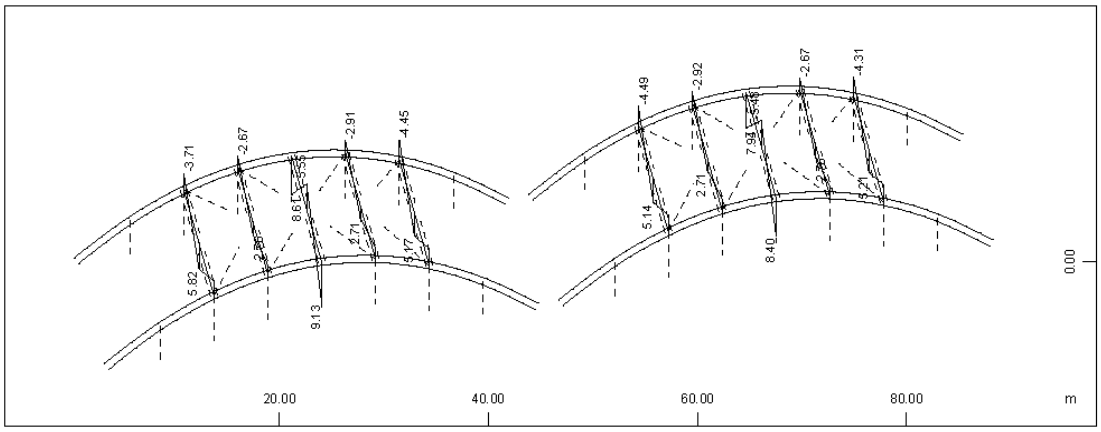

Sector of system Beam Group 3
Structure
Bending moment My of beam, Loadcase 1162 MIN-N BEAM, 1 cm 3D = 10.0 kNm (Min=-5.55) (Max=9.13)

M 1 : 600
X * 0.990
Y * 0.714
Z * 0.714

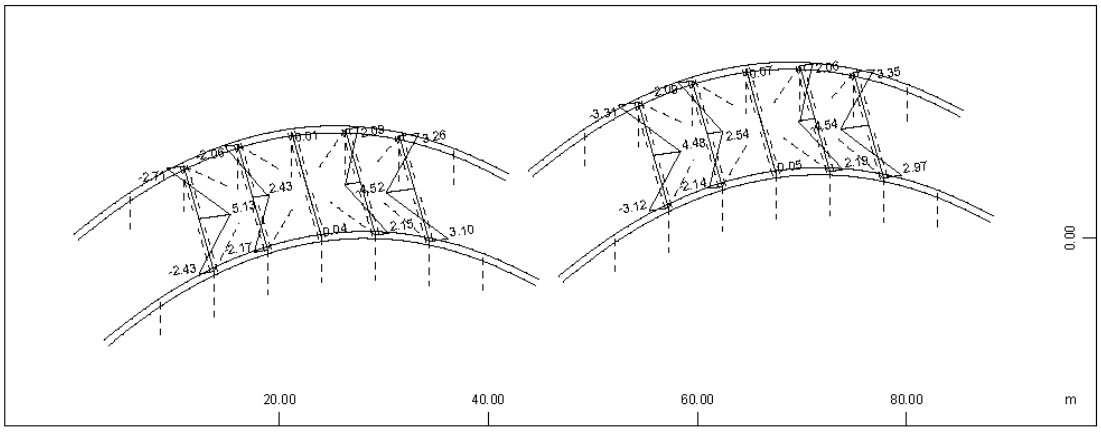

Sector of system Beam Group 3
Structure
Bending moment Mz of beam, Loadcase 1162 MIN-N BEAM, 1 cm 3D = 10.0 kNm (Min=-4.54) (Max=5.13)

M 1 : 600
X * 0.990
Y * 0.714

Scale reduced (0.9

Figure 7.9: Internal forces for the load combination with the maximum compressive force at the transverse bracing members

Σχήμα 7.9: Εντατικά μεγέθη για τον συνδυασμό φορτίσεων με τη μέγιστη θλιπτική δύναμη στα εγκάρσια μέλη των συνδέσμων δυσκαμψίας

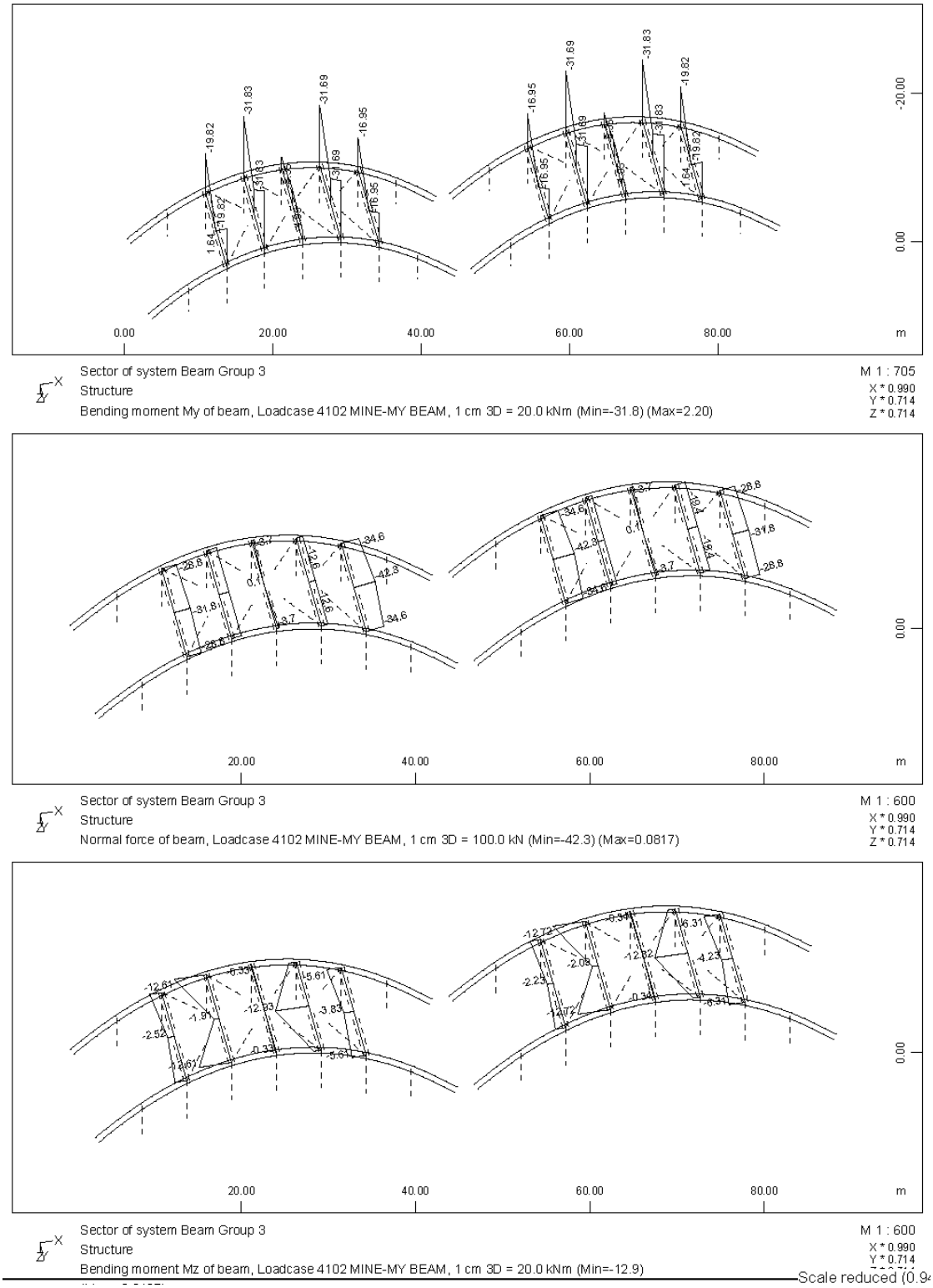

Figure 7.10: Internal forces for the load combination with the maximum bending moment at the transverse bracing members

Σχήμα 7.10: Εντατικά μεγέθη για τον συνδυασμό φορτίσεων με τη μέγιστη καμπτική ροπή στα εγκάρσια μέλη των συνδέσμων δυσκαμψίας

7.4 Diagonal bracing members

The non-dimensional slenderness for the diagonal bracing members is calculated as:

$$\bar{\lambda} = \frac{L}{\pi}\sqrt{\frac{Af_y}{EI}} = \frac{913cm}{\pi}\sqrt{\frac{33.10cm^2 \cdot 35.5kN/cm^2}{21000kN/cm^2 \cdot 720.3cm^4}} = 2.56$$

and the reduction factor χ for buckling curve c is χ=0.13. Thus, the design buckling resistance of the diagonal bracing members is:

$$N_{b,Rd} = \frac{\chi Af_y}{\gamma_{M1}} = \frac{0.13 \cdot 33.10cm^2 \cdot 35.5kN/cm^2}{1.1} = 138.87kN$$

The maximum compression force at the diagonal bracing members is developed for the seismic Load Combination 4000 and it is equal to N_{Ed}=137.2kN<$N_{b,Rd}$ (Figure 7.11).

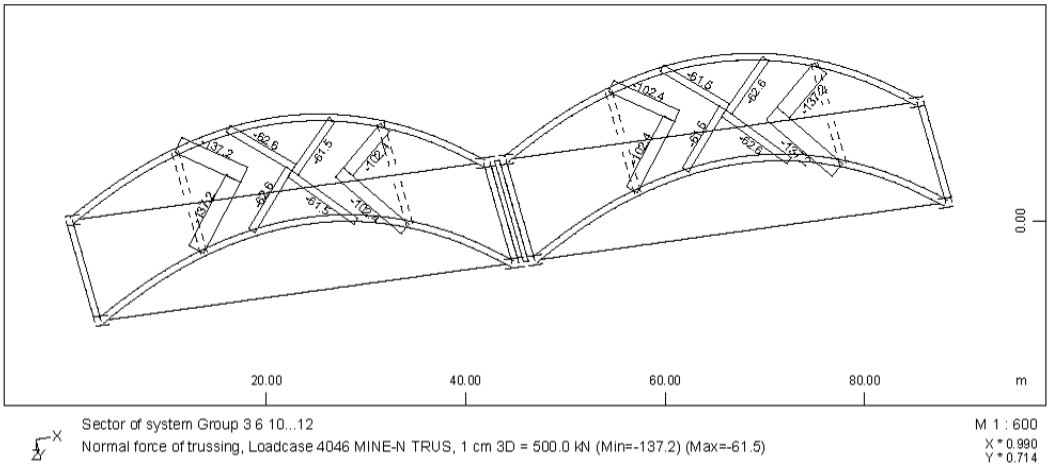

Figure 7.11: Maximum axial forces at the diagonal bracing members

Σχήμα 7.11: Μέγιστη αξονική δύναμη στα διαγώνια μέλη των συνδέσμων δυσκαμψίας

7.5 Hangers

The design tension resistance of the hangers is:

$$N_{t,Rd} = \frac{Af_y}{\gamma_{M0}} = \frac{40.29cm^2 \cdot 35.5kN/cm^2}{1.0} = 1430.30kN$$

The maximum tension force at the hangers is developed for Load Combination 1100 and it is equal to N_{Ed}=1211kN<$N_{t,Rd}$ (Figure 7.12).

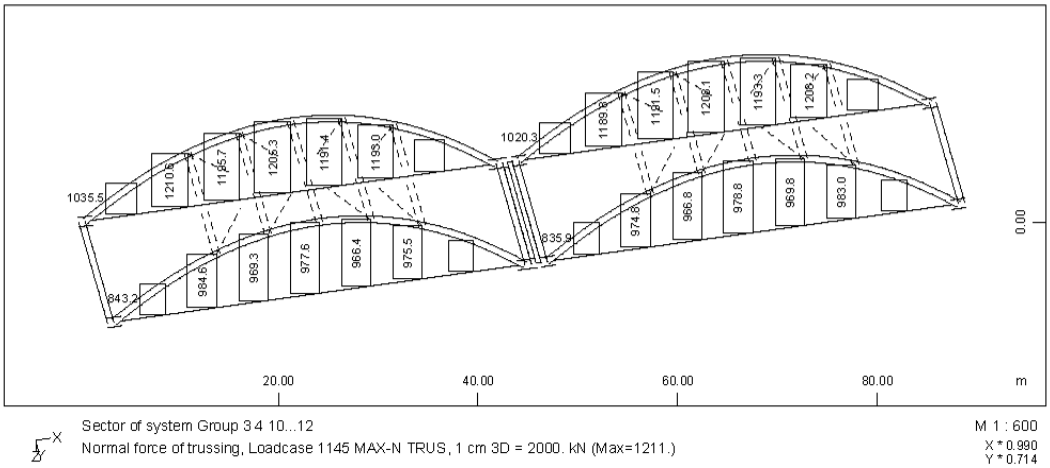

Figure 7.12: Maximum axial forces at the hangers

Σχήμα 7.12: Μέγιστη αξονική δύναμη στους αναρτήρες

7.6 Transverse Beams

During the pouring of the concrete slab the bending moment at the transverse beams due to its weight and the weight of the slab is M=521.90kNm. In Figure 7.13 the load of the slab applied on the transverse beams is illustrated and the bending moments of these beams due to self weight of the steel members and the slab are also shown. Taking into account a permanent load 0.75kN/m^2 and a variable load 0.75kN/m^2 during construction, the distributed load and the bending moment due to this load will be:

p=0.75 kN/m^2 × 2.625m=1.97kN/m

$$M = \frac{1.97\text{kN/m} \cdot (14.70\text{m})^2}{8} = 53.21\text{kNm}$$

and the design bending moment is:

M_{Ed}=1.35 × (52190kNcm+5321kNcm)+1.50 × 5321kNcm=85621.35kNcm

The critical lateral torsional buckling moment is:

$$M_{cr} = C_1 \frac{\pi^2 EI_z}{(kL_T)^2}\left\{\left[\left[\frac{k}{k_w}\right]^2 \frac{I_w}{I_z} + \frac{(kL_T)^2 GI_T}{\pi^2 EI_z} + (C_2 z_g - C_3 z_j)^2\right]^{0,5} - (C_2 z_g - C_3 z_j)\right\} \Rightarrow$$

$$M_{cr} = 1{,}132 \frac{\pi^2 \times 21000 \frac{\text{kN}}{\text{cm}^2} \times 15820\,\text{cm}^4}{(1{,}0 \times 1470\,\text{cm})^2} \times$$

$$\times \left\{\left[\left[\frac{1{,}0}{1{,}0}\right]^2 \frac{29460000\,\text{cm}^6}{15820\,\text{cm}^4} + \frac{(1{,}0 \times 1470\,\text{cm})^2 \times 8077 \frac{\text{kN}}{\text{cm}^2} \times 1137\,\text{cm}^4}{\pi^2 \times 21000 \frac{\text{kN}}{\text{cm}^2} \times 15820\,\text{cm}^4} + (0.459 \times 45\text{cm})^2\right]^{0,5} - (0.459 \times 45\text{cm})\right\} =$$

=121395.16kNcm

where z_a=90cm/2=45cm, z_s= z_j=0, z_g=z_a-z_s=45cm, k= k_w=1.00

$$G = \frac{E}{2(v+1)} = \frac{21000\,\text{kN/cm}^2}{2(0{,}3+1)} = 8077\text{kN/cm}^2$$

C_1=1.132, C_2 =0.459, C_3 =0.525, I_T=1137cm^4, I_z=15820cm^4, I_w =29460000cm^6, L_T=1470cm

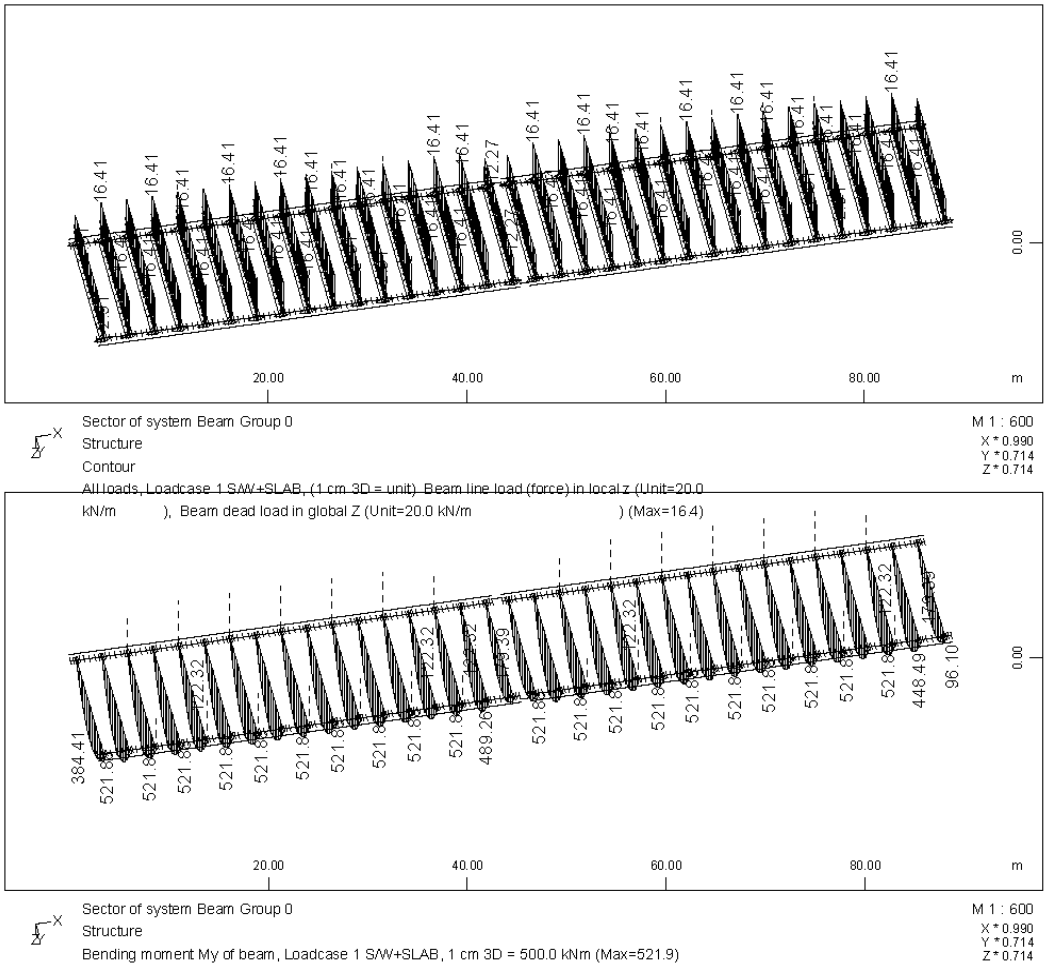

Figure 7.13: Load of the slab and bending moments at the transverse beams during construction

Σχήμα 7.13: Φορτίο καταστρώματος και καμπτικές ροπές εγκαρσίων διαδοκίδων κατά τη σκυροδέτηση

The non-dimensional slenderness for the transverse beams is calculated as:

$$\bar{\lambda}_{LT} = \sqrt{\frac{W_{pl,y} f_y}{M_{cr}}} = \sqrt{\frac{12580\,cm^3 \cdot 35.5kN/cm^2}{121395.16kNcm}} = 1.92$$

For h/b=90cm/30cm=3>2, the lateral torsional buckling curve is b, thus, χ_{LT}=0.225. The design buckling resistance moment of a laterally unrestrained beam is taken as:

$$M_{b,Rd} = \chi_{LT} \frac{W_{pl,y} f_y}{\gamma_{M1}} = 0.225 \cdot \frac{12580\,cm^3 \cdot 35.5kN/cm^2}{1.10} = 91347.95kNcm > M_{Ed}=85621.35kNcm$$

The maximum bending moment for the beams laterally restrained due to the concrete slab is calculated for Load Combination 1100 and it is equal to $M_{Ed,y}$=2032kNm. For the same combination the axial tensile force is N_{Ed}=2719kN, while the bending moment $M_{Ed,z}$ is negligible at the element with the maximum $M_{Ed,y}$ (Figure 7.14). The following criteria are satisfied:

N_{Ed}=2719kN<0.25 × $N_{pl,Rd}$=0.25 × 371.3cm² × 35.5kN/cm²=0.25 × 13181.15kN=3295.30kN

$$N_{Ed} = 2719kN < \frac{h_w t_w f_y}{\gamma_{M0}} = \frac{(90cm - 2 \cdot 3.5cm - 2 \cdot 3.0cm) \cdot 1.85cm \cdot 35.5kN/cm^2}{1.00} = 5056.98kN$$

thus, no effect of the axial force is taken into account. Hence, the design plastic moment resistance is:

$$M_{pl,y,Rd} = \frac{W_{pl,y} f_y}{\gamma_{M0}} = \frac{12580 cm^3 \cdot 35.5 kN/cm^2}{1.00} = 446590 kNcm > M_{Ed,y} = 203200 kNcm$$

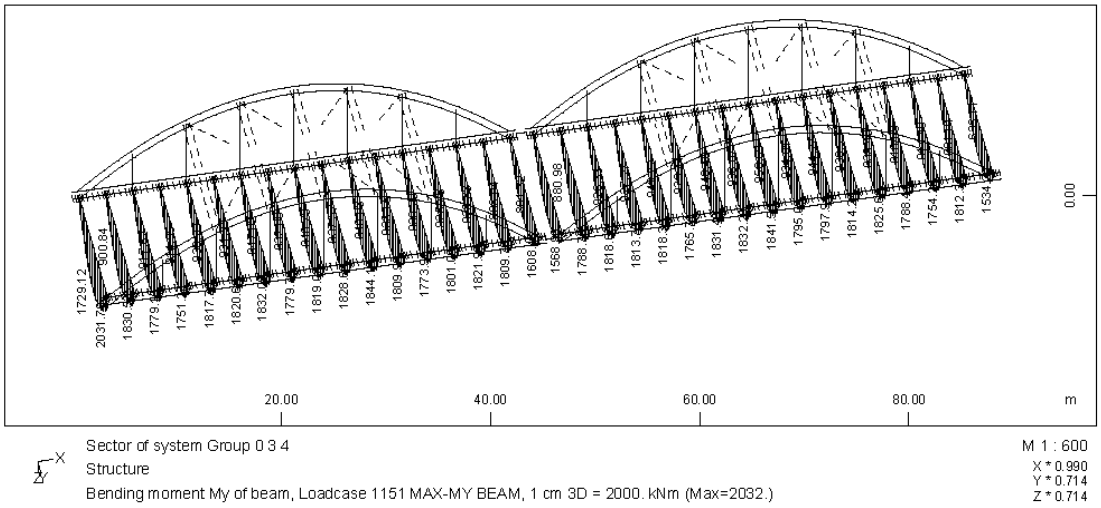

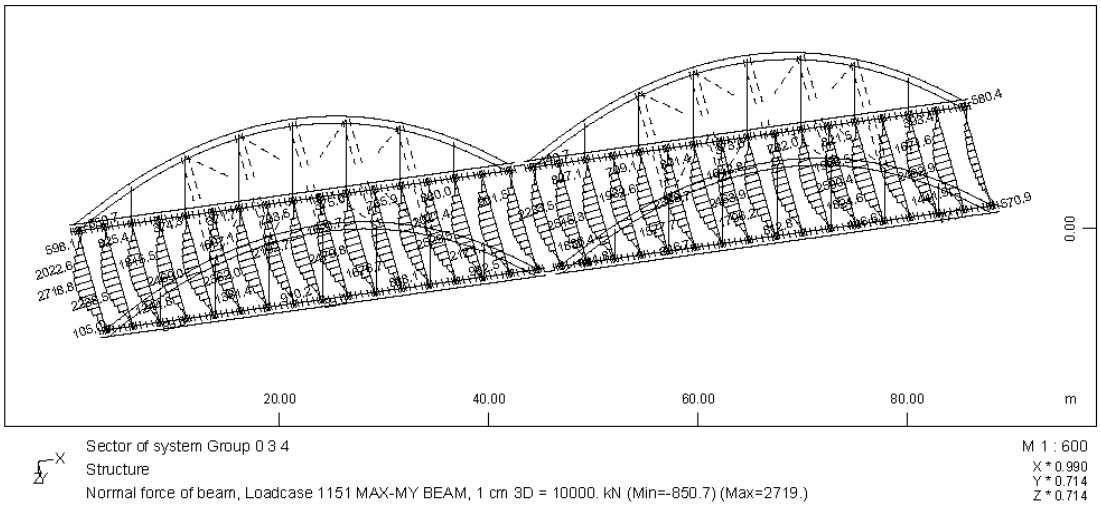

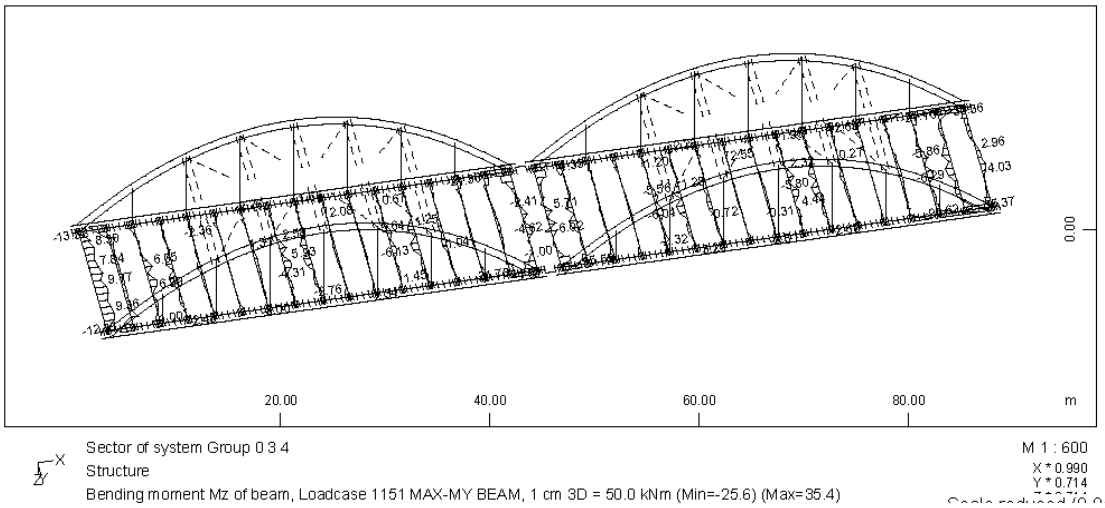

Figure 7.14: Internal forces for the load combination with the maximum bending moment at the transverse beams

Σχήμα 7.14: Εντατικά μεγέθη για τον συνδυασμό φορτίσεων με τη μέγιστη καμπτική ροπή στις διαδοκίδες

The maximum compressive axial force is computed also for Load Combination 4100, which is equal to N_{Ed}=1651kN. The maximum bending moment for the same Load Combination is $M_{Ed,y}$=676kNm, while the bending moment $M_{Ed,z}$ is negligible (Figure 7.15).

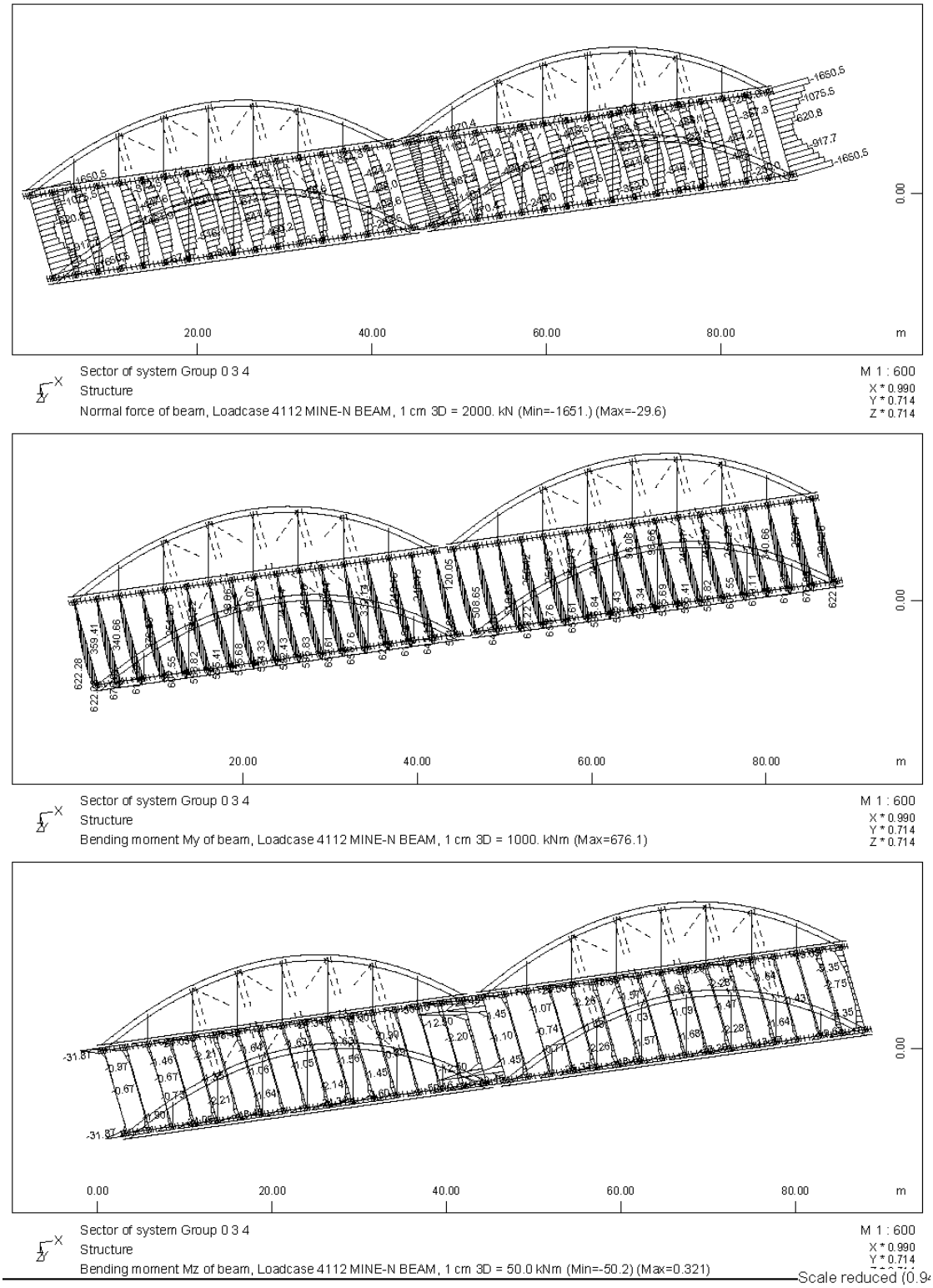

Figure 7.15: Internal forces for the load combination with the maximum compressive axial force at the transverse beams

Σχήμα 7.15: Εντατικά μεγέθη για τον συνδυασμό φορτίσεων με τη μέγιστη θλιπτική δύναμη στις διαδοκίδες

Neglecting, conservatively, the stiffness of the slab of the composite beam, the non-dimensional slenderness for the transverse beams is:

$$\bar{\lambda} = \frac{L}{\pi}\sqrt{\frac{Af_y}{EI}} = \frac{1470\text{cm}}{\pi}\sqrt{\frac{371.30\text{cm}^2 \cdot 35.5\text{kN/cm}^2}{21000\text{kN/cm}^2 \cdot 494100\text{cm}^4}} = 0.527$$

and the reduction factor χ for buckling curve b is χ=0.871. Since the slab protects the transverse beams from lateral torsional buckling, χ_{LT}=1.00. Thus, the exploitation factor for this load combination is:

$$EF = \frac{N_{Ed}}{N_{b,Rd}} + \frac{M_{y,Ed} + M_{z,Ed}}{M_{b,Rd}} = \frac{1651\text{kN}}{10437.07\text{kN}} + \frac{67600\text{kNcm}}{405990.91\text{kNcm}} = 0.32 < 1.00$$

where

$$N_{b,Rd} = \frac{\chi A f_y}{\gamma_{M1}} = \frac{0.871 \cdot 371.30\text{cm}^2 \cdot 35.5\text{kN/cm}^2}{1.1} = 10437.07\text{kN}$$

and

$$M_{b,Rd} = \frac{W_{pl,y} f_y}{\gamma_{M1}} = \frac{12580\text{cm}^3 \cdot 35.5\text{kN/cm}^2}{1.10} = 405990.91\text{kNcm}$$

7.7 Main Beams

During the pouring of the concrete slab the bending moment at the main beams due to its weight and the weight of the slab is M=779.90kNm, while the tensile axial force is 1223kN. The internal forces of the main beams during construction are illustrated in Figure 7.16. Since the following criteria are satisfied:

N_{Ed}=1223kN<0.25 × $N_{pl,Rd}$=3295.30kN

$$N_{Ed} = 1223\text{kN} < \frac{h_w t_w f_y}{\gamma_{M0}} = 5056.98\text{kN}$$

no effect of the axial force is taken into account for the cross section check. The design plastic moment resistance is:

$M_{Rd,y}$=446590kNcm>$M_{Ed,y}$=77990kNm

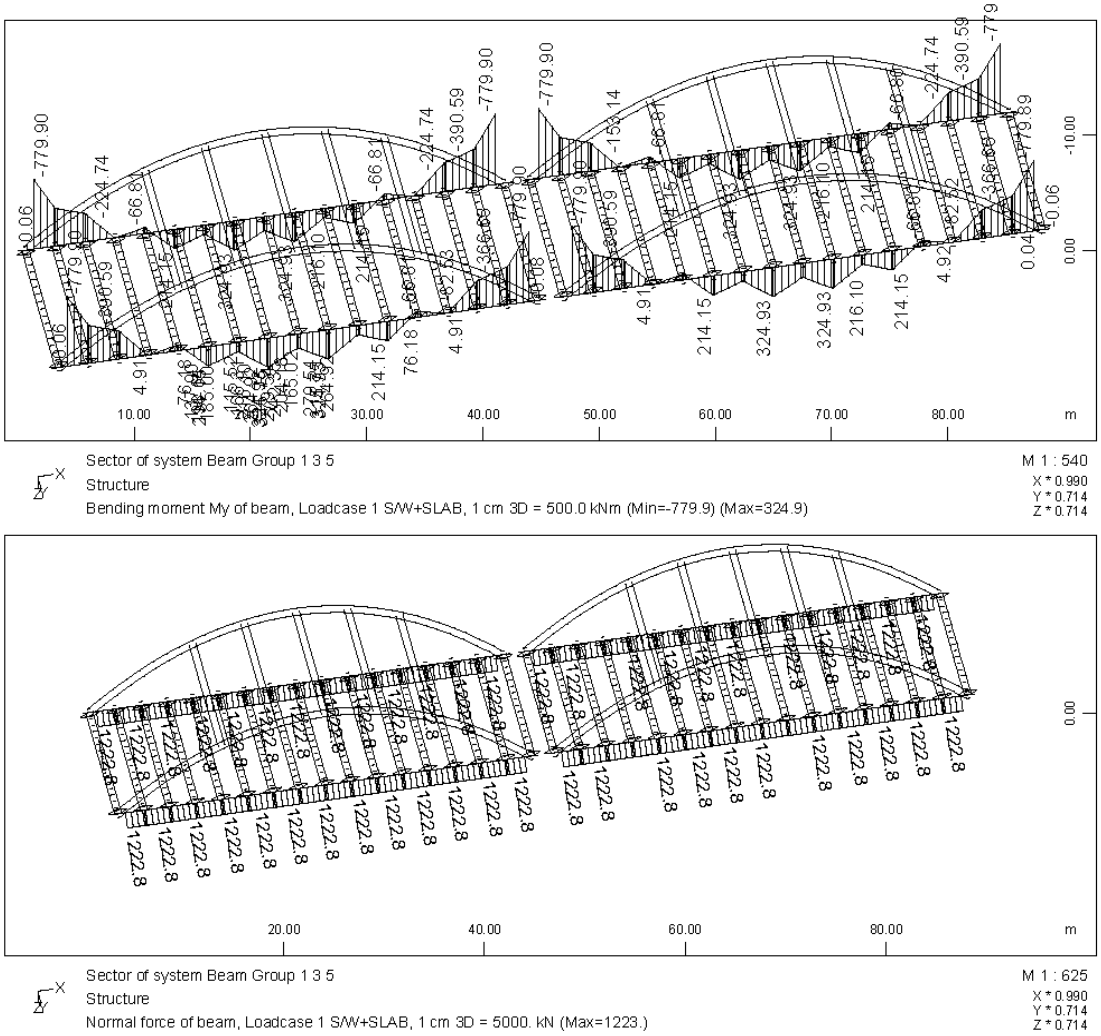

Figure 7.16: Bending moments and axial forces at the main beams during construction

Σχήμα 7.16: Καμπτικές ροπές και αξονικές δυνάμεις κυρίων δοκών κατά τη σκυροδέτηση

The maximum bending moment of the main beams is smaller than the one developed at the transverse beams. Additionally, combined with the axial force, the upper (point t) and bottom (point b) stresses of the main beams during construction are shown in Figure 7.17. The central part of the beams is entirely under tension, while only the parts close to their connections with the arches present compressive stresses at the bottom flange. The length of the main beams under partially compressive stresses is rather small, lying between the edge and the shortest hanger. Hence, no lateral buckling check of the main beams during construction is deemed necessary.

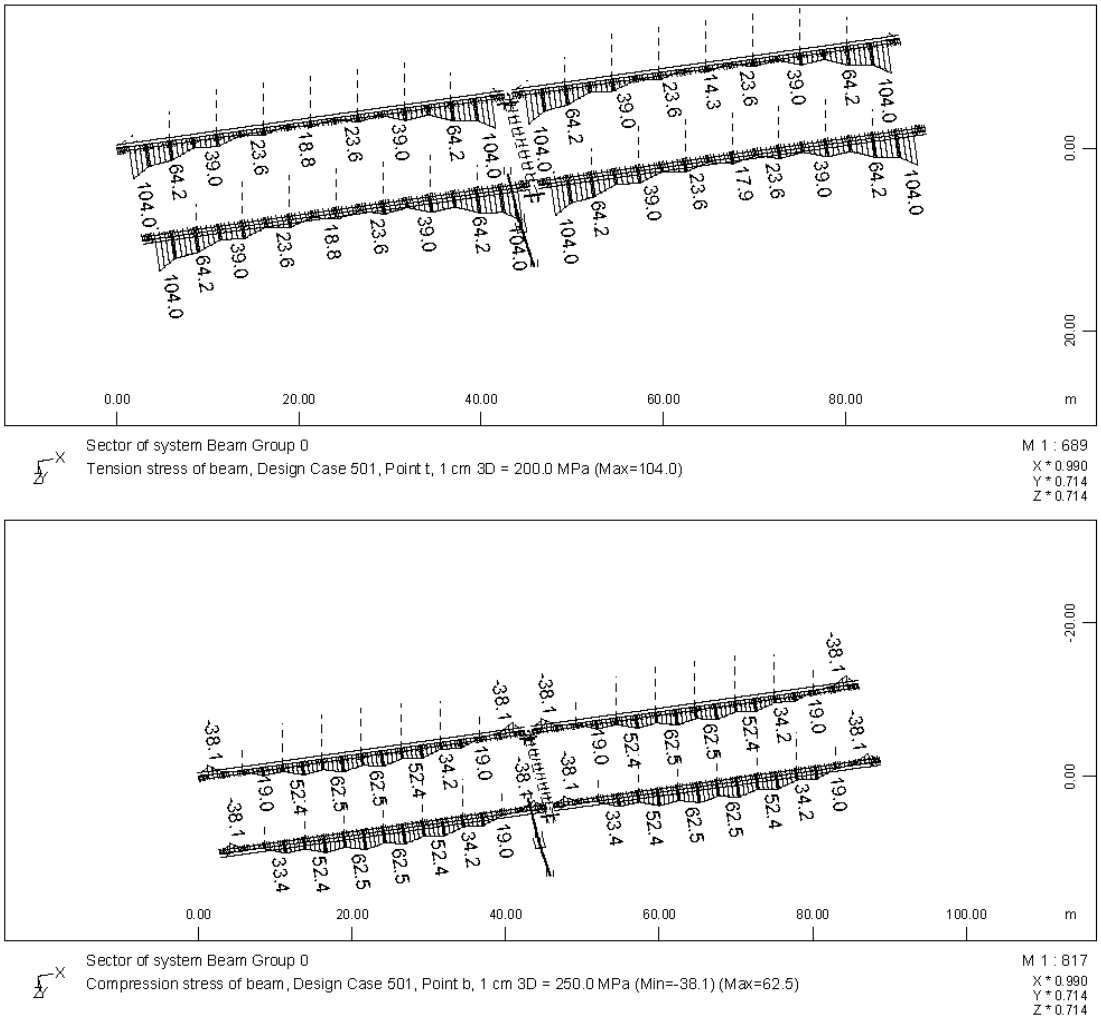

Figure 7.17: Upper and bottom stresses at the main beams during construction

Σχήμα 7.17: Τάσεις στην άνω και κάτω ίνα των κυρίων δοκών κατά τη σκυροδέτηση

The maximum tensile axial force for the main beams laterally restrained due to the concrete slab is calculated for Load Combination 1100 and it is equal to N_{Ed}=5239kN. For the same combination the bending moment is $M_{Ed,y}$=1797kNm, while the bending moment $M_{Ed,z}$ is negligible at the element with the maximum $M_{Ed,y}$ (Figure 7.18). Since the following criteria are not satisfied:

N_{Ed}=5239kN>0.25 × $N_{pl,Rd}$=3295.30kN

$$N_{Ed} = 5239\text{kN} > \frac{h_w t_w f_y}{\gamma_{M0}} = 5056.98\text{kN}$$

the effect of the axial force must be taken into account. Hence, the reduced design plastic moment resistance due to the axial force is:

$$M_{N,y,Rd} = M_{pl,y,Rd}\frac{1-n}{1-0.5\cdot a} = 446590\text{kNcm}\frac{1-0.40}{1-0.5\cdot 0.43} = 341342.68\text{kNcm} > M_{Ed,y} = 179700\text{kNcm}$$

where $n=N_{Ed}/N_{pl,Rd}$=5239kN/13181.15kN=0.40 and

$$a = \frac{A-2bt_f}{A} = \frac{371.3\text{cm}^2 - 2\cdot 30\text{cm}\cdot 3.5\text{cm}}{371.3\text{cm}^2} = 0.43 < 0.50$$

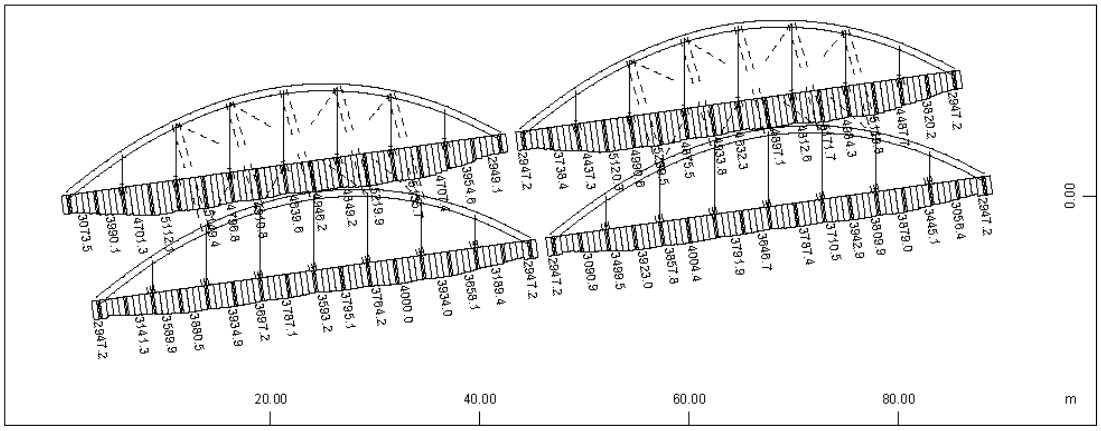

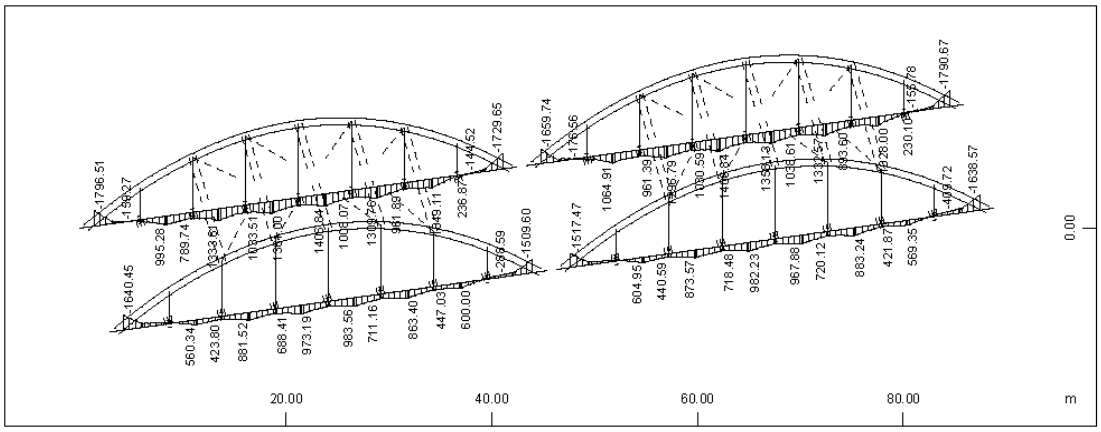

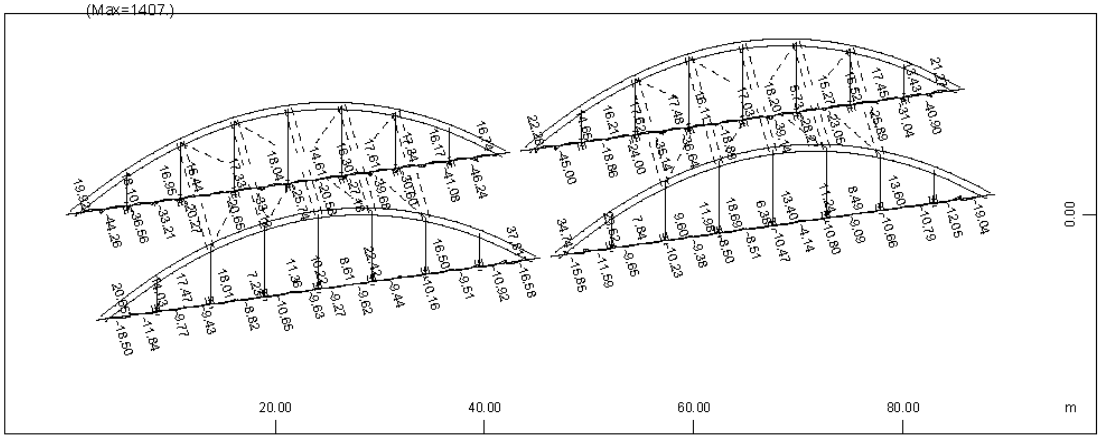

Figure 7.18: Internal forces for the load combination with the maximum tensile axial force at the main beams

Σχήμα 7.18: Εντατικά μεγέθη για τον συνδυασμό φορτίσεων με τη μέγιστη εφελκυστική αξονική δύναμη στις κύριες δοκούς

The maximum compressive axial force for the main beams laterally restrained is equal to N_{Ed}=1481kN under the seismic Load Combination 4100 (neglecting the parts of the beams outside the arches), as shown in Figure 7.19. For the same combination the maximum bending moment is $M_{Ed,y}$=1580kNm, while $M_{Ed,z}$ is negligible.

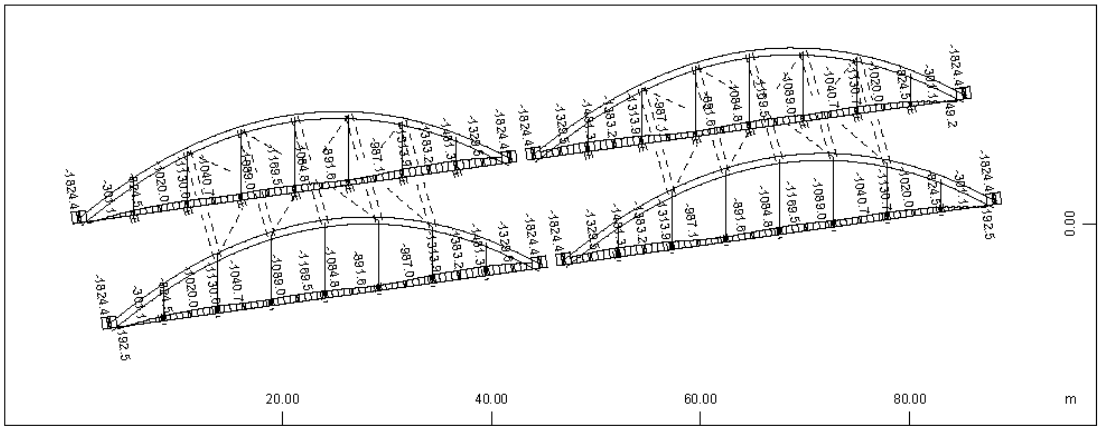

Sector of system Group 3 4
Structure
Normal force of beam, Loadcase 4112 MINE-N BEAM, 1 cm 3D = 10000. kN (Min=-1824.) (Max=192.5)

M 1 : 600
X * 0.990
Y * 0.714
Z * 0.714

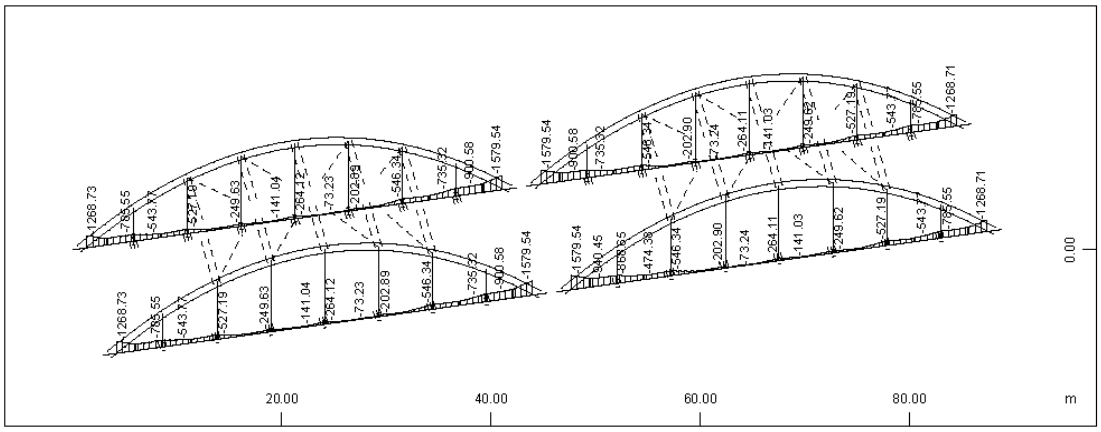

Sector of system Group 3 4
Structure
Bending moment My of beam, Loadcase 4112 MINE-N BEAM, 1 cm 3D = 5000. kNm (Min=-1580.)
(Max=-0.0055)

M 1 : 600
X * 0.990
Y * 0.714
Z * 0.714

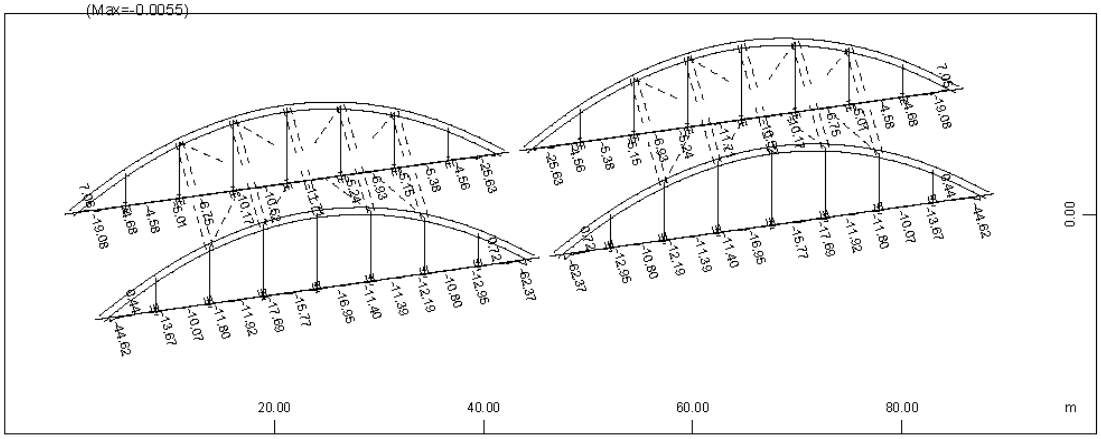

Sector of system Group 3 4
Structure
Bending moment Mz of beam, Loadcase 4112 MINE-N BEAM, 1 cm 3D = 500.0 kNm (Min=-62.4) (Max=7.06)

M 1 : 600
X * 0.990
Y * 0.714

Scale reduced (0.9

Figure 7.19: Internal forces for the load combination with the maximum compressive axial force at the main beams

Σχήμα 7.19: Εντατικά μεγέθη για τον συνδυασμό φορτίσεων με τη μέγιστη θλιπτική δύναμη στις κύριες δοκούς

In order to find the critical force N_{cr} for buckling of the main beams about their strong axis, ignoring conservatively the presence of the slab, the model of Figure 7.20 is used. The one end of the main beam is considered as pinned, while the other as roller. For a concentrated horizontal load equal to 1000kN, applied at the roller, the normal force of the main beam is

presented in Figure 7.21. The mean value of the normal force along the arch is N=966kN. The first in plane buckling mode of the beam is shown in Figure 7.22 with buckling factor equal to 35.35. Thus, the critical force of force N_{cr} in the main beams for in plane buckling is N_{cr}=35.35 × 966kN = 34148.10kN. The out of plane buckling is not taken into account, since the main beams are laterally restrained by the slab.

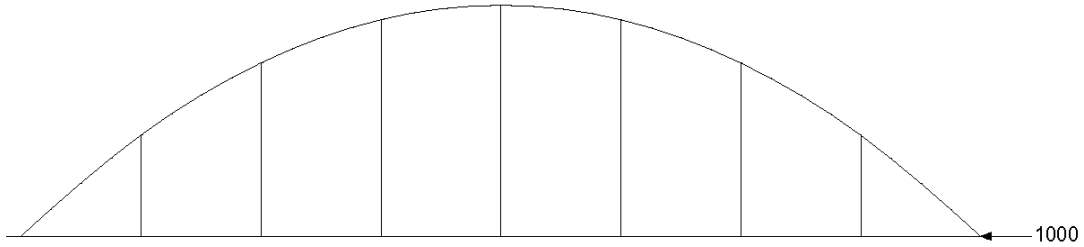

Figure 7.20: Model and load for buckling analysis of the main beams
Σχήμα 7.20: Προσομοίωμα και φορτίο για ανάλυση λυγισμού των κυρίων δοκών

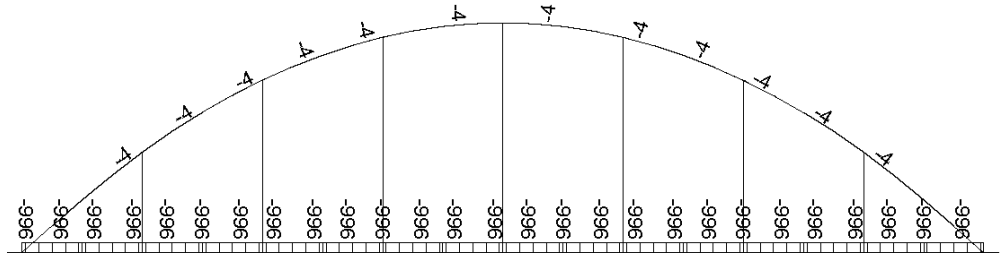

Figure 7.21: Normal force of the main beam due to concentrated horizontal load at its end
Σχήμα 7.21: Αξονική δύναμη κύριας δοκού λόγω συγκεντρωμένου οριζόντιου φορτίου στο άκρο της

Figure 7.22: The first in plane buckling mode of the main beam
Σχήμα 7.22: Η πρώτη εντός επιπέδου μορφή λυγισμού της κύριας δοκού

The non-dimensional slenderness is calculated as:

$$\bar{\lambda} = \sqrt{\frac{Af_y}{N_{cr}}} = \sqrt{\frac{371.3cm^2 \cdot 35.5kN/cm^2}{34148.10kN}} = 0.62$$

The reduction factor χ for buckling curve b is equal to χ=0.827 and the design buckling resistance of the main beams is:

$$N_{b,Rd} = \frac{\chi Af_y}{\gamma_{M1}} = \frac{0.827 \cdot 371.3cm^2 \cdot 35.5kN/cm^2}{1.1} = 9909.83kN$$

According to the second method, presented in EC3 – Part 1.1, the interaction factor k_{yy} is given as:

$$k_{yy} = C_{my}\left(1 + (\bar{\lambda}_y - 0.2)\frac{N_{Ed}}{\chi_y N_{Rd} / \gamma_{M1}}\right) = 0.4 \cdot \left(1 + (0.62 - 0.2)\frac{1481\text{kN}}{9909.83\text{kN}}\right) = 0.43$$

Since the slab protects the main beams from lateral torsional buckling, χ_{LT}=1.00. Thus, the exploitation factor for this load combination is:

$$EF = \frac{N_{Ed}}{N_{b,Rd}} + \frac{k_{yy} M_{y,Ed}}{M_{b,Rd}} = \frac{1481\text{kN}}{9909.83\text{kN}} + \frac{0.43 \cdot 158000\text{kNcm}}{1.00 \cdot \frac{446590\text{kNcm}}{1.1}} = 0.32 < 1.00$$

For reasons of constructability of the connection of the transverse beams on the main ones, the same profile is used for both groups of beams, although the exploitation factor of the main beams is much smaller than 1.

Chapter 8

PERFORMANCE AT SERVICEABILITY LIMIT STATE

8.1 Maximum compressive stress of the deck slab

As mentioned in section 5.5 for the characteristic load combination, the compressive stress of the concrete slab should not exceed the value of $0.60f_{ck}$=21MPa. The maximum compressive stress is obtained for load combination 1600 and it is equal to 17.3MPa (Figure 8.1).

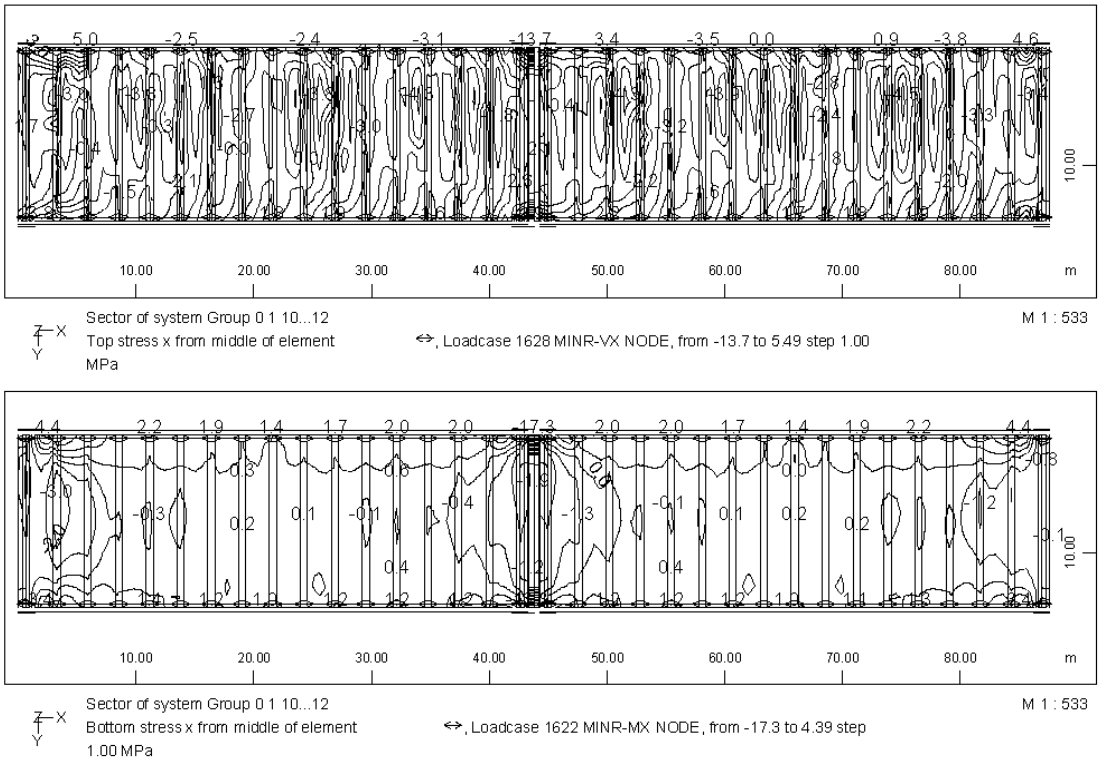

Figure 8.1: Maximum compressive stresses of the deck slab for SLS (characteristic) load combination

Σχήμα 8.1: Μέγιστη θλιπτική τάση στην πλάκα καταστρώματος για τους συνδυασμούς λειτουργικότητας (χαρακτηριστικός)

8.2 Maximum deformation of the deck

As mentioned in section 5.5 the deformation of the deck is calculated for the frequent load combination. In Figure 8.2 the maximum deflection of the main and transverse beams is illustrated, arising at 60.3mm for the main beams (60.3mm< L/300=42000/300=140mm) and 79.9mm-60.3mm=19.6mm for the transverse ones (19.6mm<L/300=14700mm/300=49mm).

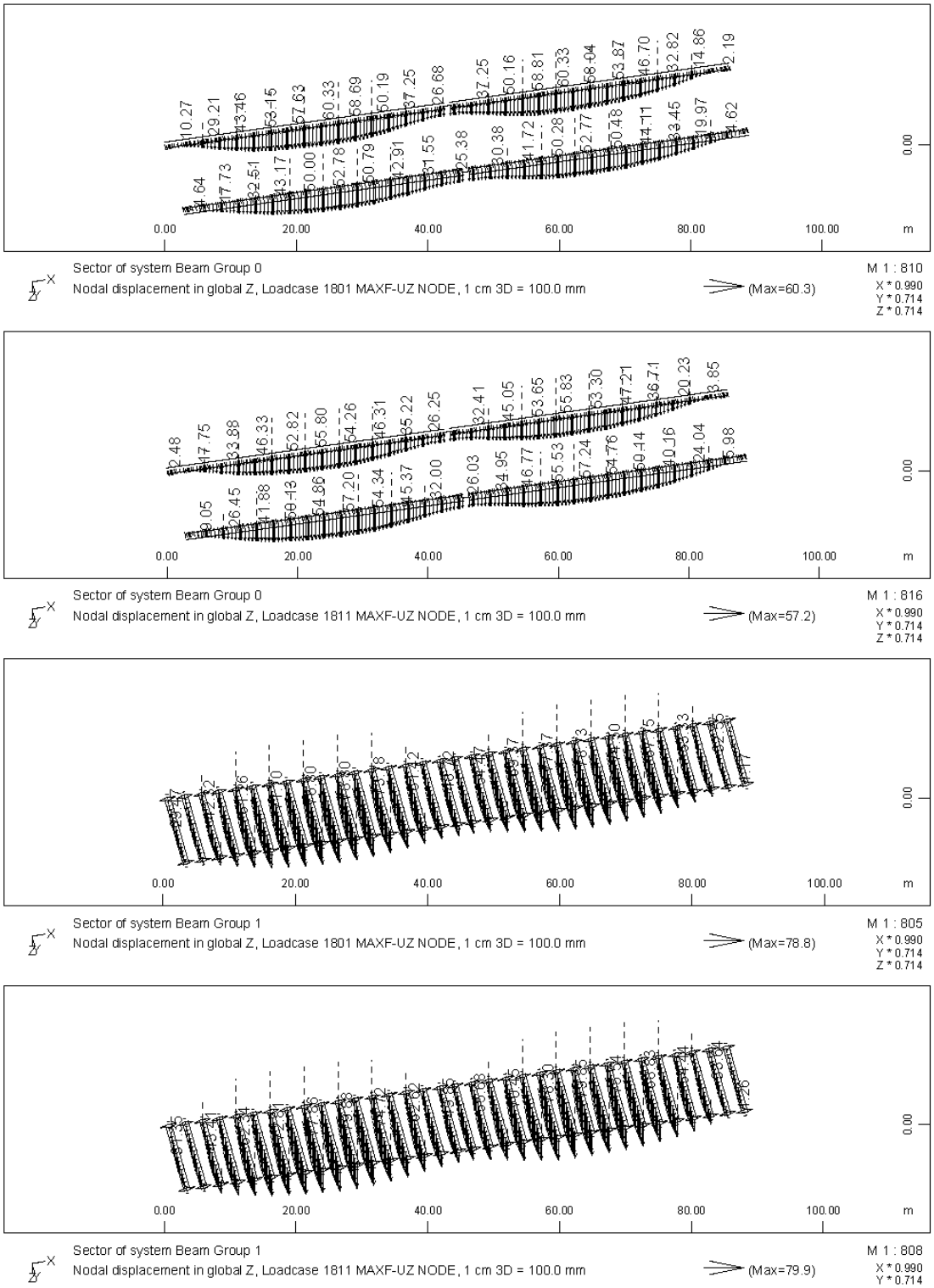

Figure 8.2: Deflection of the deck's beams for SLS (frequent) load combination

Σχήμα 8.2: Βέλος δοκών καταστρώματος για τους συνδυασμούς λειτουργικότητας (συχνός)

Chapter 9

CHECK OF BEARINGS AND EXPANSION JOINTS

9.1 Check of bearings

	parallel to axis:	x		y	
Dimensions:		70	x	80	cm^2
Number of elastomeric layers:				10	
Thickness of an indivicual elastomeric layer:				15	mm
Total thickness:				150	mm

Axial loads	most loaded bearing		
Permanent:	1347.00 kN		
Superimposed:	845.00 kN	: N_g =	2192.00 KN
Traffic load:	1430.70 kN	: N_p =	1430.70 KN
Earthquake z-z:	866.50 kN	$N_{max,st}$ =	3622.70 KN
	less loaded bearing		
Permanent:	1347.00 kN		
Superimposed:	845.00 kN	$N_{min,st}$ =	2192.00 KN
Earthquake z-z:	866.50 kN		

Displacements	
Braking load:	24.50 mm
Shrinkage:	4.00 mm
Uniform difference of temperature $\Delta T = -41^{\circ}C$:	18.00 mm
Earthquake x-x:	238.90 mm
Earthquake y-y:	209.80 mm

Rotations				
permanent:	α_x =	0.180 x 10^{-3} rad	α_y =	0.296 x 10^{-3} rad
superimposed:	α_x =	0.556 x 10^{-3} rad	α_y =	0.324 x 10^{-3} rad
traffic load:	α_x =	3.043 x 10^{-3} rad	α_y =	2.989 x 10^{-3} rad

A. Check for static combinations (according to DIN 4141 / Part 14)

Total displacement d_{td} = 46.50 mm

Shear strain		γ_{td} = 0.31	<	$\gamma_{\varepsilon n}$ = 0.69	OK
Design pressure	$\sigma_{max}=N_{o\vee}/A=$	6.47 MPa	<	15,00 MPa	
	$\sigma_{min}=N_g/A=$	3.91 MPa	<	5.00 MPa	ANCHORAGE IS REQUIRED
Angular rotation about x	$\varphi_{td,x}=$	0.0038 rad	<	$\varphi_{\varepsilon n}=n\times\varphi_{1,\varepsilon n}$ = 0.0150 rad	OK
Angular rotation about y	$\varphi_{td,y}=$	0.0036 rad	<	$\varphi_{\varepsilon n}=n\times\varphi_{1,\varepsilon n}$ = 0.0200 rad	OK

B. Check for seismic combinations (according to EC8-2)

Apparent conventional shear modulus:	G_g=	900 kPa			
Shear modulus:	G_b=	1125 kPa			
Lower bound design properties:	$G_{b,min}$=	1125 kPa			
Upper bound design properties:	$G_{b,max}$=	1350 kPa			
Displacement +x:	d_{Edx} =	251.9 mm			
Displacement +y:	d_{Edy} =	62.9 mm			
Total displacement	d_{Ed} =	259.6 mm			
Design shear strain due to horizontal displacement	$\varepsilon_{q,d}$=	1.73	<2.0		OK
	S =	12.44			
	A_r =	3333.18 cm^2			
	N_{sd} =	2738.09 kN			
	σ_e =	8214.65 kPa			
Design strain due to compressive load	$\varepsilon_{c,d}$ =	0.88			
Design strain due to design angular rotation	$\varepsilon_{a,d}$ =	0.32			
Maximum design strain	$\varepsilon_{t,d}$ =	2.93	<$\varepsilon_{u,k}$ /γ_m=	7.00	OK

C. Stability

One of the following criteria should be satisfied:

$b_{min}>4\Sigma t_i$	=>	70 cm	>	60 cm	OK
$\sigma_e<2b_{min}G_{b,min}S/3\Sigma t_i$	=>	8214.65 kPa	<	43555.56 kPa	OK

D. Anchorage

Minimum vertical design force:	N_{Ed} =	1932.05 KN		
Minimum design pressure:	σ_e =	5.80 N/mm^2	>3,00	
Stiffness:	K = $G_{b,max}$ x A / T =	5040.0 KN/m		
Maximum shear force:	V_{Ed} = K d_{Ed} =	1308.61 KN		
	V_{Ed} / N_{Ed} =	0.677		
	α =	0.100		
	β =	0.300		
	μ_e= $\alpha + \beta/\sigma_e$ =	0.152		

Check: V_{Ed} / N_{Ed} > $\alpha + \beta/\sigma_e$ ANCHORAGE IS REQUIRED

E. Uplift of the bearings

The minimum vertical load at the bearings due to the seismic load combinations is:

minN_{Ed}= 1325.50 kN COMPRESSIVE FORCE, OK

9.2 Check of expansion joints

Displacements:

Braking load:	24.50 mm
Shrinkage:	4.00 mm
Uniform difference of temperature ΔT = -41°C:	18.00 mm
Uniform difference of temperature ΔT = +59°C:	25.90 mm
Earthquake x-x:	238.90 mm
Earthquake y-y:	209.80 mm

Total displacement

Static combination

Maximum negative	$d'_{Ed}=-d_G-1.50*d_{TR}-1.5*0.60*d_{t(-41)}=$	-56.95 mm
Maximum positive	$d'_{Ed}=-d_G+1.50*d_{TR}+1.50*0.6*d_{t(+59)}=$	56.06 mm

Seismic combination

Maximum negative	$d'_{Ed}=-0.4*d_E-d_G-0.5*d_{t(-41)}=$	111.44 mm
Maximum positive	$d'_{Ed}=0.4*d_E-d_G+0.5*d_{t(+59)}=$	107.50 mm

Minimum displacements of the expansion joint

Static combination	114 mm
Seismic combination	223 mm

Minimum gap

$d'_{Ed}=d_E-d_G+0.5*dt_{(+59)}=$ 260 mm

An expansion joint of type Algaflex TM480 or similar is chosen

PART II: INNOVATIVE SOLUTION

Chapter 10

BRIDGE DESCRIPTION

10.1 Geometry and cross sections

The bridge under investigation is situated over a riverbank and it is a steel arch road bridge with two simply supported spans, with total length 87.60m. The total width of the deck is equal to 15.00m, while at the supports it becomes 15.55m. The steel members of each span include two (2) main beams, seventeen (17) transverse beams, two (2) arches connected with transverse and diagonal bracing members. Each main beam is suspended by each arch with seven (7) hangers. The distance of the transverse steel beams is 2.625m. A composite deck is formed using trapezoidal profiles of type SYMDECK 150 and a concrete slab. The total thickness of the composite slab is 35cm. The concrete slab is connected with the transverse and main beams through steel shear connectors in order to ensure composite action. The characteristics of the bridge's steel members are listed in Table 10.1. The elevation view of a single span is illustrated in Figure 10.1, the arrangement in plan view of the main and transverse beams is shown in Figure 10.2, the plane view of the bridge in Figure 10.3 and the section of the bridge at mid span in Figure 10.4.

Table 10.1: Characteristics of the bridge's steel members

Πίνακας 10.1: Χαρακτηριστικά των μεταλλικών στοιχείων της γέφυρας

Type	Total number	Cross section	Length of each member	Theoretical span/rise
Main beams	4	HEB900	43.30m	42.00m
Transverse beams	34	HEB900	14.30m	14.70m
Arches	4	CHS750/20	47.70m	42.00m / 10.00m
Transverse bracing members	10	CHS244.5/8	13.95m	14.70m
Diagonal bracing members	16	CHS168.3/12.5	8.45m	9.13m
Hangers	28	CHS168.3/8	3.90m – 9.625m	4.375m – 10.00m

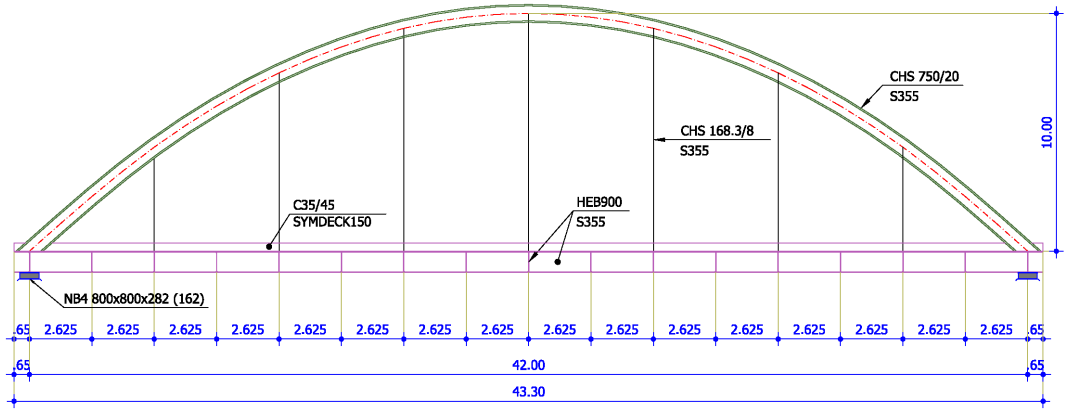

Figure 10.1: Elevation view of a single span

Σχήμα 10.1: Όψη εντός ανοίγματος γέφυρας

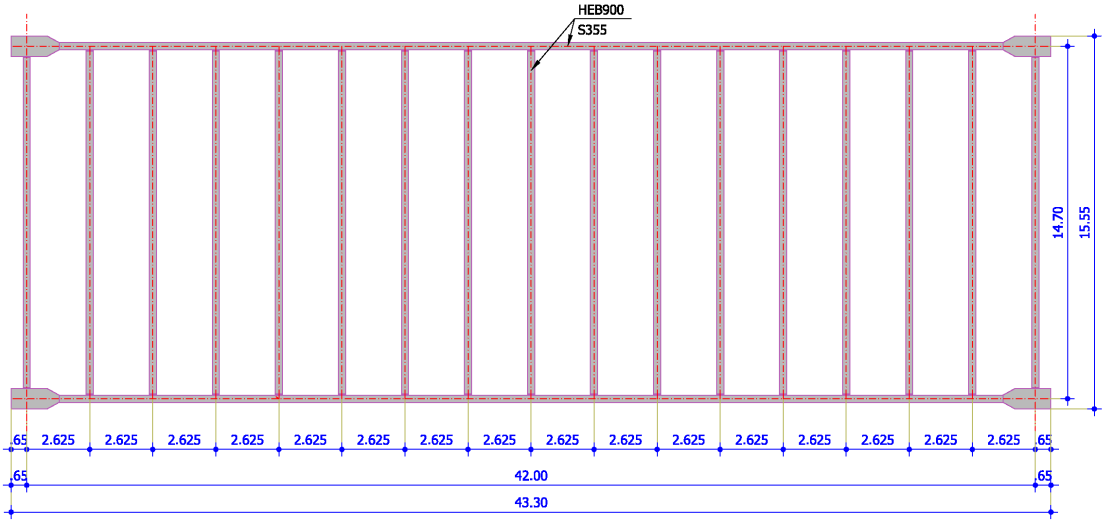

Figure 10.2: Arrangement in plan view of the deck's beams of a single span

Σχήμα 10.2: Διάταξη δοκών καταστρώματος εντός ανοίγματος γέφυρας

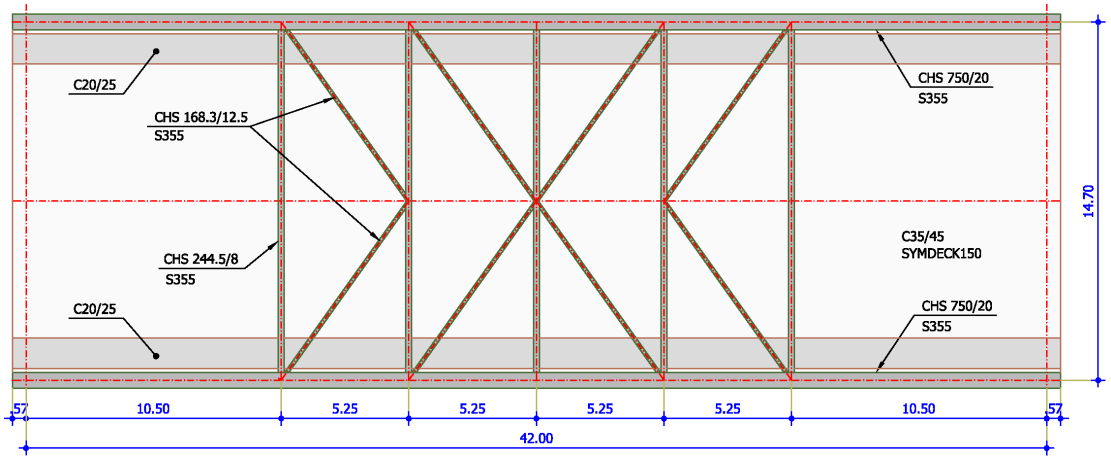

Figure 10.3: Plan view of a single span

Σχήμα 10.3: Κάτοψη εντός ανοίγματος γέφυρας

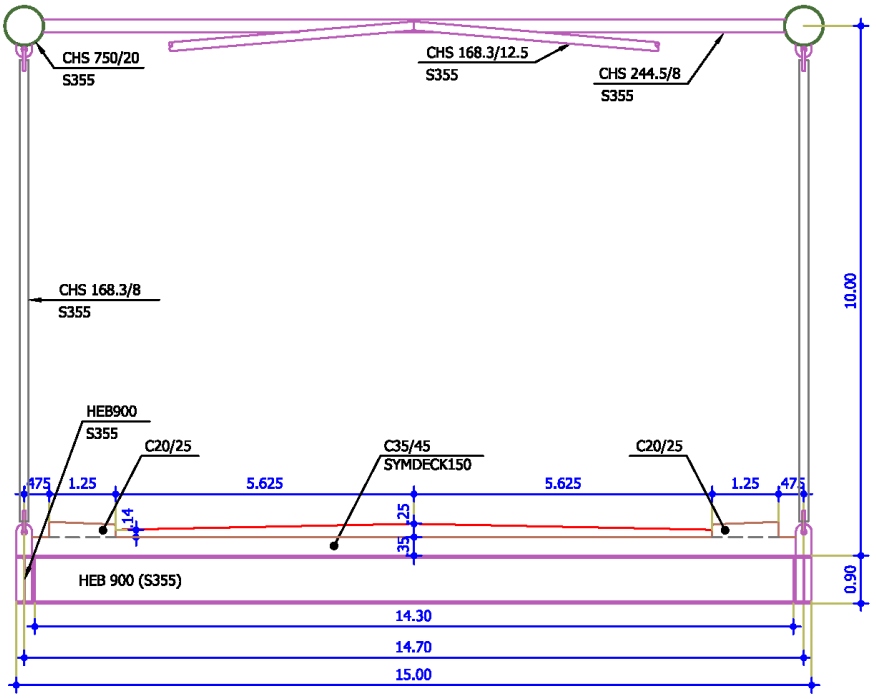

Figure 10.4: Section of the bridge at midspan

Σχήμα 10.4: Εγκάρσια τομή γέφυρας στο μέσον του ανοίγματος

The pier consists of three circular reinforced concrete columns, 8.00m tall, having a circular cross section of 1.50m diameter. The distance between the three columns is equal to 7.35m. They are connected at the top with a 17.00m long concrete beam, having the cross – section of Figure 10.5a. The dimensions of the pier's footing are 17.70m × 6.70m and its thickness is 2.00m (Figure 10.5b). The section of the bridge at the pier is given in Figure 10.6. The elevation view of the bridge is illustrated in Figure 10.7.

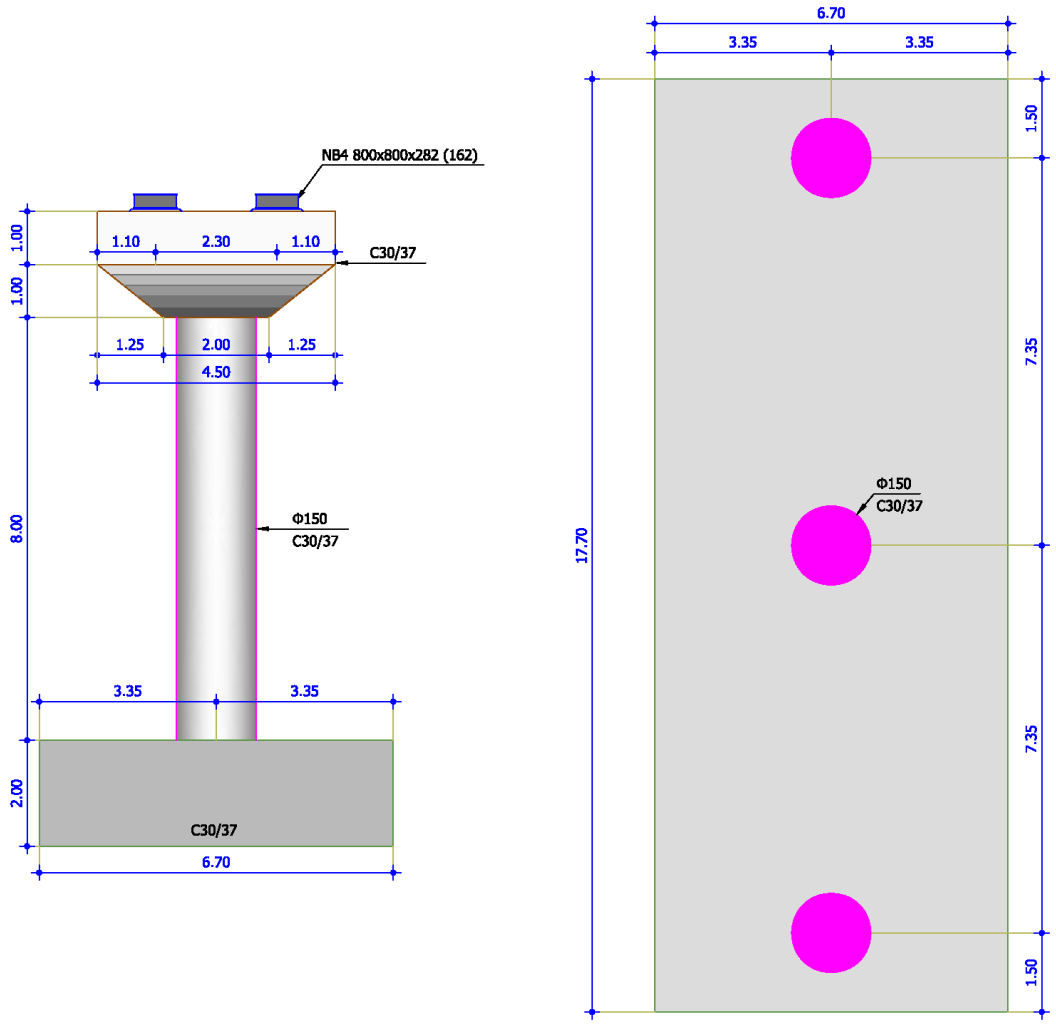

(a) (b)

Figure 10.5: (a) Geometry of the pier in longitudinal section, (b) Geometry of the pier's footing

Σχήμα 10.5: (a) Γεωμετρία μεσοβάθρου στη διαμήκη έννοια, (b) Γεωμετρία πεδίλου μεσοβάθρου

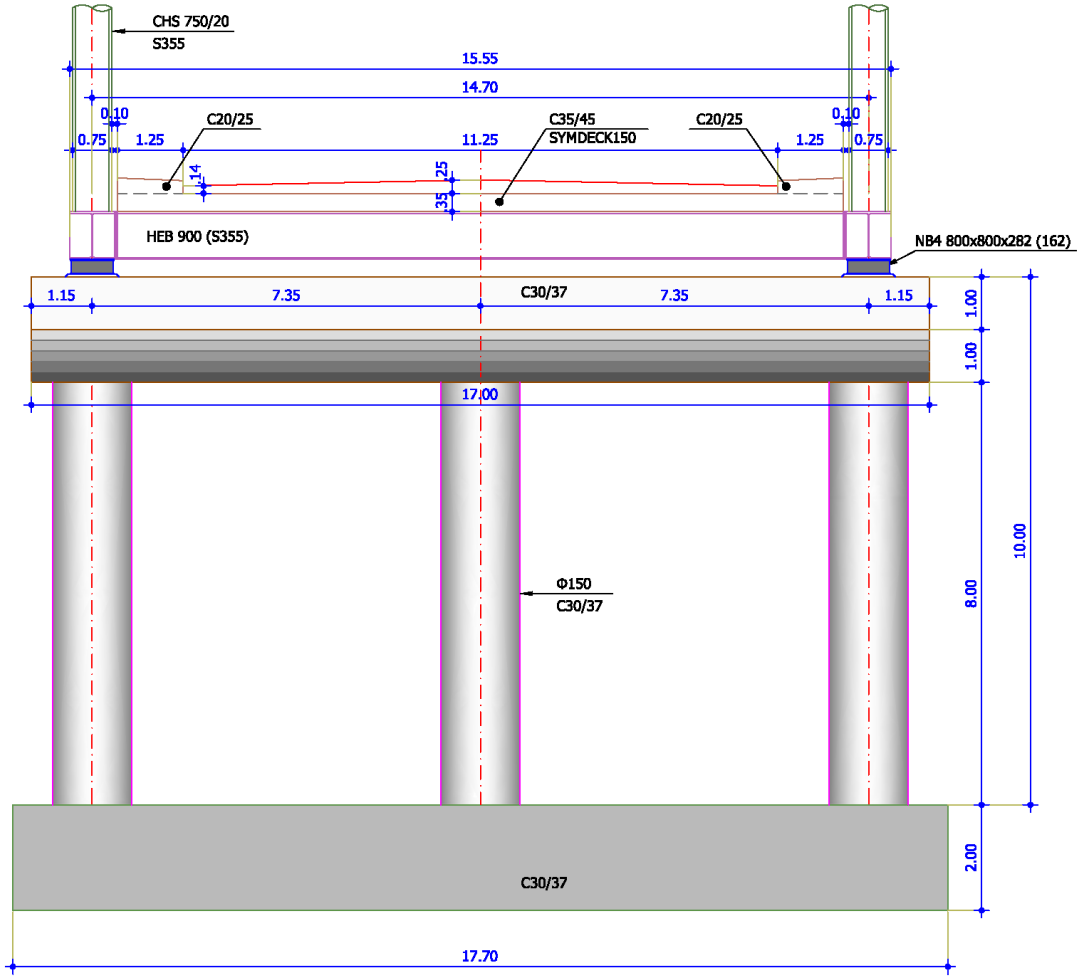

Figure 10.6: Section of the bridge at the pier

Σχήμα 10.6: Εγκάρσια τομή γέφυρας στη θέση μεσοβάθρου

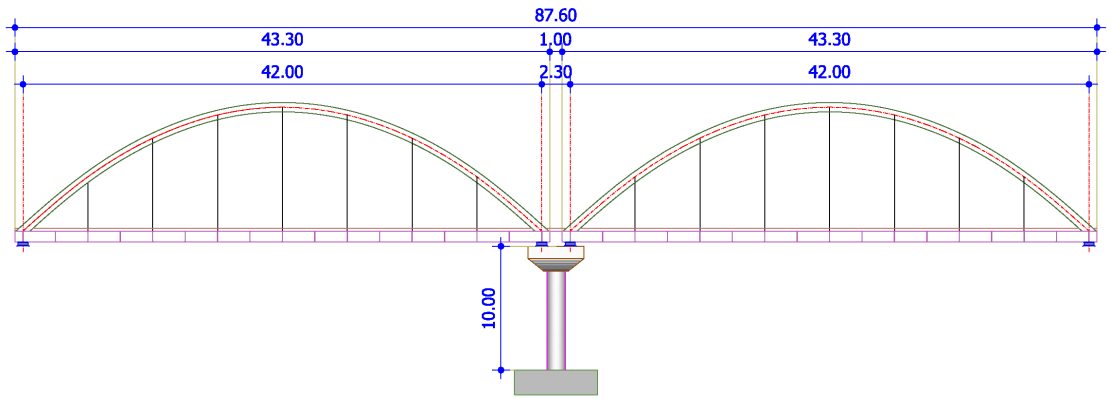

Figure 10.7: Elevation view of the bridge

Σχήμα 10.7: Όψη γέφυρας

The connection of the deck and the pier and the abutments is realized with anchored elastomeric bearings type NB4 800x800x282 (162). The bearings consist of nine (9) layers of elastomer, with thickness t_e=0.018m. The total thickness of the elastomer is t=0.162m. Details of the bearings are shown in Figure 10.8.

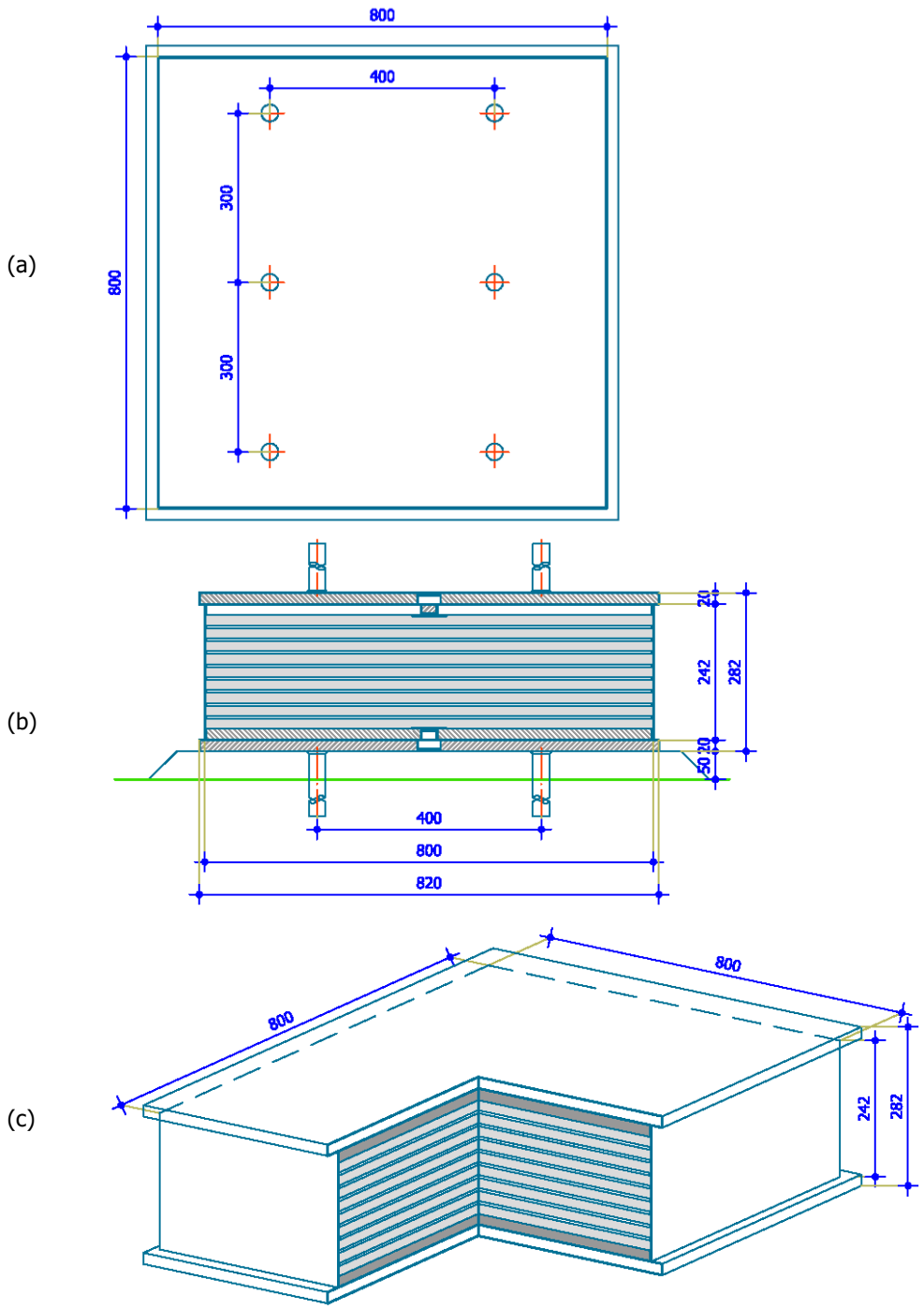

Figure 10.8: Details of the elastomeric bearings: (a) plan view, (b) vertical section, (c) perspective view

Σχήμα 10.8: Λεπτομέρειες ελαστομερικών εφεδράνων: (a) κάτοψη (β) κατακόρυφη τομή (γ) προοπτικό

10.2 Materials

All steel members are made of S355 structural steel. For the composite deck reinforced concrete C35/45 is used, for the sidewalks C20/25, for the footing, the columns and the beam of the pier C30/37. The reinforcement steel is B500C.

10.3 Footing design and dimensions of the crust

For the evaluation of the dimensions of the pier's footing and the crust, the total static load q_o is considered, which includes the permanent loads (consisting of the self weight of the bridge and footing and of the superimposed load) and 20% of the live load, which is the percentage considered in the seismic combinations. With respect to the embedment depth D the footing is considered to be seated at 2.50m below the soil surface. The dimensions of the footing and the crust are appropriately chosen so that the degraded factor of safety, $F.S._{deg}$ is equal or larger than 1.10, according to Table 10.2 for the seismic load combination, while Figure 10.9 shows the basic notation for the design of the improved crust. The thickness of the crust is chosen equal to 3.20m, while its width and length are 10.00m and 21.00m, respectively (Figure 10.10).

Table 10.2: Evaluation of the pier's footing and the crust's dimensions
Πίνακας 10.2: Καθορισμός διαστάσεων πεδίλου μεσοβάθρου και κρούστας

Input	
Soil Properties	
Relative Density of the natural soil, $D_{r,o}$ (%)	60
Excess Pore Pressure ratio in the improved zone, $r_{u,design}$	0.30
Buoyant unit weight, γ' (kN/m^3)	9.81
Soil Geometry	
Total Thickness of the liquefiable layer, Z_{tot} (m)	20
Thickness of the improved zone, Hi_{mp}(m)	3.20
Thickness of the liquefiable layer, Z_{liq} (m)	14.3
Width of the improved zone, L_{imp}(m)	10.00
Excitation	
Maximum input acceleration, a_{max} (g)	0.17
Predominant period, T (sec)	0.25
Number of cycles, N	12
Footing Properties	
Footing width, B(m)	6.70
Footing Length, L(m)>B(m) [use 0 for strip footing]	17.70
Embedment depth, D(m)	2.50
Total static load from footing, q_o (kPa)	180.94

Output	
Improved Soil	
Length of the improved zone (m)	21.00
Volume of the improved zone (m^3)	672.00
Replacement ratio, a_s	0.122
Relative Density of the improved zone, $D_{r,imp}$ (%)	80
Friction Angle of the improved zone, φ_{imp} (deg)	40
Permeability of the improved zone, k_{eq} (m/s)	1.39E-03
Infinite Improvement	
Degraded factor of safety, $F.S._{deginf}$	1.29
Seismic settlements, $\rho_{dyn,inf}$(m)	0.069
Differential settlements, δ(m)	0.046
Rotation, θ(degrees)	0.226
Finite Improvement	
Degraded factor of safety, $F.S._{deg}$	**1.10**
Seismic settlements, ρ_{dyn}(m)	0.080
Differential settlements, δ(m)	0.054
Rotation, θ(degrees)	0.262

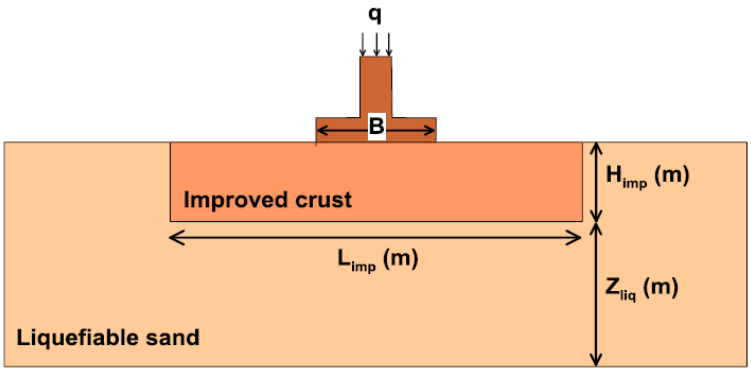

Figure 10.9: Notation used for the design of the improved crust

Σχήμα 10.9: Ορισμός βασικών συμβόλων για το σχεδιασμό της βελτιωμένης επιφανειακής κρούστας

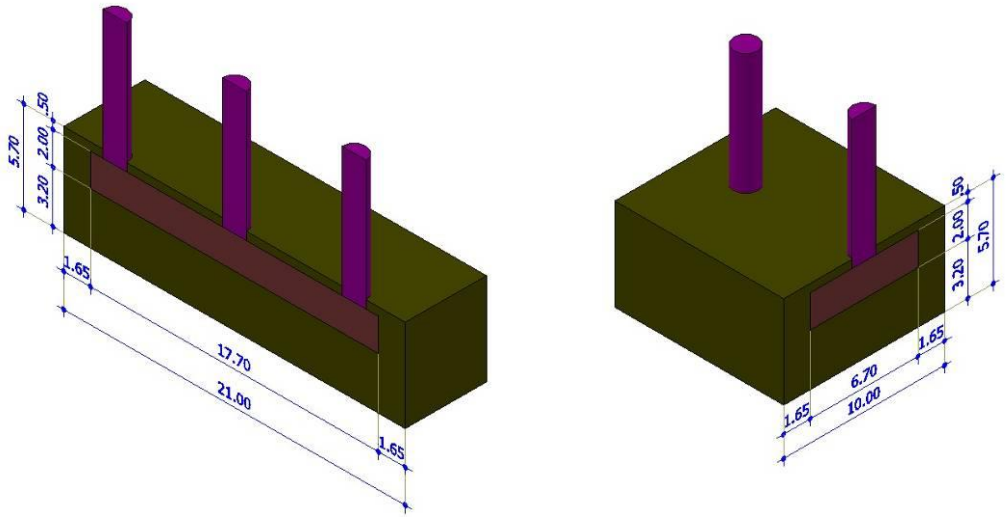

(a) (b)

Figure 10.10: (a) Transverse section and (b) longitudinal section of the pier's footing and crust

Σχήμα 10.10: (a) Εγκάρσια τομή και (b) διαμήκης τομή θεμελίου μεσοβάθρου και κρούστας

Chapter 11

SEISMIC CONDITIONS

11.1 Seismic response spectra with no liquefaction

In order to define seismic actions, without liquefaction, the design spectrum of Eurocode 8 is taken into consideration, for soil type D, soil factor S=0.96 and peak ground acceleration PGA_b=0.22g, accounting for Seismic Scenario 1, with the following characteristics:

- return period T_{ret} = 225 years
- earthquake magnitude Mw = 6.2
- peak ground acceleration at outcropping bedrock PGA_b = 0.22g

Additionally, the following parameters are considered:

- Behavior factor q_h=1.50, q_v=1.00
- Damping ratio ζ=3%
- Damping correction factor $n = \sqrt{\frac{10}{5+3}} = 1.118$
- Peak ground acceleration $PGA_{b,h}$=0.22g, $PGA_{b,v}$=0.90×0.22g=0.198g
- Periods for horizontal component (T_B=0.20s, T_C=0.80s, T_D=2.00s, S=0.96)
- Periods for vertical component (T_B=0.05s, T_C=0.15s, T_D=1.00s)

The horizontal elastic response spectrum for the case without liquefaction is illustrated in Figure 11.1a, while Figure 11.1b shows the vertical one.

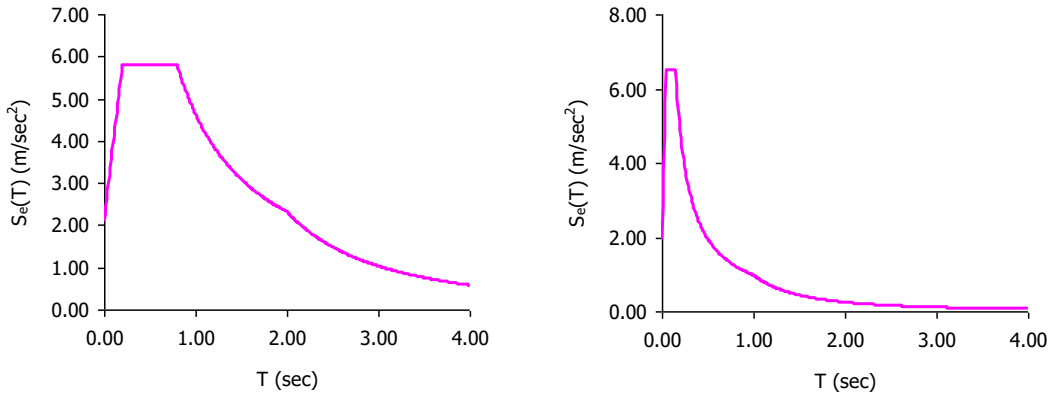

(a) (b)

Figure 11.1: (a) Horizontal elastic response spectrum, (b) Vertical elastic response spectrum without liquefaction

Σχήμα 11.1: (a) Οριζόντιο ελαστικό φάσμα απόκρισης, (b) Κατακόρυφο ελαστικό φάσμα απόκρισης χωρίς ρευστοποίηση

11.2 Seismic response spectra with liquefaction

In case of liquefaction, the seismic actions are defined according to the design spectrum of Eurocode 8, for soil type C, soil factor S=0.50 and peak ground acceleration PGA_b=0.32g, accounting for Seismic Scenario 2, with the following characteristics:

- return period T_{ret} = 1000 years
- earthquake magnitude Mw = 7.0
- peak ground acceleration at outcropping bedrock PGA_b = 0.32g

Additionally, the following parameters are considered:

- Behavior factor q_h=1.50, q_v=1.00
- Damping ratio ζ=3%
- Damping correction factor $n = \sqrt{\frac{10}{5+3}} = 1.118$
- Peak ground acceleration $PGA_{b,h}$=0.32g, $PGA_{b,v}$=0.90×0.32g=0.288g
- Periods for horizontal component (T_B=0.20s, T_C=0.60s, T_D=2.00s, S=0.50)
- Periods for vertical component (T_B=0.05s, T_C=0.15s, T_D=1.00s)

The horizontal elastic response spectrum with liquefaction is illustrated in Figure 11.2a, while Figure 11.2b shows the vertical one.

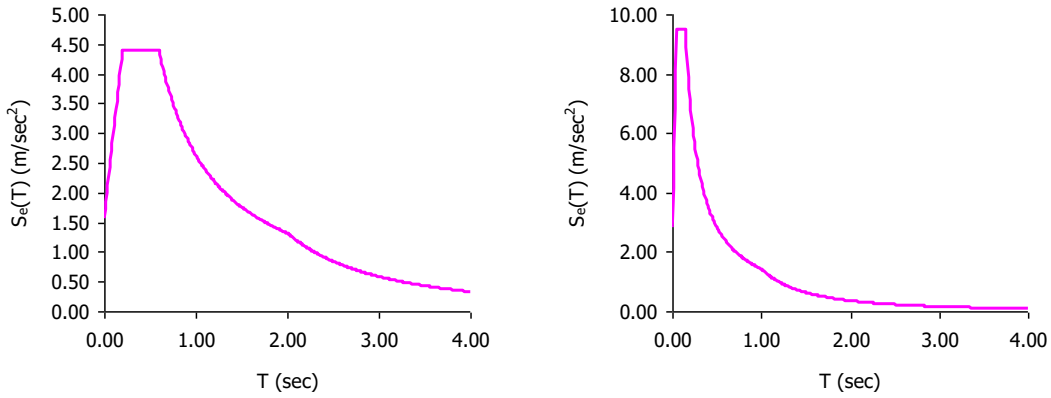

(a) (b)

Figure 11.2: (a) Horizontal elastic response spectrum, (b) Vertical elastic response spectrum with liquefaction

Σχήμα 11.2: (a) Οριζόντιο ελαστικό φάσμα απόκρισης, (b) Κατακόρυφο ελαστικό φάσμα απόκρισης με ρευστοποίηση

11.3 Modal response spectrum analysis

A modal analysis is performed to calculate the natural frequencies and vibration modes of the bridge. The inertial effects of the design seismic action are evaluated by taking into account the presence of the masses associated with all gravity loads appearing in the following combination of actions:

$\sum_{j\geq 1} G_{kj} "+" \sum_{i\geq 1} \psi_E \cdot Q_{ki}$ where ψ_E=0.20 for road traffic loads.

It is ensured that the sum of the effective modal masses for the modes taken into account is at least 90% of the total mass of the structure. The maximum displacements, internal loads and stresses are superimposed according to CQC (Complete Quadratic Combination) method.

Chapter 12

ANALYSIS OF THE BRIDGE

12.1 Model of the bridge

The main and transverse beams, the horizontal bracing members of the arches and the arches are modeled with beam elements. Moment releases are applied at the ends of the transverse beams. The hangers and the diagonal bracing members of the arches are modeled with truss elements. The concrete slab is simulated using shell elements with a thickness of 25cm, accounting for the mean value of the slab's thickness. The bearings at the abutments and the pier are modeled with equivalent elastic springs, with different stiffness for static and seismic combinations. Thus, for the horizontal springs the stiffness of the bearings for static load combinations is:

$$K_{h,st} = \frac{G_g \times A}{t} = \frac{900kN/m^2 \times 0.8m \times 0.8m}{0.162m} = 3556kN/m \quad (12.1)$$

while for displacements under seismic load combinations the stiffness of the horizontal springs is given as:

$$K_{h,se} = \frac{1.25 \times G_g \times A}{t} = 1.25 \times 3556kN/m = 4444kN/m \quad (12.2)$$

and for the calculation of the internal forces under seismic load combinations, the corresponding stiffness of the horizontal springs is:

$$K_{h,se,In} = \frac{1.20 \times 1.25 \times G_g \times A}{t} = 1.20 \times 4444kN/m = 5333kN/m \quad (12.3)$$

with G_g=900kN/m^2 the conventional shear modulus, A the overall plan area of the bearing and t the total thickness of the elastomer layers. The vertical springs have a stiffness constant equal to:

$$K_v = \frac{A}{\sum t_i \times \left(\frac{1}{5 \times G \times S^2} + \frac{1}{E_b} \right)} =$$

$$= \frac{0.80m \times 0.80m}{0.162m \times \left(\frac{1}{5 \times 1.25 \times 900kN/m^2 \times 11.11^2} + \frac{1}{2000000kN/m^2} \right)} = 2.04 \times 10^6 kN/m \quad (12.4)$$

where S is the shape factor of the elastomeric bearing equal to:

$$S = \frac{A}{L \times t_e} = \frac{0.80m \times 0.80m}{2 \times (0.80m + 0.80m) \times 0.018m} = 11.11 \qquad (12.5)$$

with L the perimeter of the bearing and t_e the effective thickness of an individual elastomer layer and the bulk modulus is taken equal to E_b=2000MPa.

The numerical model of the bridge is shown in Figure 12.1. The finite element analysis software that is used is Sofistik.

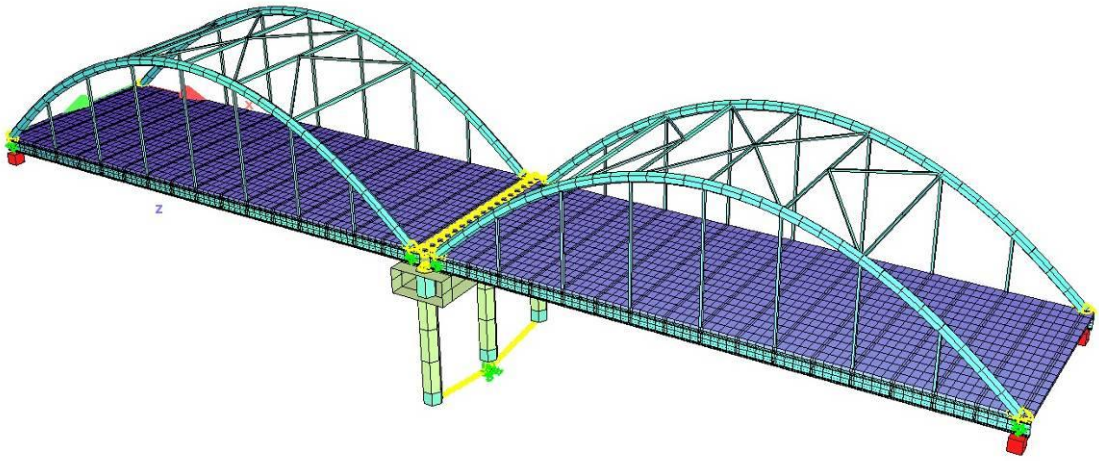

Figure 12.1: Model of the bridge
Σχήμα 12.1: Προσομοίωμα γέφυρας

12.2 Modeling of the pier's footing

The bases of the three columns are connected via rigid links with a common "master" node. The soil-structure interaction is taken into account with equivalent springs and damping elements connected to this common node at the base of the pier. More specifically, for the orientation of the designed pier's footing of Figure 12.2, shown in Figure 12.2, the static values of the spring's constants are given in Table 12.1.

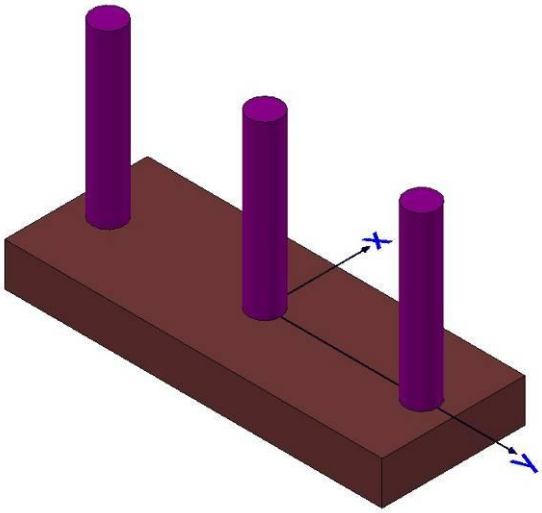

Figure 12.2: Orientation of the pier's footing
Σχήμα 12.2: Προσανατολισμός θεμελίου μεσοβάθρου

Table 12.1: Static stiffness of equivalent springs at the base of the pier

Πίνακας 12.1: Στατική δυσκαμψία ισοδύναμων ελατηρίων στη βάση του μεσοβάθρου

Direction	Static stiffness k_{static}
Horizontal, (longitudinal x axis)	2.91E+05 kN/m
Horizontal (transverse y axis)	3.04E+05 kN/m
Vertical, z	3.70E+05 kN/m
Rocking (around longitudinal x axis)	1.81E+07 kNm/rad
Rocking (around transverse y axis)	4.41E+06 kNm/rad

In case of dynamic response under seismic loads, the dynamic correction factors are calculated for both cases, with and without liquefaction (see Annex I). They are considered common for both horizontal directions. Factors $k_1(T)$, referring to the dynamic spring constants, are given in Table 12.2 for several periods, while the dynamic springs are calculated as:

$$k_{dynamic}=k_0 \times k_1(T) \tag{12.6}$$

where the values of k_0 are listed in Table 12.3.

Table 12.2: Dynamic correction factor $k_1(T)$ of equivalent springs at the base of the pier

Πίνακας 12.2: Δυναμικός συντελεστής $k_1(T)$ ισοδύναμων ελατηρίων στη βάση του μεσοβάθρου

No liquefaction							
	T(sec)						
Direction	**0.20**	**0.40**	**0.60**	**0.80**	**1.00**	**1.25**	**1.50**
Horizontal	1.00	0.85	0.87	0.88	0.89	0.92	0.95
Vertical	0.57	0.78	0.81	0.92	0.95	0.96	0.98
Rocking	0.84	0.95	0.98	0.99	0.99	1.00	1.00
With liquefaction							
	T(sec)						
Direction	**0.20**	**0.40**	**0.60**	**0.80**	**1.00**	**1.25**	**1.50**
Horizontal	1.20	1.04	0.96	0.91	0.97	0.85	0.77
Vertical	0.42	0.73	0.76	0.55	0.59	0.65	0.72
Rocking	0.83	0.92	0.94	0.94	0.96	0.97	0.99

Table 12.3: Stiffness k_0 of equivalent springs at the base of the pier

Πίνακας 12.3: Δυσκαμψία k_0 ισοδύναμων ελατηρίων στη βάση του μεσοβάθρου

	Static stiffness k_0	
Direction	**No liquefaction**	**With liquefaction**
Horizontal, (longitudinal x axis)	2.54E+06 kN/m	1.26E+06 kN/m
Horizontal (transverse y axis)	2.34E+06 kN/m	1.16E+06 kN/m
Vertical, z	2.99E+06 kN/m	8.34E+05 kN/m
Rocking (around longitudinal x axis)	1.61E+08 kNm/rad	9.84E+07 kNm/rad
Rocking (around transverse y axis)	3.94E+07 kNm/rad	2.42E+07 kNm/rad

For vibration modes about horizontal axes, the eigenperiod is close to 1.50sec, which also applies for the rocking about the horizontal axes, while for vertical oscillation, the eigenperiod is approximately 0.50sec, as shown in Table 12.7 (for the case without liquefaction) and Table 12.8 (for the case with liquefaction), as well as in Figure 12.3. Thus for the case without liquefaction:

$$k_{1,h}(1.50\text{sec})=0.95 \tag{12.7}$$

$$k_{1,v}(0.50\text{sec})=0.80 \tag{12.8}$$

$$k_{1,r}(1.50sec)=1.00 \quad (12.9)$$

while for the case with liquefaction, the corresponding values become equal to:

$$k_{1,h}(1.50sec)=0.77 \quad (12.10)$$

$$k_{1,v}(0.50sec)=0.75 \quad (12.11)$$

$$k_{1,r}(1.50sec)=0.99 \quad (12.12)$$

Hence, the stiffness coefficients of the equivalent springs at the base of the pier that will be used for the dynamic analysis are given in Table 12.4. They are calculated according to Eq. (12.6), using the values of Table 12.3 and the dynamic correction factors of Eqs. (12.7) – (12.12).

Table 12.4: Dynamic stiffness of equivalent springs at the base of the pier

Πίνακας 12.4: Δυναμική δυσκαμψία ισοδύναμων ελατηρίων στη βάση του μεσοβάθρου

	Dynamic stiffness $k_{dynamic}$	
Direction	**No liquefaction**	**With liquefaction**
Horizontal, (longitudinal x axis)	2.41E+06 kN/m	9.70E+05 kN/m
Horizontal (transverse y axis)	2.22E+06 kN/m	8.93E+05 kN/m
Vertical, z	2.39E+06 kN/m	6.26E+05 kN/m
Rocking (around longitudinal x axis)	1.61E+08 kNm/rad	9.77E+07 kNm/rad
Rocking (around transverse y axis)	3.94E+07 kNm/rad	2.40E+07 kNm/rad

Factors $k_2(T)$, depending also on the structure's eigenperiod, refer to the dashpot coefficient, which is activated only for seismic loads and it is expressed as:

$$C=k_0\times k_2(T)\times T/2\pi \quad (12.13)$$

Table 12.5: Dynamic correction factor $k_2(T)$ of equivalent dashpot at the base of the pier

Πίνακας 12.5: Δυναμικός συντελεστής $k_2(T)$ ισοδύναμων αποσβεστήρων στη βάση του μεσοβάθρου

No liquefaction							
	T(sec)						
Direction	**0.20**	**0.40**	**0.60**	**0.80**	**1.00**	**1.25**	**1.50**
Horizontal	0.59	0.45	0.20	0.16	0.09	0.07	0.05
Vertical	0.81	0.31	0.09	0.06	0.06	0.06	0.06
Rocking	0.18	0.07	0.06	0.06	0.06	0.06	0.06
With liquefaction							
	T(sec)						
Direction	**0.20**	**0.40**	**0.60**	**0.80**	**1.00**	**1.25**	**1.50**
Horizontal	1.62	0.96	0.72	0.58	0.51	0.50	0.50
Vertical	2.11	1.09	1.01	0.75	0.43	0.32	0.24
Rocking	0.40	0.18	0.15	0.12	0.09	0.08	0.08

Thus for the case without liquefaction:

$$k_{2,h}(1.50sec)=0.05 \quad (12.14)$$

$$k_{2,v}(0.50sec)=0.20 \quad (12.15)$$

$$k_{2,r}(1.50sec)=0.06 \quad (12.16)$$

while for the case with liquefaction, the corresponding values become equal to:

$$k_{2,h}(1.50sec)=0.50 \quad (12.17)$$

$$k_{2,v}(0.50sec)=1.05 \quad (12.18)$$

$$k_{2,r}(1.50sec)=0.08 \quad (12.19)$$

The dashpot coefficients C are listed in Table 12.6, which is calculated according to Eq. (12.13), taking into account the eigenperiods of the bridge, the values of the stiffness k_0 of the springs (Table 12.3) and the factors $k_2(T)$ given in Eqs. (12.14) – (12.19).

Table 12.6: Dashpot coefficient C of damping elements at the base of the pier
Πίνακας 12.6: Συντελεστής απόσβεσης C στοιχείων απόσβεσης στη βάση του μεσοβάθρου

	Dashpot coefficient C	
Direction	**No liquefaction**	**With liquefaction**
Horizontal, (longitudinal x axis)	3.03E+04 kN/m	1.50E+05 kN/m
Horizontal (transverse y axis)	2.79E+04 kN/m	1.38E+05 kN/m
Vertical, z	4.76E+04 kN/m	6.97E+04 kN/m
Rocking (around longitudinal x axis)	2.31E+06 kNm/rad	1.88E+06 kNm/rad
Rocking (around transverse y axis)	5.64E+05 kNm/rad	4.62E+05 kNm/rad

12.3 Vibration modes and natural frequencies

The natural frequencies and periods of the first six vibration modes are listed in Table 12.7, for the case without liquefaction, and in Table 12.8, when liquefaction occurs, taking into account the corresponding values of springs and damping elements at the base of the pier, as described in section 12.1. The modal shapes are the same for the first six (6) vibration modes for both cases, as shown in Figure 12.3.

Table 12.7: Eigenfrequencies and eigenperiods of the bridge for the case of no liquefaction
Πίνακας 12.7: Ιδιοσυχνότητες και ιδιοπερίοδοι της γέφυρας για την περίπτωση μη ρευστοποίησης

Mode number	Eigenfrequency (rad/sec)	Eigenfrequency (Hz)	Period (sec)
1	4.014	0.639	1.565
2	4.212	0.670	1.492
3	5.221	0.831	1.203
4	12.861	2.046	0.489
5	13.379	2.129	0.470
6	15.431	2.456	0.407

Table 12.8: Eigenfrequencies and eigenperiods of the bridge for the case of liquefaction
Πίνακας 12.8: Ιδιοσυχνότητες και ιδιοπερίοδοι της γέφυρας για την περίπτωση ρευστοποίησης

Mode number	Eigenfrequency (rad/sec)	Eigenfrequency (Hz)	Period (sec)
1	3.980	0.634	1.579
2	4.187	0.666	1.501
3	5.220	0.831	1.204
4	12.661	2.015	0.496
5	13.154	2.094	0.478
6	14.835	2.361	0.424

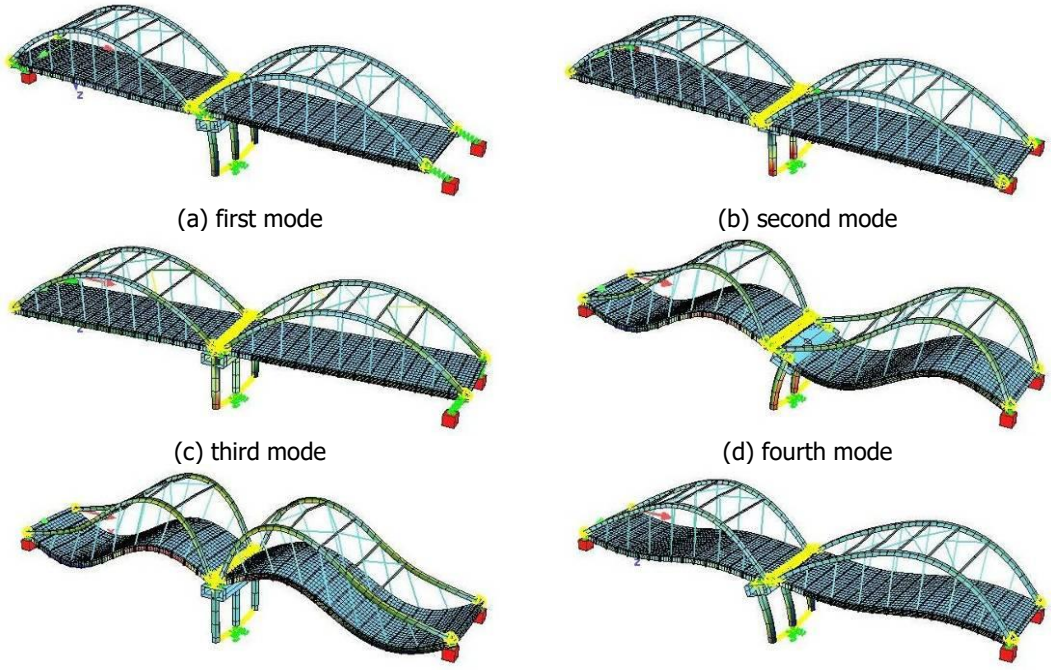

(a) first mode (b) second mode

(c) third mode (d) fourth mode

(e) fifth mode (f) sixth mode

Figure 12.3: Eigenmodes of the bridge

Σχήμα 12.3: Ιδιομορφές γέφυρας

12.4 Horizontal liquefaction-induced differential displacements

According to the proposed methodology, except for the settlements and rotations due to liquefaction, the superstructure should be able to accommodate the maximum liquefaction-induced differential horizontal displacements between the abutments and the pier. Due to the response spectrum method limitations, one and only spectrum can be applied to all the support points (i.e. pier footings and abutments) for each loading case. However, it is recognized that the seismic excitation differs significantly between the pier and the abutments since the latter are founded on non-liquefaction susceptible soil while the pier on potentially liquefiable soil. To overcome this inconsistency, additional displacements due to liquefaction are imposed to the footings of the pier. Specifically, the expected level of the imposed horizontal displacements due to liquefaction is defined as a separate loading case. The design value of the horizontal differential displacement is derived from the geotechnical study of the particular soil profile. The peak and average transient displacements of the liquefied ground are summarized in Table 12.9. The design value of the horizontal differential displacement is considered equal to 12.00cm.

Table 12.9: Peak and average transient displacements of the liquefied ground (from Appendix C of Deliverable D4: Elastic Response Spectra for Liquefiable soils)

Πίνακας 12.9: Μέγιστες και μέσες εδαφικές μετακινήσεις ρευστοποιημένου εδάφους (από Παράρτημα Γ Παραδοτέου Π4: Ελαστικά Φάσματα Σχεδιασμού για Ρευστοποιήσιμα Εδάφη)

	Excitation	Peak horizontal displacement, (cm)				
		Outcropping bedrock	Ground Surface			
			w/ improved top layer		w/o improved top layer	
			Absolute	Relative	Absolute	Relative
1	ITALY_BAG	13.13	19.12	10.49	27.64	20.59
2	ITALY_VLT	1.28	2.81	3.20	4.03	4.39
3	KOBE_TDO	13.47	17.17	20	14.46	21.47
4	LOMAP_AND	10.20	21.16	22.17	11.23	9.31
5	LOMAP_GIL	11.68	12.59	4.99	13.07	4.87
average		**9.95**	**14.57**	**12.17**	**14.09**	**12.13**

The previously extracted displacements are then considered according to the combination rule:

$$\pm\delta_x \pm 0.30\ \delta_y \quad (12.20)$$

$$\pm 0.30\ \delta_x \pm \delta_y \quad (12.21)$$

where δ_x, δ_y are the displacements along the longitudinal and the transversal bridge axes, respectively. These displacements are then further combined with gravity (G), live (Q) loads and seismic loads (E) using the partial factors for actions according to the applied code. Finally, the following combinations of actions are examined:

$G + 0.2Q \pm E_x \pm 0.30E_y \pm 0.30E_z + 0.30\ (\pm\delta_x \pm 0.30\delta_y)$

$G + 0.2Q \pm 0.30E_x \pm E_y \pm 0.30E_z + 0.30\ (\pm 0.30\delta_x \pm \delta_y)$

$G + 0.2Q \pm 0.30E_x \pm 0.30E_y \pm E_z + 0.30\ (\pm 0.30\delta_x \pm 0.30\delta_y)$

$G + 0.2Q + 0.30\ (\pm E_x \pm 0.30E_y \pm 0.30E_z) + (\pm\delta_x \pm 0.30\delta_y)$

$G + 0.2Q + 0.30\ (\pm 0.30E_x \pm E_y \pm 0.30E_z) + (\pm 0.30\delta_x \pm \delta_y)$

$G + 0.2Q + 0.30\ (\pm 0.30E_x \pm 0.30E_y \pm E_z) + (\pm 0.30\delta_x \pm 0.30\delta_y)$

12.5 Load Cases

The load cases considered are the following:

LC 1: Self weight

LC 2: Superimposed

Pavement and future layer: $g=0.20m\times24kN/m^3+0.50kN/m^2=5.30kN/m^2$

Each sidewalk with parapets: $g=(0.33m^2\times25kN/m^3 + 0.95kN/m) / 1.25m = 7.36kN/m^2$

Earth weight on the footing $g=0.50m \times 20\ kN/m^3= 10kN/m^2$.

LC 3: Shrinkage and creep

An equivalent uniform decrease of temperature is used to simulate the shrinkage of the concrete slab, equal to -13^o.

LC 4: Braking load

The total braking load is:

$Q_{ik}=0.6\alpha_{Q1}(2Q_{1k})+0.10\alpha_{q1}\ q_{1k}\ w_1\ L=0.6\times0.9\times2\times300+0.10\times1.0\times9\times3\times87.60=560.52kN$

It is: $180\times\alpha_{Q1}<=Q_{ik}<=900 \Rightarrow 180\times0.9<=Q_{ik}<=900 \Rightarrow 162<=Q_{ik}<=900$.

The distributed uniform horizontal load over the bridge's deck is:

$Q_{ik}/(14.70m \times 87.60m)=0.43\ kN/m^2$

LC 5-6: Uniform difference of temperature for check of elastomeric bearings and expansion joints.

For the check of bearings and expansion joints the uniform difference of temperature is calculated as:

$\Delta T_{N,con}$-20ºC=-41ºC, $\Delta T_{N,exp}$+20ºC=59ºC.

As in LC 15 and 16, the temperature variations are applied on the steel members of the superstructure and the slab of the deck.

LC 7: Wind action y

Considering a wind velocity V_b=30m/sec, a uniform load is applied at the members of the bridge towards +y (depending on their exposed dimension):

Piers: 0.0238kN/m

Deck: 0.415kN/m^2

Hangers: 0.11-0.13kN/m

Arches: 0.56kN/m

Diagonal bracing members: 0.09kN/m

LC 8: Wind action x

Similarly, considering a wind velocity V_b=30m/sec, a uniform load is applied at the members of the bridge towards +x:

Piers: 0.0323kN/m

Deck: 0.104kN/m^2

Hangers: 0.11-0.13kN/m

Arches: 0.56kN/m

Diagonal bracing members: 0.07kN/m

Horizontal bracing members:: 0.19kN/m

LC 9: Wind action z

Considering a wind velocity V_b=30m/sec, a uniform load is applied at the members of the bridge towards +z:

Half Deck: 1.01kN/m^2

Arches: 0.56kN/m

Diagonal bracing members: 0.11kN/m

Horizontal bracing members: 0.19kN/m

LC 10, 11, 12: Settlement of 1cm at the pier and 1cm at the abutments. These load cases are used for the static combinations, in case no liquefaction occurs.

LC 13, 14: Horizontal ground displacements. A horizontal displacement is applied at the base of the pier, equal to 12cm, in the longitudinal and transverse direction of the bridge,

respectively. These Load Cases are taken into account in the seismic loading combinations only if liquefaction takes place.

LC 15-16: Uniform difference of temperature on deck.

Considering an initial temperature T_0=+10ºC, a minimum shade air temperature T_{min}=-15ºC and a maximum one T_{max}=+45ºC, the uniform temperature components are determined by EC1. Part.1-5 for a composite bridge (Type 2) and are equal to $T_{e,min}$=-11ºC and $T_{e,max}$=+49ºC. Thus:

$\Delta T_{N,con}=T_0-T_{e,min}$=-21ºC, $\Delta T_{N,exp}= T_{e,max} - T_0$ =+39ºC.

The temperature variations are applied on the steel members of the superstructure and the slab of the deck.

LC 17: Settlement of 8cm at the pier as calculated in Table 10.2. This load case is used for the static combinations, in case liquefaction takes place and it is combined with LC18 and 19.

LC 18, 19: Rotation of the pier's footing. A rotation about x and y axes, equal to θ=0.05×8cm=0.4º (0.007rad) is applied at the base of the pier, respectively. These Load Cases are taken into account in the static loading combinations only if liquefaction takes place and they are combined with LC17.

LC 20-99: Tandem System of Traffic Load Model 1

The carriageway width is 11.25m, thus, three lanes are considered with width 3.00m and a tandem system is applied at varied positions of the bridge, as:

Lane 1: 0.9×150kN=135kN/wheel (four wheels)

Lane 2: 0.9×100kN=90kN/wheel (four wheels)

Lane 3: 0.9×50kN=45kN/wheel (four wheels)

LC 101-103: UDL System of Traffic Load Model 1

A distributed load is applied on the deck equal to 2.5kN/m^2

LC 121-123, 141-143: UDL System of Traffic Load Model 1

At Lane 1 an additional distributed load is applied, equal to 6.5kN/m^2.

LC 201-260: Tandem System of Traffic Load Model 2

A single axle load is applied at different positions of the bridge with value: 0.9×200kN=180kN/wheel (two wheels)

LC 320-399: Tandem System of Traffic Load Model 1 with cracked deck concrete

LC 401-403: UDL System of Traffic Load Model 1 with cracked deck concrete

LC 421-423, 441-443: UDL System of Traffic Load Model 1 with cracked deck concrete

LC 501-560: Tandem System of Traffic Load Model 2 with cracked deck concrete

LC600: Uniform road traffic loads

This load case is used for the seismic combinations, taking into account Load Model 1. The loads considered for this LC are listed in Table 5.2. A uniform load is applied to the shell elements equal to 4.67kN/m^2.

LC2010: Earthquake x-x

LC2011: Earthquake y-y

LC2012: Earthquake z-z

12.6 Load Combinations at Ultimate Limit State (ULS)

The load combination at ULS is described as:

$$\sum_{j\geq 1} \gamma_{Gj} \cdot G_{kj} "+" \gamma_{Q1} \cdot Q_{k1} "+" \sum_{i\geq 1} \gamma_{Qi} \cdot \psi_{0i} \cdot Q_{ki} \qquad (12.22)$$

where the partial factors γ_G and γ_Q are listed in Table 5.3.

The following ULS load combinations are considered:

LC 1100 and 1200: This combination includes the following load cases:

LC1	Self weight
+LC2	Superimposed
+LC3	Shrinkage
+LC4	Braking load
+LC7 or LC8	Wind action ±x or ± y
+LC9	Wind action ±z
+LC10, 11, 12	Settlements at the pier and the abutments (only for the design of superstructure) (only if liquefaction does not occur)
+LC17	Settlements at the pier's footing (only if liquefaction takes place)
+LC18 (±1.0 or ±0.3)	Settlements at the pier's footing (only if liquefaction takes place)
+LC19 (±0.3 or ±1.0)	Settlements at the pier's footing (only if liquefaction takes place)
+LC15, 16	Thermal loads
+LC20-99	Tandem System (LM1)
+LC101-103	UDL 2.5kN/m^2 (LM1)
+LC121-123 or 141-143	UDL 6.50kN/m^2 (LM1)

LC 1300: This combination includes the following load cases:

LC1	Self weight
+LC2	Superimposed
+LC3	Shrinkage
+LC4	Braking load
+LC7 or LC8	Wind action ±x or ± y
+LC9	Wind action ±z
+LC10, 11, 12	Settlements at the pier and the abutments (only for the design of superstructure) (only if liquefaction does not occur)
+LC17	Settlements at the pier's footing (only if liquefaction takes place)
+LC18 (±1.0 or ±0.3)	Settlements at the pier's footing (only if liquefaction takes place)
+LC19 (±0.3 or ±1.0)	Settlements at the pier's footing (only if liquefaction takes place)
+LC15, 16	Thermal loads
+LC201-260	Traffic load (LM2)

In case liquefaction occurs, the static combinations 1100, 1200 and 1300 including LC 17, 18 and 19, take into the full settlement combined with 100% of the rotation in one direction and 30% of the rotation in the other direction.

12.7 Load Combinations at Serviceability Limit State (SLS)

The load combinations at the SLS are:

$$\text{Characteristic combination: } \sum_{j\geq 1} G_{kj} \text{"+"} Q_{k1} \text{"+"} \sum_{i\geq 1} \psi_0 \cdot\cdot Q_{ki} \qquad (12.23)$$

$$\text{Frequent combination: } \sum_{j\geq 1} G_{kj} \text{"+"} \psi_{1,1} \cdot Q_{k1} \text{"+"} \sum_{i\geq 1} \psi_{2i} \cdot\cdot Q_{ki} \qquad (12.24)$$

where the ψ factors for road bridges are given in Table 5.4.

The SLS load combinations are:

LC 1600: Characteristic Load Combination

For this combination the tensile stress in the concrete reinforcement should not exceed $0.80f_{yk}$, otherwise the reinforcement is increased. Additionally, the compressive stress in the concrete slab should be less or equal to $0.60f_{ck}$.

LC1	Self weight
+LC2	Superimposed

+LC3	Shrinkage
+LC4	Braking load
+LC7 or LC8	Wind action ±x or ± y
+LC9	Wind action ±z
+LC15, 16	Thermal loads
+LC20-99	Tandem System (LM1)
+LC101-103	UDL 2.5kN/m^2 (LM1)
+LC121-123 or 141-143	UDL 6.50kN/m^2 (LM1)

LC 1700: Characteristic Load Combination

For this combination the tensile stress in the reinforcement should not exceed $0.80f_{yk}$, otherwise the reinforcement is increased. Additionally, the compressive stress in the slab concrete should be less or equal to $0.60f_{ck}$.

LC1	Self weight
+LC2	Superimposed
+LC3	Shrinkage
+LC4	Braking load
+LC7 or LC8	Wind action ±x or ± y
+LC9	Wind action ±z
+LC15, 16	Thermal loads
+LC201-260	Traffic load (LM2)

LC 1800: Frequent Load Combination (Calculation of deformations taking into account cracked deck concrete)

LC1	Self weight
+LC2	Superimposed
+LC3	Shrinkage
+LC15, 16	Thermal loads
+LC320-399	Tandem System (LM1)
+LC401-403	UDL 2.5kN/m^2 (LM1)
+LC421-423 or 441-443	UDL 6.50kN/m^2 (LM1)

12.8 Seismic Load Combinations

The seismic load combination is described as:

$$\sum_{j\geq 1} G_{kj} "+" \sum_{i\geq 1} \psi_{Ei} \cdot\cdot Q_{ki} "+" E \qquad (12.25)$$

where Q are the variable loads, including traffic and thermal loads, while E represents the following earthquake combinations:

E_{Edx} "+" 0.30 E_{Edy} "+" 0.30 E_{Edz}

0.30 E_{Edx} "+" E_{Edy} "+" 0.30 E_{Edz}

0.30 E_{Edx} "+" 0.30 E_{Edy} "+" E_{Edz}

The ψ_E factors for the variable loads are listed in Table 5.5.

The load cases included in the seismic load combinations are:

LC 4000: This combination concerns the pier's columns and the superstructure. It includes the following load cases:

LC1	Self weight
+LC2	Superimposed
+LC3	Shrinkage
+LC600	Uniform traffic load
+LC15, 16	Thermal loads
+LC13*0.3 (±1.0 or ±0.3)	Longitudinal displacement of the pier's footing
+LC14*0.3 (±0.3 or ±1.0)	Transverse displacement of the pier's footing
+LC2010 (±1.0 or ±0.3)/1.50	Earthquake X
+LC2011 (±1.0 or ±0.3)/1.50	Earthquake Y
+LC2012 (±1.0 or ±0.3)	Earthquake Z

LC 13, 14 are taken into account only if the liquefaction is activated, and only if they act unfavorably. Combination 4000 includes 100% of the seismic action and 30% of the pier's footing settlement and rotation, assuming that the movement of the pier's footing will not coincide with the maximum seismic action. In case of liquefaction, another seismic combination is considered, assuming 30% of the seismic action and 100% of the pier's footing settlement and rotation. Thus:

LC 4200: This combination concerns the pier's columns and the superstructure. It includes the following load cases:

LC1	Self weight
+LC2	Superimposed
+LC3	Shrinkage

+LC600	Uniform traffic load
+LC15, 16	Thermal loads
+LC13 (±1.0 or ±0.3)	Longitudinal displacement of the pier's footing
+LC14 (±0.3 or ±1.0)	Transverse displacement of the pier's footing
+LC2010 0.3(±1.0 or ±0.3)/1.50	Earthquake X
+LC2011 0.3(±1.0 or ±0.3)/1.50	Earthquake Y
+LC2012 0.3(±1.0 or ±0.3)	Earthquake Z

12.9 Analyses

Two analyses are carried out for the same bridge:

1. No liquefaction: assuming Seismic Scenario 1 with return period T_{ret} = 225 years (see section 11.1).

2. With liquefaction: assuming Seismic Scenario 2 with return period T_{ret} = 1000 years (see section 11.2). As already mentioned in section 12.8, in this case, the footing movements described by LC17 – LC19 are taken into consideration in the seismic loading combination.

For each case, the corresponding springs and the damping elements at the base of the pier are taken into account, as given in Table 12.4 and Table 12.6, respectively.

Chapter 13

DESIGN OF CONCRETE MEMBERS

13.1 Evaluation of the results

Among the two analyses described in section 12.9, the most unfavorable for the pier is the first case, for which the phenomenon of the liquefaction does not take place. The required reinforcement is similar for the deck's concrete slab for both analyses. The results for the concrete components of the bridge are summarizing in Table 13.1.

Table 13.1: Analyses' results/requirements for concrete members

Πίνακας 13.1: Αποτελέσματα/απαιτήσεις αναλύσεων για στοιχεία από οπλισμένο σκυρόδεμα

Members	Results / Requirement	Analysis 1 (no liquefaction)	Analysis 2 (with liquefaction)
Pier	Longitudinal Reinforcement	187.10cm^2	94.30cm^2
	Stirrups	16.60cm^2	16.60cm^2
	Max compressive force (LC1100)	10081kN	10654kN
Deck slab	Longitudinal Reinforcement	41.2cm^2	46.8cm^2
	Transverse Reinforcemnt	20.3cm^2	27.6cm^2

13.2 Reinforcement of the pier

The maximum required reinforcement of the pier's columns is equal to 187.10cm^2 (Figure 13.1) for the first analysis (no liquefaction). A minimum percentage of 1% is considered and 45Φ25 (220.95cm^2) are used for the columns of the pier.

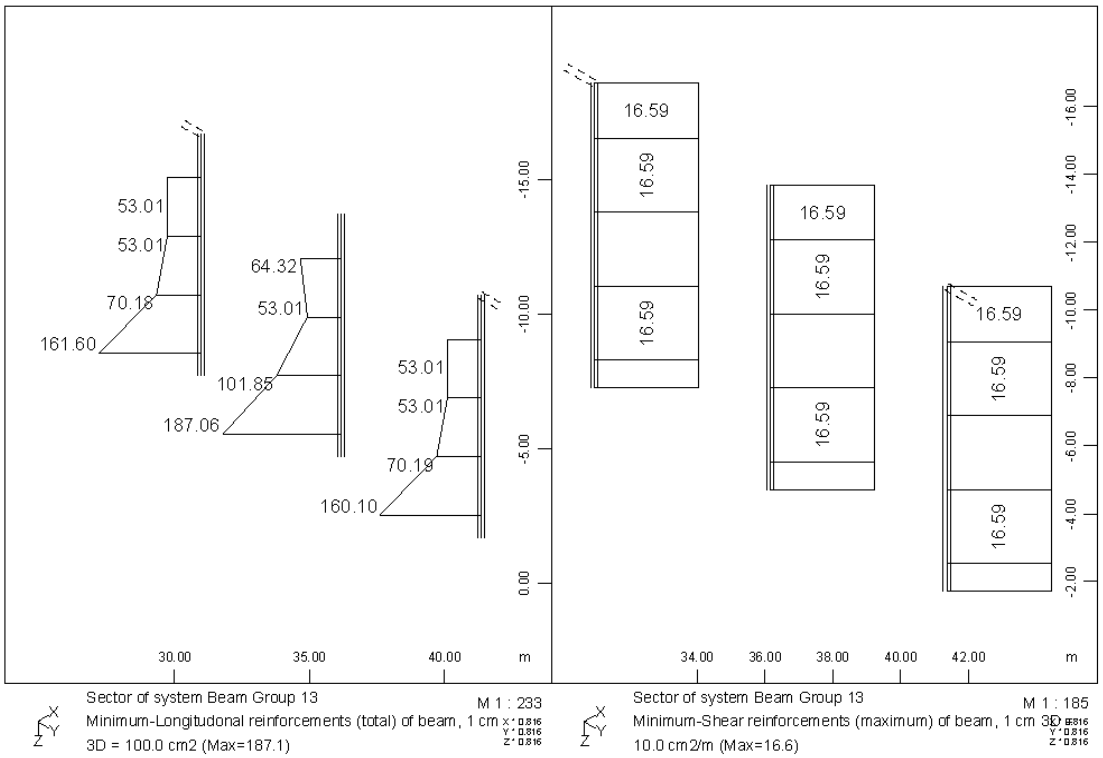

Figure 13.1: Required reinforcement of the pier

Σχήμα 13.1: Απαιτούμενος οπλισμός στύλων μεσοβάθρου

13.3 Pier's Confinement

The maximum compressive load of the piers is for Load Combination 1200 and it is equal to N_c=10654kN (Figure 13.2).

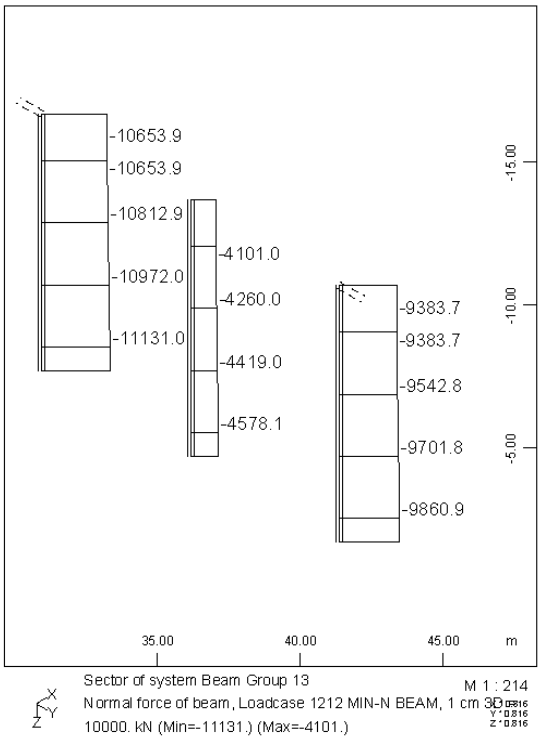

Figure 13.2: Maximum axial force at the pier

Σχήμα 13.2: Μέγιστο αξονικό φορτίο στους στύλους μεσοβάθρου

Since the normalized axial force n_k exceeds the limit of 0.08, as:

$$n_k = \frac{N_c}{f_{ck} A_c} = 10654 / (30000 \times 3.14 \times 1.50^2/4) = 0.20 > 0.08$$

confinement should be provided. The minimum amount of confining reinforcement for a spiral is:

$$\omega_{min} = 1.40 \cdot \frac{A_c}{A_{cc}} \cdot \lambda \cdot n_k \geq 0.18 = 1.40 \times 1.50^2 / 1.34^2 \times 0.37 \times 0.20 = 0.13 < 0.18 \rightarrow \omega = 0.18$$

The mechanical reinforcement ratio is:

$$\min \rho_w = \omega_{min} \frac{f_{cd}}{f_{yd}} \Rightarrow \min \rho_w = 0.18 \times \frac{\frac{30 \times 10^3}{1.5}}{\frac{500 \times 10^3}{1.15}} \Rightarrow \min \rho_w = 0.008$$

Stirrups 2Φ16/15 are used with a volumetric ratio:

$$\rho_w = \frac{4 A_{sp}}{D_{sp} s_L} = 2 \times 4 \times 2.00 cm^2 / (134 cm \times 15 cm) \Rightarrow \rho_w = 0.008 = \min \rho_w$$

The spacing of the stirrups satisfies the limits of:

$s_L = 15cm = 6 d_{bL} = 6 \times 2.5cm = 15cm$ where d_{bL} is the longitudinal bar diameter and

$s_L = 15cm < D_{cc}/5 = 134cm/5 = 26.8cm$ where D_{cc} is the diameter of the confined concrete core.

13.4 Reinforcement of deck slab

The required reinforcement of the deck slab is similar for both analyses. Figure 13.3 shows the one from the second analysis, where the principal direction is parallel to x-axis, while the cross one is parallel to y-axis. The maximum values at the corners of the slab are ignored, as well as the local picks. In the longitudinal direction Φ14/10 is used for the upper and lower reinforcement, while in the transverse direction Φ12/10 is chosen.

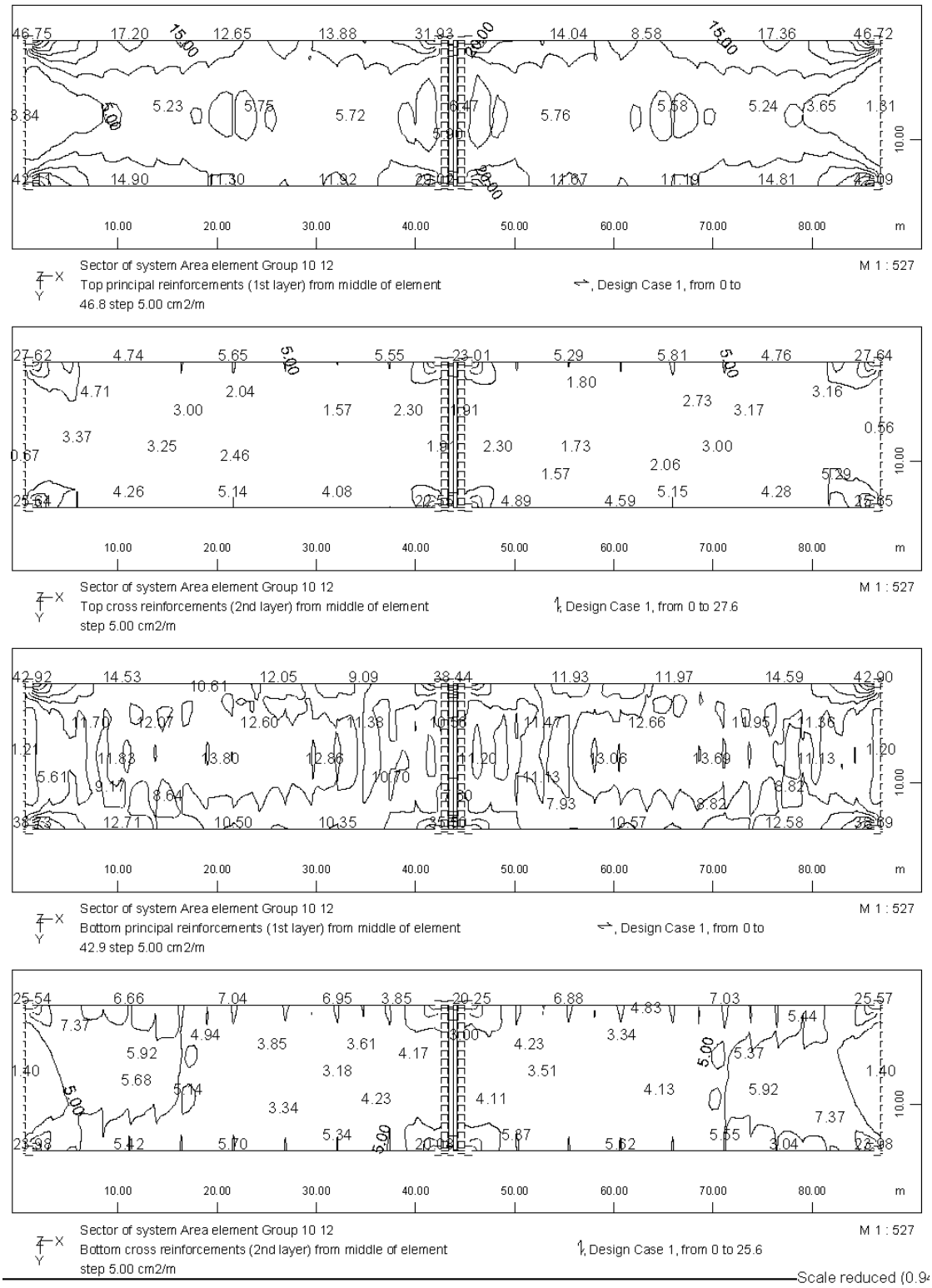

Figure 13.3: Required reinforcement of the concrete deck slab

Σχήμα 13.3: Απαιτούμενος οπλισμός πλάκας καταστρώματος

Chapter 14

DESIGN OF STEEL MEMBERS

14.1 Evaluation of the results

Among the two analyses described in section 12.9, the maximum internal forces in the steel members are encountered for the static combination of the second analysis (with liquefaction). The analyses' results are listed in Table 14.1.

Table 14.1: Analyses' results for the steel members

Πίνακας 14.1: Αποτελέσματα αναλύσεων για τα μεταλλικά στοιχεία

Members	Results	Analysis 1 (no liquefaction)	Analysis 2 (with liquefaction)	Max. Exploitation Factor
Arches	minN (LC1100)	-6260kN	-6497kN	0.98
	maxM_y (LC1100)	1035kNm	1064kNm	
	maxM_z (LC1100)	875kNm	1544kNm	
Transverse bracing	maxN (LC1100)	157.9kN	345.4kN	0.49
	minN (LC1100)	-124.1kN	-223.1kN	
	maxM_y (LC1100)	29.1kNm	32.9kNm	
	maxM_z (LC1100)	14.1kNm	14.8kNm	
Diagonal bracing	minN (LC1100)	-119.3kN	-323.2kN	0.96
Hangers	maxN (LC1100)	1212kN	1245kN	0.87
Transverse beams	maxN (LC1100)	3326kN	3356kN	0.94
	minN	-1121kN (LC4100)	-1554kN (LC1100)	
	maxM_y (LC1100)	2032kNm	2038kNm	
	maxM_z (LC1100)	75kNm	115.9kNm	
Main beams	maxN (LC1100)	5275kN	5746kN	0.60
	minN (LC1100)	-1066kN	-1539kN	
	maxM_y (LC1100)	1412kNm	2166kNm	
	maxM_z (LC1100)	81.2kNm	135.9kNm	

14.2 Arches

As concluded in section 7.2, for the check of the arches the critical force in the arches will be considered equal to N_{cr}=36073kN. The non-dimensional slenderness is calculated as:

$$\bar{\lambda} = \sqrt{\frac{Af_y}{N_{cr}}} = \sqrt{\frac{458.67cm^2 \cdot 35.5kN/cm^2}{36073kN}} = 0.67$$

The reduction factor χ for buckling curve c (cold formed hollow sections) is equal to χ=0.742 and the design buckling resistance of the arches is:

$$N_{b,Rd} = \frac{\chi A f_y}{\gamma_{M1}} = \frac{0.74 \cdot 458.67 cm^2 \cdot 35.5 kN/cm^2}{1.1} = 10953.87 kN$$

Since circular hollow sections are not susceptible to lateral torsional buckling, χ_{LT}=1.00. Considering also conservatively k_{yy}=k_{yz}=1.0, all elements of the arches should satisfy:

$$EF = \frac{N_{Ed}}{N_{b,Rd}} + \frac{M_{y,Ed} + M_{z,Ed}}{M_{b,Rd}} \leq 1.00$$

where

$$M_{b,Rd} = \frac{W_{pl} f_y}{\gamma_{M1}} = \frac{10660.67 cm^3 \cdot 35.5 kN/cm^2}{1.1} = 344049 kNcm$$

The maximum compression force and bending moments $M_{Ed,y}$ and $M_{Ed,z}$ are observed for Load Combination 1100 of the second analysis (with liquefaction). Figure 14.1 illustrates the diagrams of the maximum axial force and the corresponding bending moments. In Figure 14.2 the maximum bending moment $M_{Ed,y}$ is shown with the corresponding axial force and bending moment $M_{Ed,z}$ are plotted, while the corresponding diagrams for the Load Combination of the maximum bending moment $M_{Ed,z}$ are given in Figure 14.3. The maximum exploitation factor for the arches is EF=0.98<1.00.

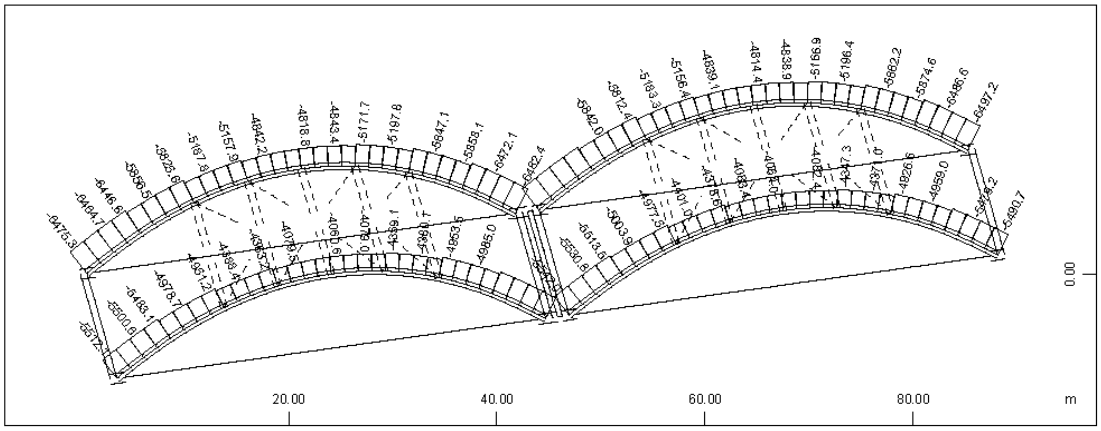

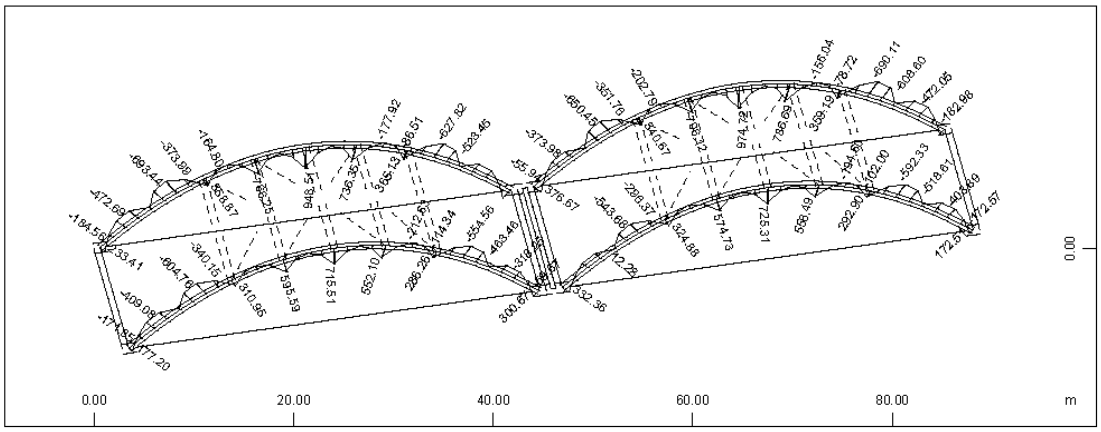

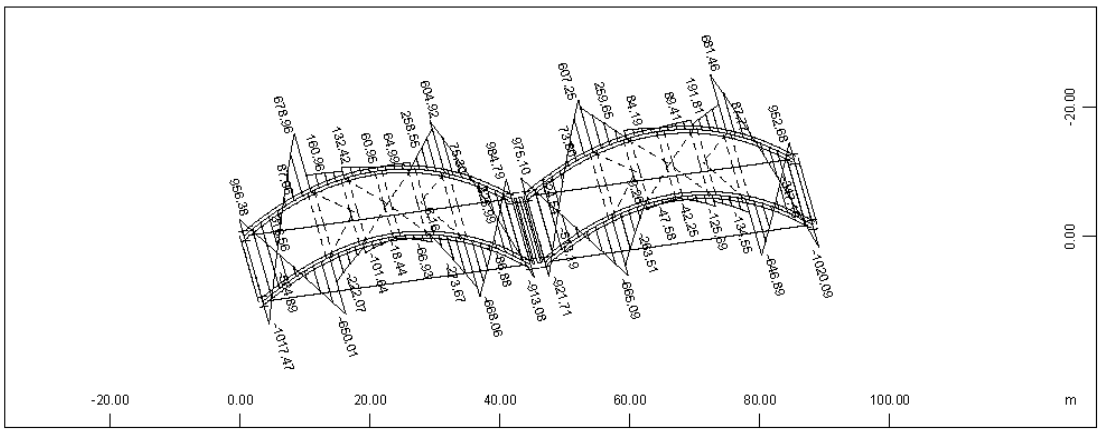

Figure 14.1: Internal forces for the load combination with the maximum axial force at the arches

Σχήμα 14.1: Εντατικά μεγέθη για τον συνδυασμό φορτίσεων με τη μέγιστη αξονική δύναμη στα τόξα

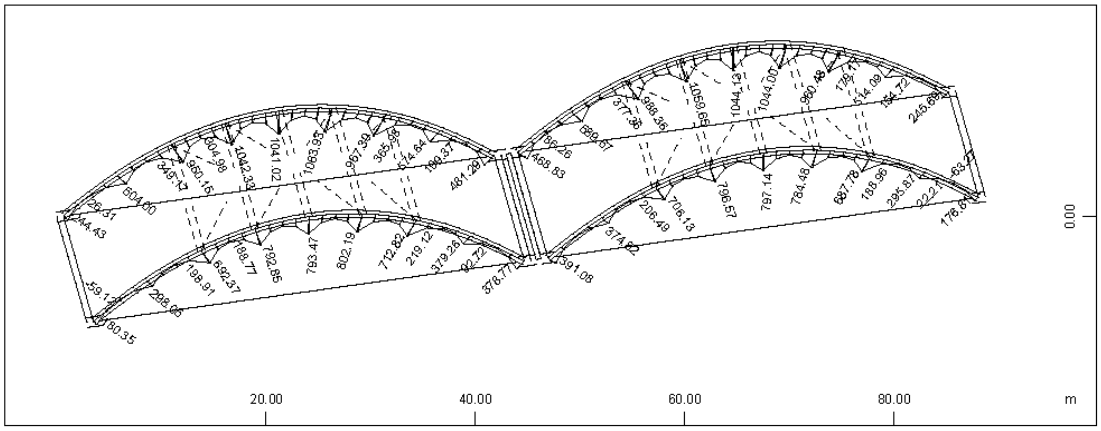

Sector of system Group 3 10...12
Bending moment My of beam, Loadcase 1101 MAX-MY BEAM, 1 cm 3D = 2000. kNm (Min=-63.3)
(Max=1064.)
M 1 : 600
X * 0.990
Y * 0.714
Z * 0.714

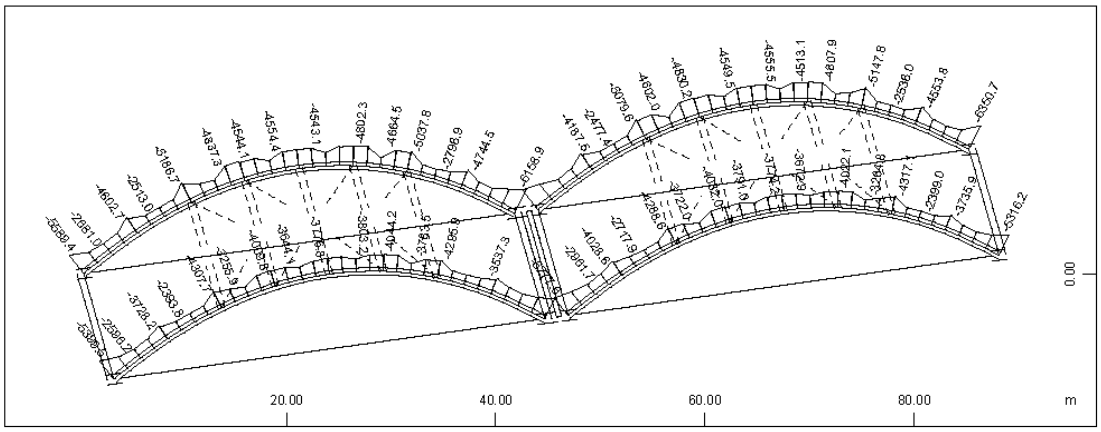

Sector of system Group 3 10...12
Normal force of beam, Loadcase 1101 MAX-MY BEAM, 1 cm 3D = 15000. kN (Min=-6351.) (Max=-2309.)
M 1 : 600
X * 0.990
Y * 0.714
Z * 0.714

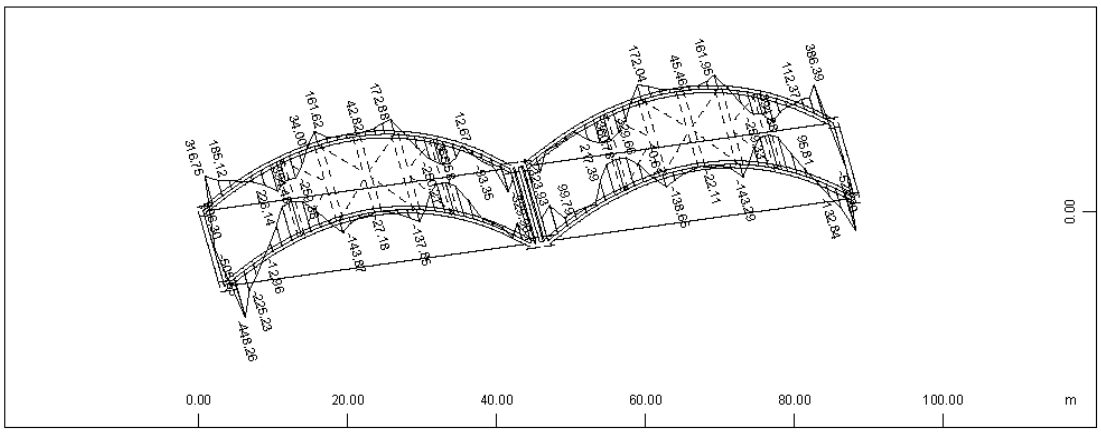

Sector of system Group 3 10...12
Bending moment Mz of beam, Loadcase 1101 MAX-MY BEAM, 1 cm 3D = 500.0 kNm (Min=-522.2)
(Max=506.3)
M 1 : 843
X * 0.990
Y * 0.714
Scale reduced (0.9

Figure 14.2: Internal forces for the load combination with the maximum bending moment $M_{Ed,y}$ at the arches

Σχήμα 14.2: Εντατικά μεγέθη για τον συνδυασμό φορτίσεων με τη μέγιστη καμπτική ροπή $M_{Ed,y}$ στα τόξα

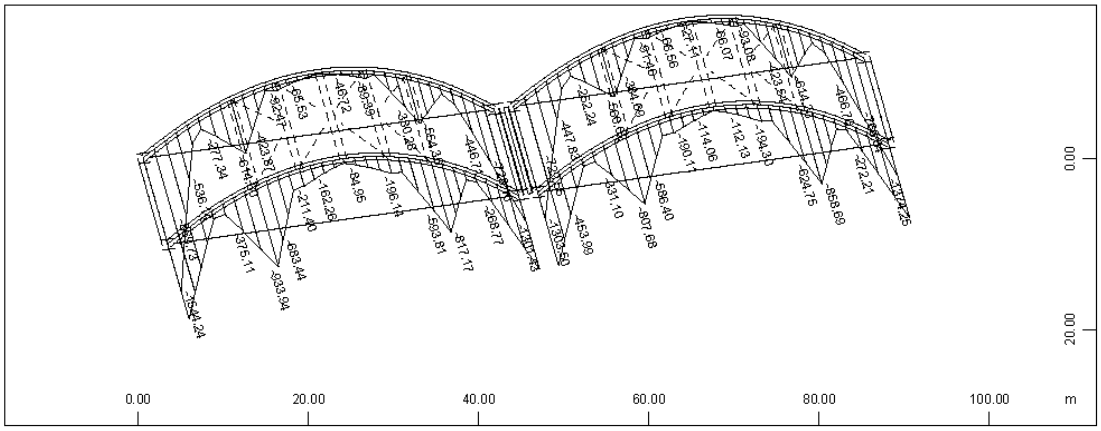

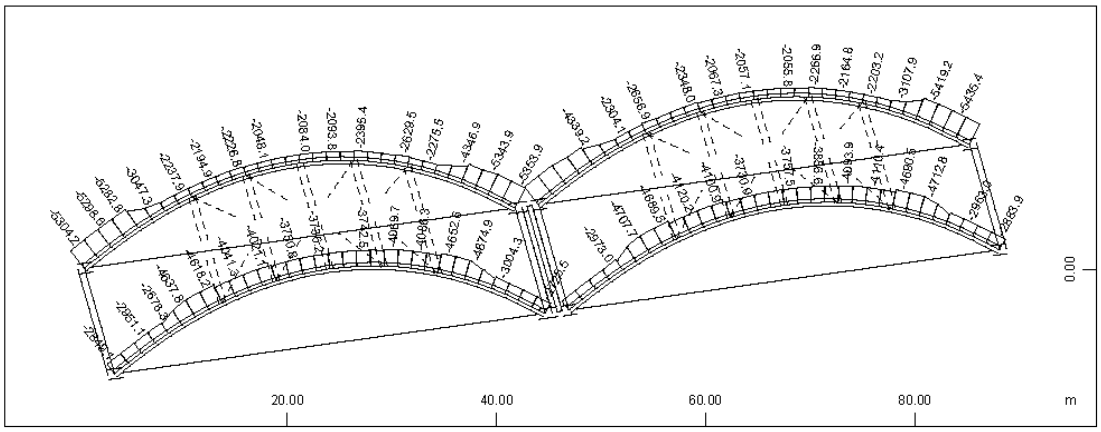

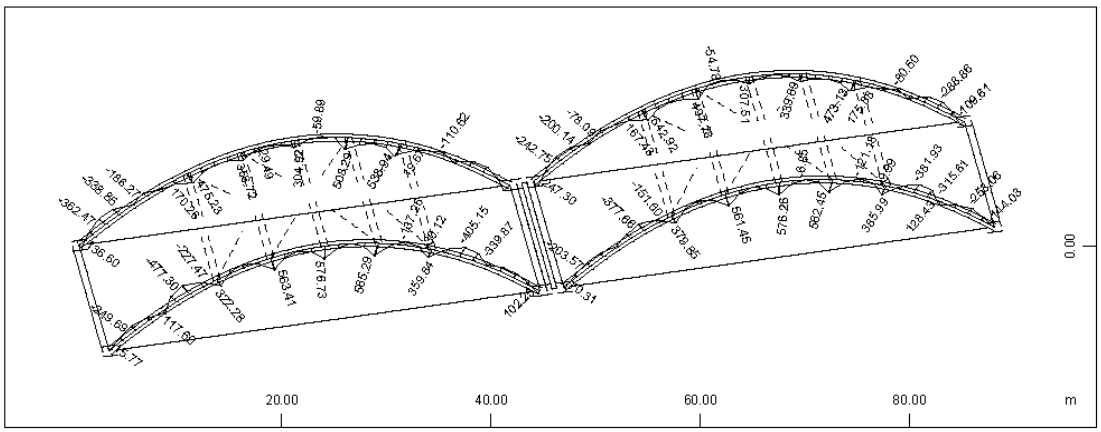

Figure 14.3: Internal forces for the load combination with the maximum bending moment $M_{Ed,z}$ at the arches

Σχήμα 14.3: Εντατικά μεγέθη για τον συνδυασμό φορτίσεων με τη μέγιστη καμπτική ροπή $M_{Ed,z}$ στα τόξα

14.3 Transverse bracing members

The non-dimensional slenderness for the transverse bracing members is calculated as:

$$\bar{\lambda} = \frac{L}{\pi}\sqrt{\frac{Af_y}{EI}} = \frac{1470cm}{\pi}\sqrt{\frac{59.44cm^2 \cdot 35.5kN/cm^2}{21000kN/cm^2 \cdot 4160cm^4}} = 2.30$$

and the reduction factor χ for buckling curve c is χ=0.15. Thus, the design buckling resistance of the transverse bracing members is:

$$N_{b,Rd} = \frac{\chi A f_y}{\gamma_{M1}} = \frac{0.15 \cdot 59.44cm^2 \cdot 35.5kN/cm^2}{1.1} = 287.74kN$$

The maximum compression force at the transverse bracing members is developed for the Load Combination 1100 of the second analysis (with liquefaction) and it is equal to N_{Ed}=223.1kN<$N_{b,Rd}$. For this combination the bending moment is negligible (Figure 14.4). The maximum bending moment appears for the same Load Combination 1100 with N_{Ed}=244.7kN (tensile force), N_{Ed}=-49.4kN (compressive force), $M_{y,Ed}$=32.9kNm, $M_{z,Ed}$=12.5kNm (Figure 14.4). Since the following criterion is satisfied:

N_{Ed}=244.7kN<0.25 × $N_{pl,Rd}$=0.25 × 2110.12kN=527.53kN

where

$N_{pl,Rd}$=Af_y=59.44cm^2 × 35.5kN/cm^2=2110.12kN

no effect of the axial force is taken into account. Hence:

$$\left[\frac{M_{y,Ed}}{M_{Rd}}\right]^2 + \left[\frac{M_{z,Ed}}{M_{Rd}}\right]^2 = \left[\frac{3290kNcm}{14446.24kNcm}\right]^2 + \left[\frac{1350kNcm}{14446.24kNcm}\right]^2 = 0.06 < 1.00$$

where

$$M_{Rd} = \frac{W_{pl} f_y}{\gamma_{M1}} = \frac{447.63cm^3 \cdot 35.5kN/cm^2}{1.1} = 14446.24kNcm$$

Since circular hollow sections are not susceptible to lateral torsional buckling, χ_{LT}=1.00. Considering also conservatively k_{yy}=k_{yz}=1.0, the transverse bracing members should satisfy:

$$EF = \frac{N_{Ed}}{N_{pl,Rd}} + \frac{M_{y,Ed} + M_{z,Ed}}{M_{b,Rd}} \le 1.00 \Rightarrow EF = \frac{244.70kN}{2110.12kN} + \frac{3290kNcm + 1350kNcm}{14446.24kNcm} = 0.44 < 1.00$$

and

$$EF = \frac{N_{Ed}}{N_{b,Rd}} + \frac{M_{y,Ed} + M_{z,Ed}}{M_{b,Rd}} \le 1.00 \Rightarrow EF = \frac{49.40kN}{287.74kN} + \frac{3290kNcm + 1350kNcm}{14446.24kNcm} = 0.49 < 1.00$$

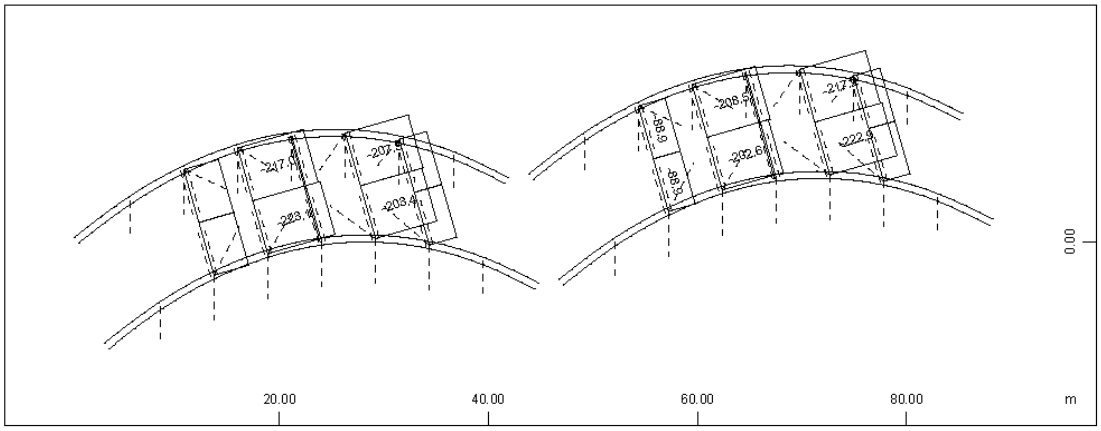

Sector of system Beam Group 3
Structure
Normal force of beam, Loadcase 1112 MIN-N BEAM, 1 cm 3D = 200.0 kN (Min=-223.1) (Max=5.45)

M 1 : 600
X * 0.990
Y * 0.714
Z * 0.714

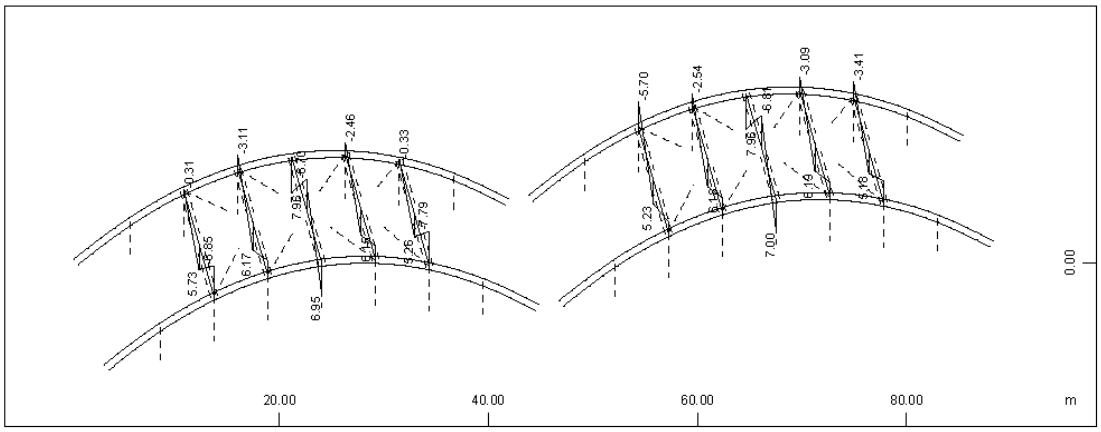

Sector of system Beam Group 3
Structure
Bending moment My of beam, Loadcase 1112 MIN-N BEAM, 1 cm 3D = 10.0 kNm (Min=-7.79) (Max=7.96)

M 1 : 600
X * 0.990
Y * 0.714
Z * 0.714

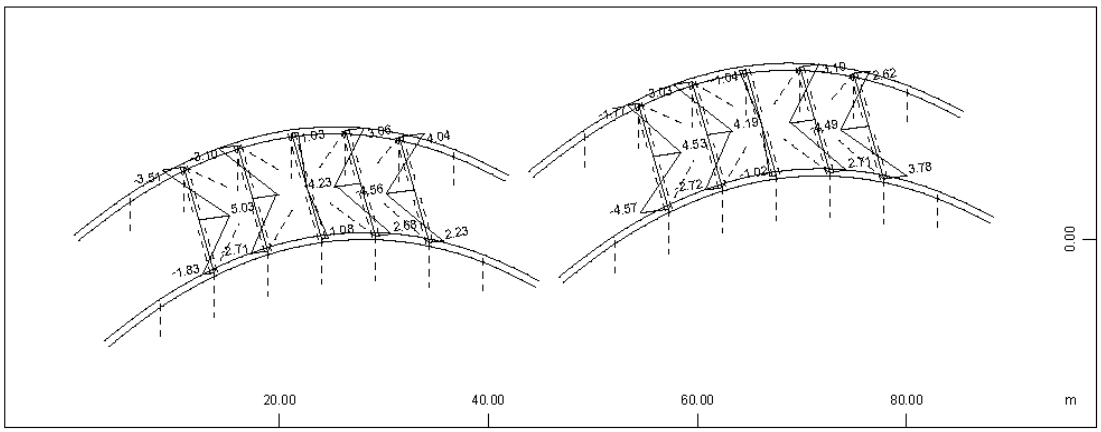

Sector of system Beam Group 3
Structure
Bending moment Mz of beam, Loadcase 1112 MIN-N BEAM, 1 cm 3D = 10.0 kNm (Min=-4.57) (Max=5.03)

M 1 : 600
X * 0.990
Y * 0.714

Scale reduced (0.9

Figure 14.4: Internal forces for the load combination with the maximum axial force at the transverse bracing members

Σχήμα 14.4: Εντατικά μεγέθη για τον συνδυασμό φορτίσεων με τη μέγιστη αξονική δύναμη στα εγκάρσια μέλη των συνδέσμων δυσκαμψίας

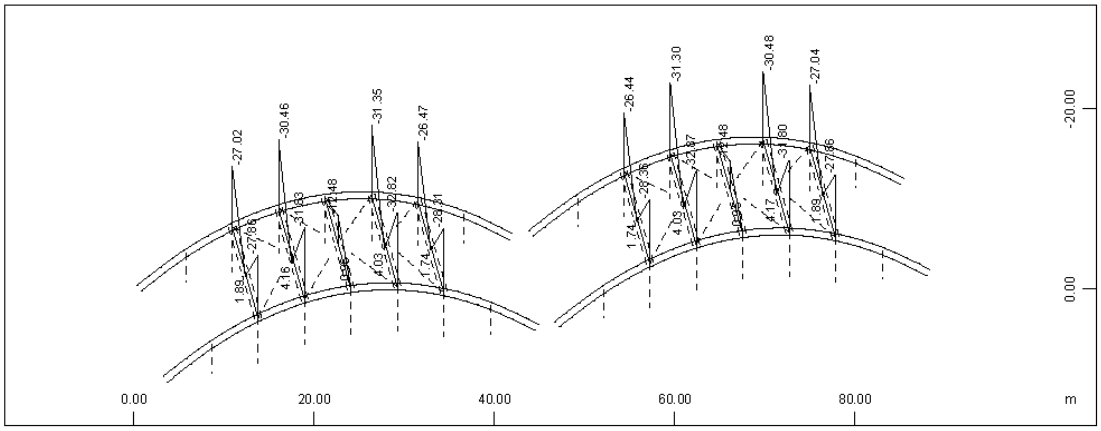

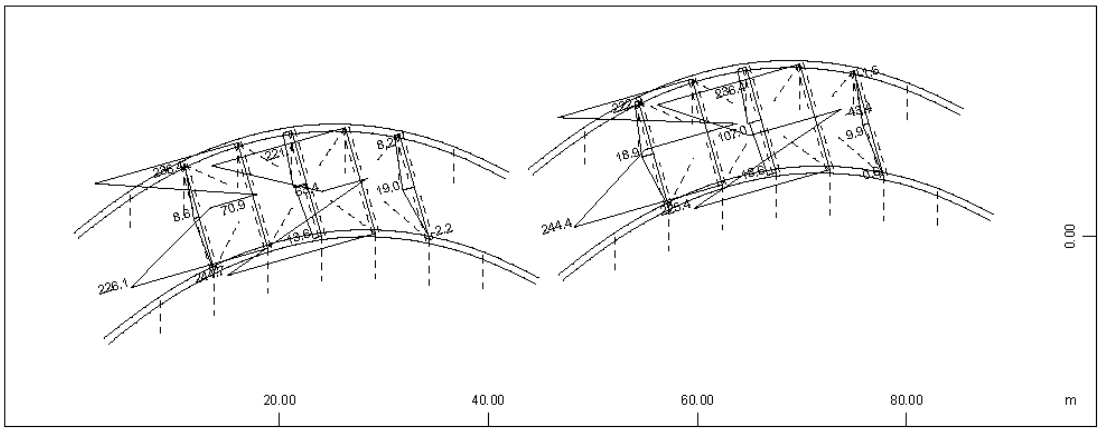

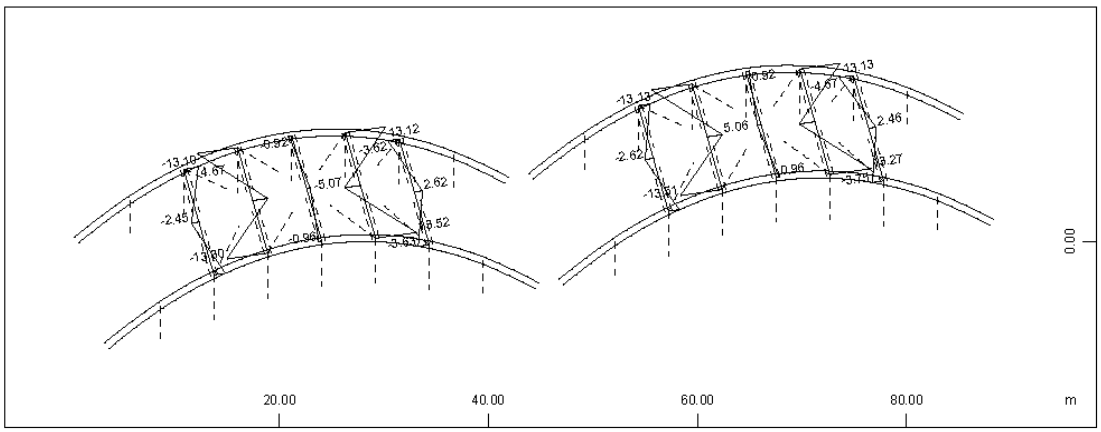

Figure 14.5: Internal forces for the load combination with the maximum bending moment at the transverse bracing members

Σχήμα 14.5: Εντατικά μεγέθη για τον συνδυασμό φορτίσεων με τη μέγιστη καμπτική ροπή στα εγκάρσια μέλη των συνδέσμων δυσκαμψίας

14.4 Diagonal bracing members

The non-dimensional slenderness for the diagonal bracing members is calculated as:

$$\bar{\lambda} = \frac{L}{\pi}\sqrt{\frac{Af_y}{EI}} = \frac{913cm}{\pi}\sqrt{\frac{61.18cm^2 \cdot 35.5kN/cm^2}{21000kN/cm^2 \cdot 1868cm^4}} = 2.16$$

and the reduction factor χ for buckling curve c is χ=0.17. Thus, the design buckling resistance of the diagonal bracing members is:

$$N_{b,Rd} = \frac{\chi A f_y}{\gamma_{M1}} = \frac{0.17 \cdot 61.18cm^2 \cdot 35.5kN/cm^2}{1.1} = 335.66kN$$

The maximum compression force at the diagonal bracing members is developed for the seismic Load Combination 1100 of the second analysis (with liquefaction) and it is equal to N_{Ed}=323.2kN<$N_{b,Rd}$ (Figure 14.6).

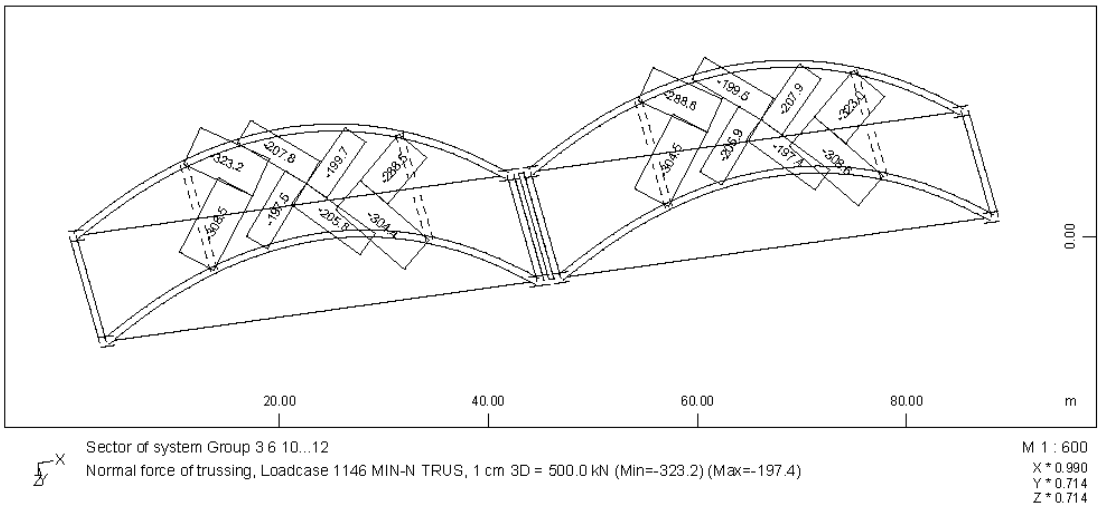

Figure 14.6: Maximum axial forces at the diagonal bracing members

Σχήμα 14.6: Μέγιστη αξονική δύναμη στα διαγώνια μέλη των συνδέσμων δυσκαμψίας

14.5 Hangers

The design tension resistance of the hangers is:

$$N_{t,Rd} = \frac{Af_y}{\gamma_{M0}} = \frac{40.29cm^2 \cdot 35.5kN/cm^2}{1.0} = 1430.30kN$$

The maximum tension force at the hangers is developed for Load Combination 1100 for the second analysis (with liquefaction) and it is equal to N_{Ed}=1245kN<$N_{t,Rd}$ (Figure 14.7).

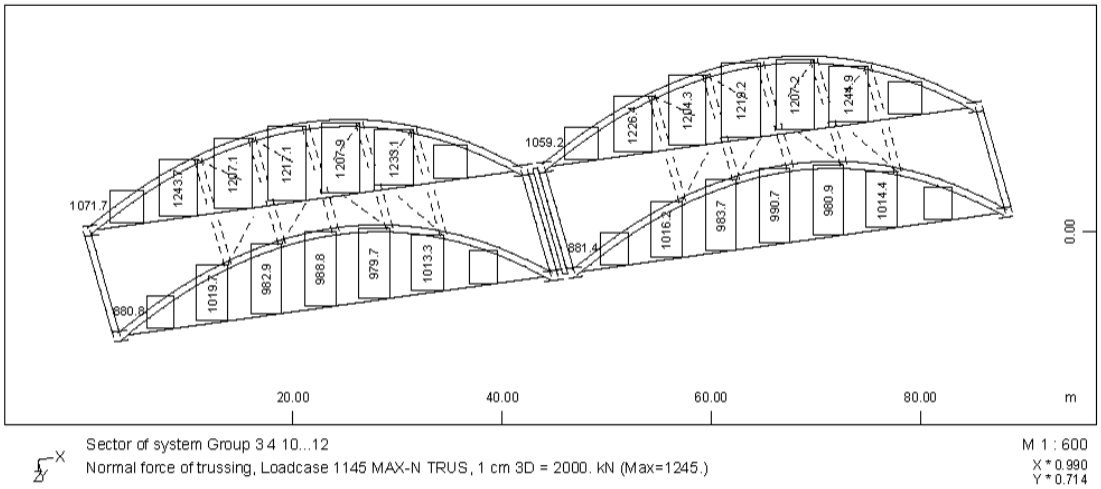

Figure 14.7: Maximum axial forces at the hangers

Σχήμα 14.7: Μέγιστη αξονική δύναμη στους αναρτήρες

14.6 Transverse Beams

The check of the transverse beams during the pouring of the concrete slab given in section 7.6 is also valid for the conventional solution. The maximum bending moment for the beams laterally restrained due to the concrete slab is calculated for Load Combination 1100 for the second analysis (with liquefaction) and it is equal to $M_{Ed,y}$=2038kNm. For the same combination the axial tensile force is N_{Ed}=2753kN, while the bending moment $M_{Ed,z}$ is negligible at the element with the maximum $M_{Ed,y}$ (Figure 14.8).

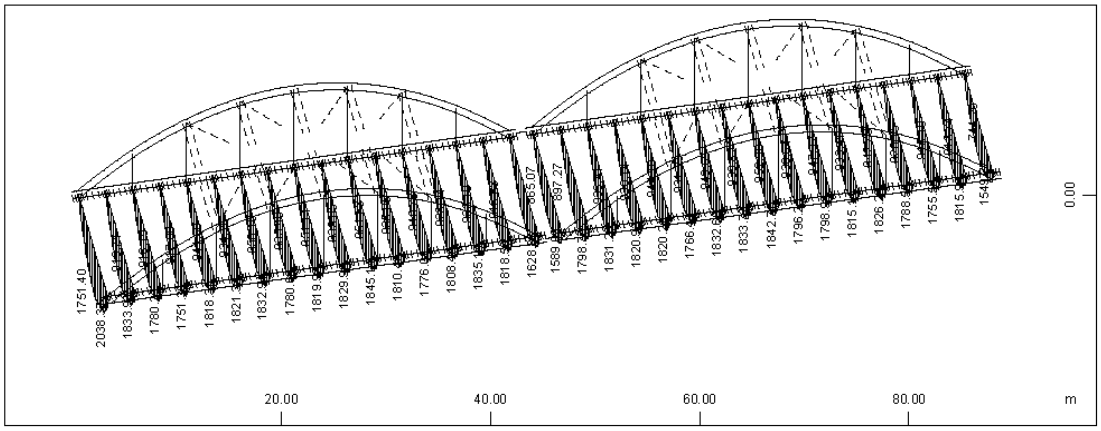

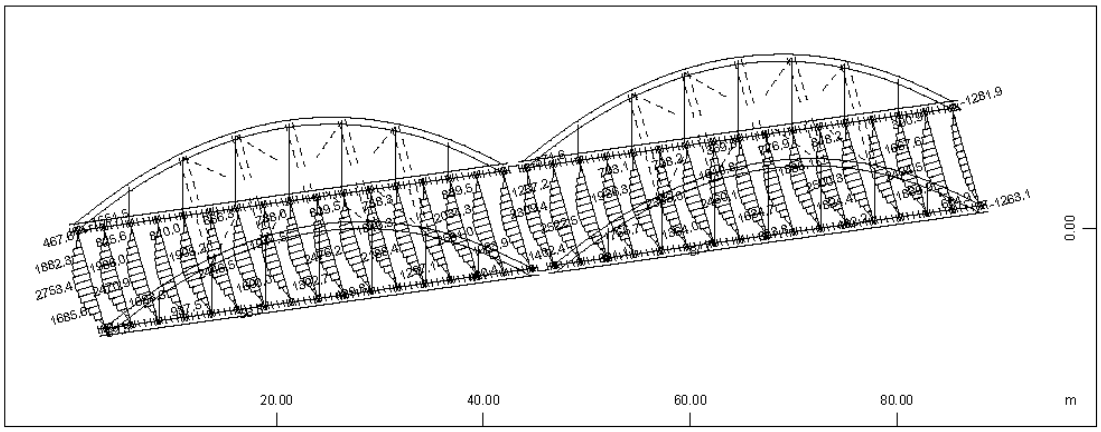

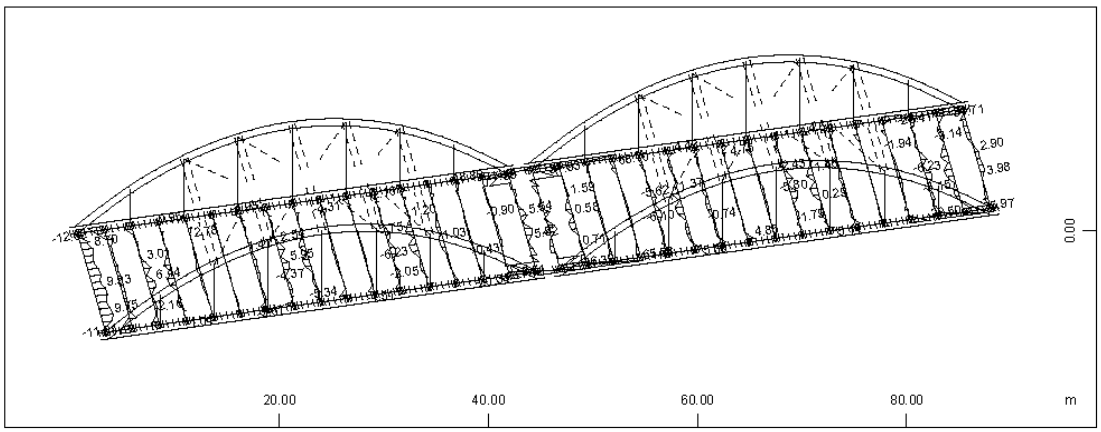

Figure 14.8: Internal forces for the load combination with the maximum bending moment at the transverse beams

Σχήμα 14.8: Εντατικά μεγέθη για τον συνδυασμό φορτίσεων με τη μέγιστη καμπτική ροπή στις διαδοκίδες

The following criteria are satisfied:

$N_{Ed}=2753kN<0.25 \times N_{pl,Rd}=0.25 \times 371.3cm^2 \times 35.5kN/cm^2=0.25 \times 13181.15kN=3295.30kN$

$$N_{Ed} = 2753kN < \frac{h_w t_w f_y}{\gamma_{M0}} = \frac{(90cm - 2 \cdot 3.5cm - 2 \cdot 3.0cm) \cdot 1.85cm \cdot 35.5kN/cm^2}{1.00} = 5056.98kN$$

thus, no effect of the axial force is taken into account. Hence, the design plastic moment resistance is:

$$M_{pl,y,Rd} = \frac{W_{pl,y} f_y}{\gamma_{M0}} = \frac{12580cm^3 \cdot 35.5kN/cm^2}{1.00} = 446590kNcm > M_{Ed,y} = 203800kNcm$$

The maximum compressive axial force is computed also for Static Load Combination 1100, which is equal to N_{Ed}=1554kN for the second analysis (with liquefaction). The maximum bending moment for the same Load Combination is $M_{Ed,y}$=893kNm, while the bending moment $M_{Ed,z}$ is negligible (Figure 14.9). Neglecting, conservatively, the stiffness of the slab of the composite beam, the non-dimensional slenderness for the transverse beams is:

$$\bar{\lambda} = \frac{L}{\pi}\sqrt{\frac{Af_y}{EI}} = \frac{1470cm}{\pi}\sqrt{\frac{371.30cm^2 \cdot 35.5kN/cm^2}{21000kN/cm^2 \cdot 494100cm^4}} = 0.527$$

and the reduction factor χ for buckling curve b is χ=0.871. Since the slab protects the transverse beams from lateral torsional buckling, χ_{LT}=1.00. Thus, the exploitation factor for this load combination is:

$$EF = \frac{N_{Ed}}{N_{b,Rd}} + \frac{M_{y,Ed} + M_{z,Ed}}{M_{b,Rd}} = \frac{1554kN}{10437.07kN} + \frac{89300kNcm}{405990.91kNcm} = 0.37 < 1.00$$

where

$$N_{b,Rd} = \frac{\chi A f_y}{\gamma_{M1}} = \frac{0.871 \cdot 371.30cm^2 \cdot 35.5kN/cm^2}{1.1} = 10437.07kN$$

and

$$M_{b,Rd} = \frac{W_{pl,y} f_y}{\gamma_{M1}} = \frac{12580cm^3 \cdot 35.5kN/cm^2}{1.10} = 405990.91kNcm$$

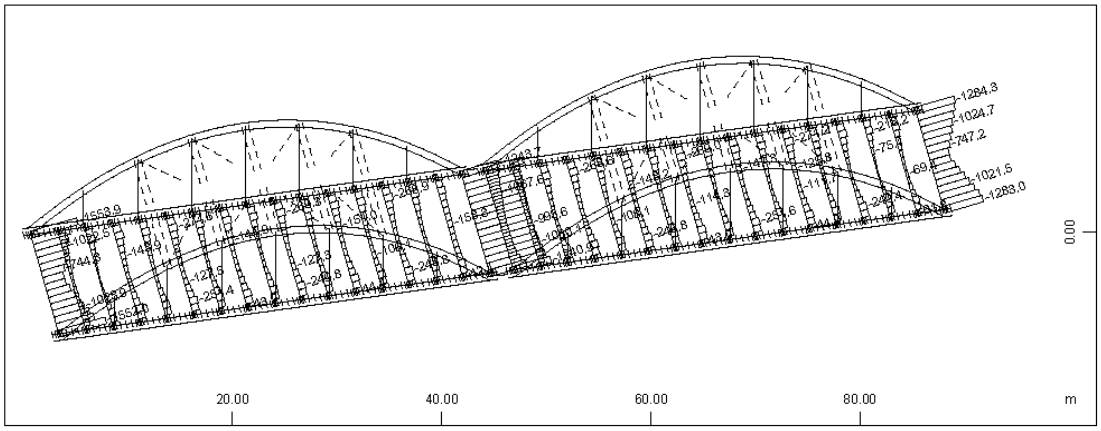

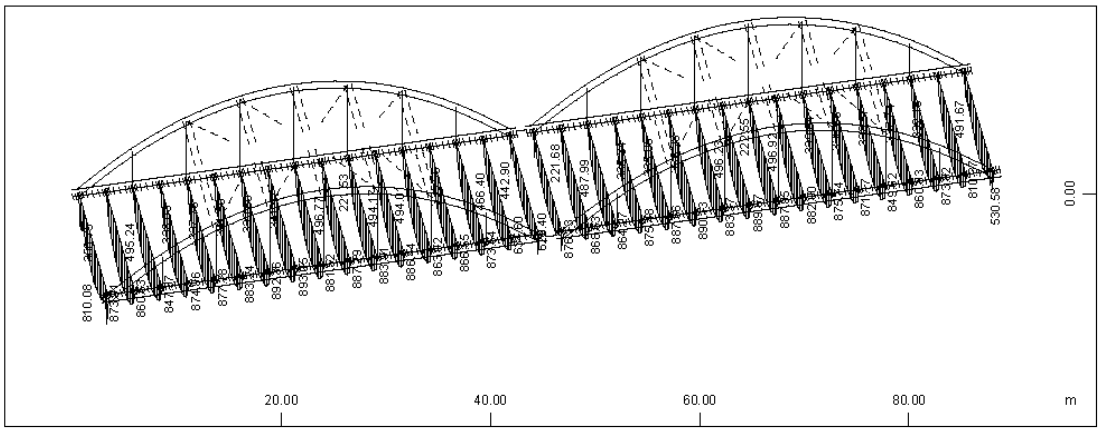

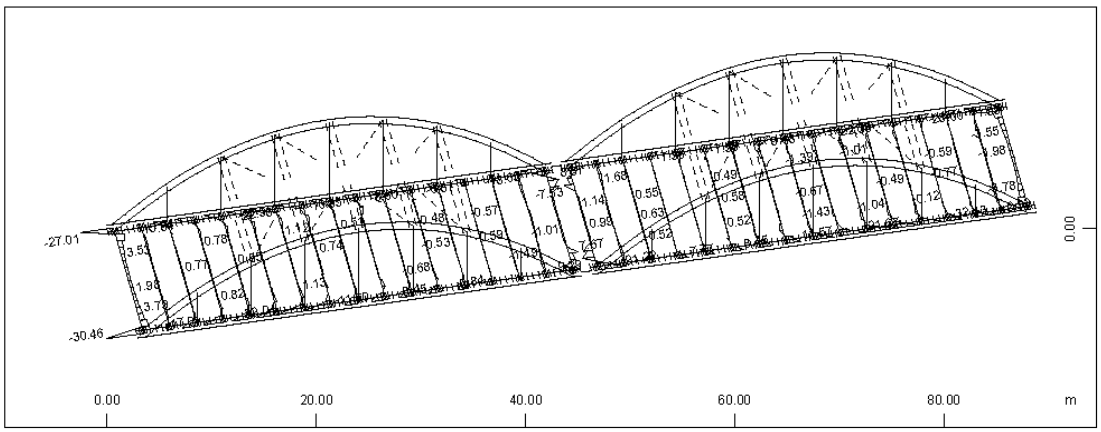

Figure 14.9: Internal forces for the load combination with the maximum compressive axial force at the transverse beams

Σχήμα 14.9: Εντατικά μεγέθη για τον συνδυασμό φορτίσεων με τη μέγιστη θλιπτική δύναμη στις διαδοκίδες

14.7 Main Beams

The check of the main beams during the pouring of the concrete slab is provided in section 7.7. The maximum tensile axial force for the main beams laterally restrained due to the

concrete slab is calculated for Load Combination 1100 of the second analysis (with liquefaction) and it is equal to N_{Ed}=5746kN. For the same combination the bending moment is $M_{Ed,y}$=1914kNm, while the bending moment $M_{Ed,z}$ is negligible at the element with the maximum $M_{Ed,y}$ (Figure 14.10).

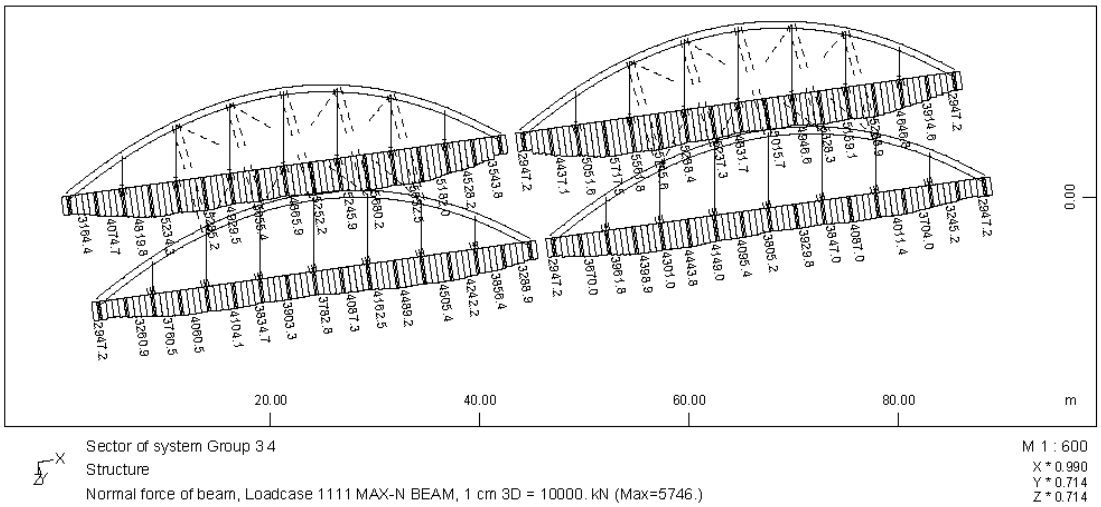

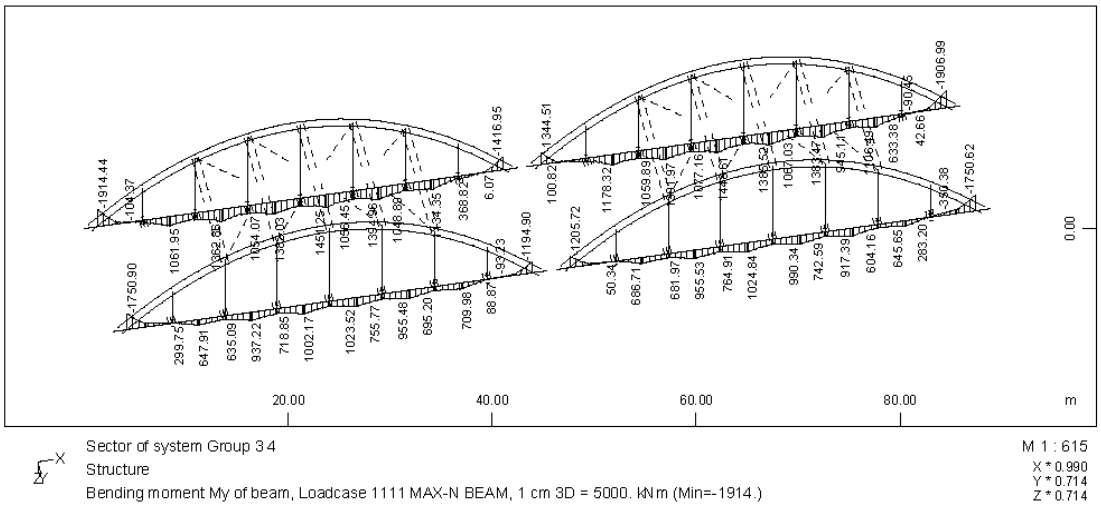

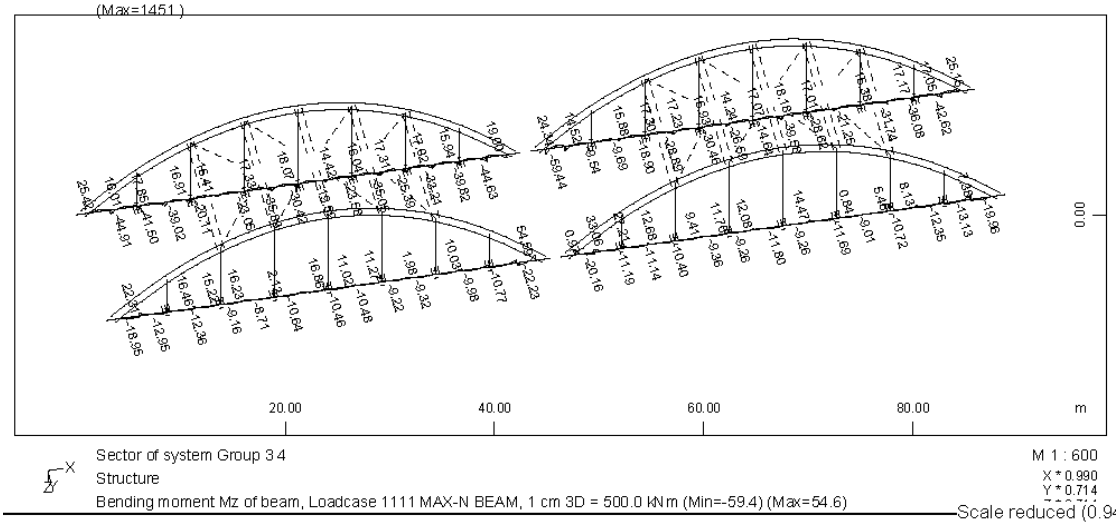

Figure 14.10: Internal forces for the load combination with the maximum tensile axial force at the main beams

Σχήμα 14.10: Εντατικά μεγέθη για τον συνδυασμό φορτίσεων με τη μέγιστη εφελκυστική αξονική δύναμη στις κύριες δοκούς

Since the following criteria are not satisfied:

N_{Ed}=5746kN>0.25 × $N_{pl,Rd}$=3295.30kN

$$N_{Ed} = 5746\text{kN} > \frac{h_w t_w f_y}{\gamma_{M0}} = 5056.98\text{kN}$$

the effect of the axial force must be taken into account. Hence, the reduced design plastic moment resistance due to the axial force is:

$$M_{N,y,Rd} = M_{pl,y,Rd}\frac{1-n}{1-0.5\cdot a} = 446590\text{kNcm}\frac{1-0.44}{1-0.5\cdot 0.43} = 318586.50\text{kNcm} > M_{Ed,y} = 191400\text{kNcm}$$

where n=N_{Ed}/$N_{pl,Rd}$=5746kN/13181.15kN=0.44 and

$$a = \frac{A-2bt_f}{A} = \frac{371.3\text{cm}^2 - 2\cdot 30\text{cm}\cdot 3.5\text{cm}}{371.3\text{cm}^2} = 0.43 < 0.50$$

The maximum compressive axial force for the main beams laterally restrained is equal to N_{Ed}=1539kN under Load Combination 1100 of the second analysis (neglecting the parts of the beams outside the arches), as shown in Figure 14.11. For the same combination the maximum bending moment is $M_{Ed,y}$=797.4kNm, while $M_{Ed,z}$ is negligible.

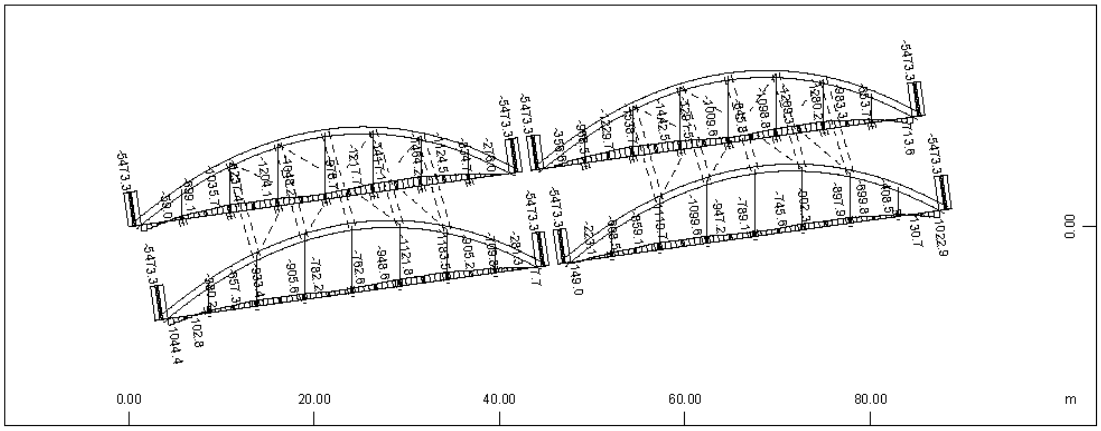

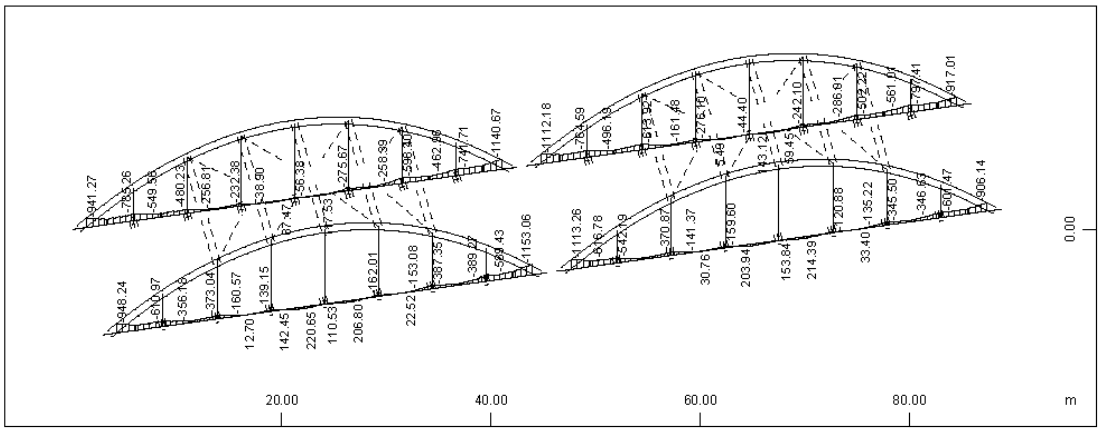

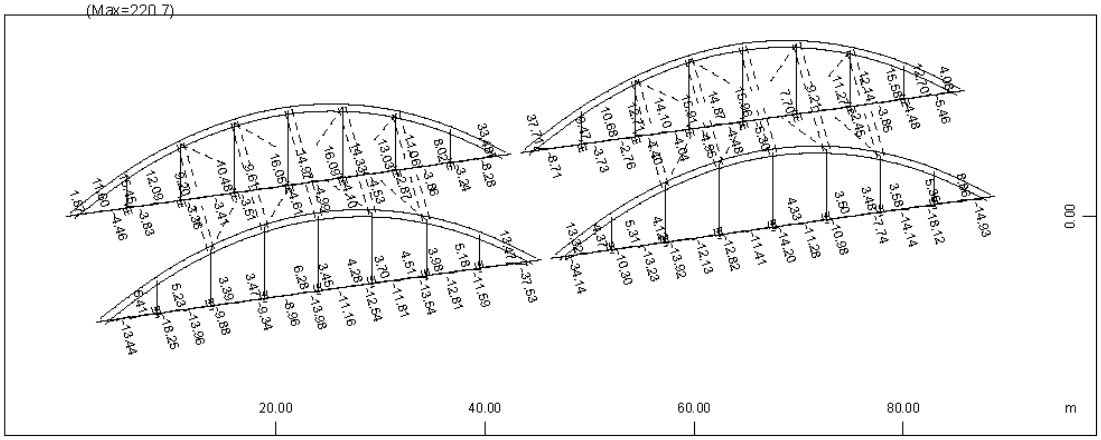

Figure 14.11: Internal forces for the load combination with the maximum compressive axial force at the main beams

Σχήμα 14.11: Εντατικά μεγέθη για τον συνδυασμό φορτίσεων με τη μέγιστη θλιπτική δύναμη στις κύριες δοκούς

As calculated in section 7.7, the critical force of force N_{cr} in the main beams for in plane buckling is N_{cr}=34148.10kN the reduction factor χ for buckling curve b is equal to χ=0.827 and the design buckling resistance of the main beams is $N_{b,Rd}$=9909.83kN.

According to the second method, presented in EC3 – Part 1.1, the interaction factor k_{yy} is given as:

$$k_{yy} = C_{my}\left(1 + (\bar{\lambda}_y - 0.2)\frac{N_{Ed}}{X_y N_{Rd} / \gamma_{M1}}\right) = 0.4 \cdot \left(1 + (0.62 - 0.2)\frac{1539\text{kN}}{9909.83\text{kN}}\right) = 0.43$$

Since the slab protects the main beams from lateral torsional buckling, χ_{LT}=1.00. Thus, the exploitation factor for this load combination is:

$$EF = \frac{N_{Ed}}{N_{b,Rd}} + \frac{k_{yy} M_{y,Ed}}{M_{b,Rd}} = \frac{1539\text{kN}}{9909.83\text{kN}} + \frac{0.43 \cdot 79700\text{kNcm}}{1.00 \cdot \frac{446590\text{kNcm}}{1.1}} = 0.24 < 1.00$$

For reasons of constructability of the connection of the transverse beams on the main ones, the same profile is used for both groups of beams, although the exploitation factor of the main beams is much smaller than 1.

Chapter 15

PERFORMANCE AT SERVICEABILITY LIMIT STATE

15.1 Maximum compressive stress of the deck slab

As mentioned in section 12.7 for the characteristic load combination, the compressive stress of the concrete slab should not exceed the value of $0.60f_{ck}$=21MPa. The maximum compressive stress is obtained for load combination 1600 of both analyses and it is equal to 16.6MPa (Figure 15.1).

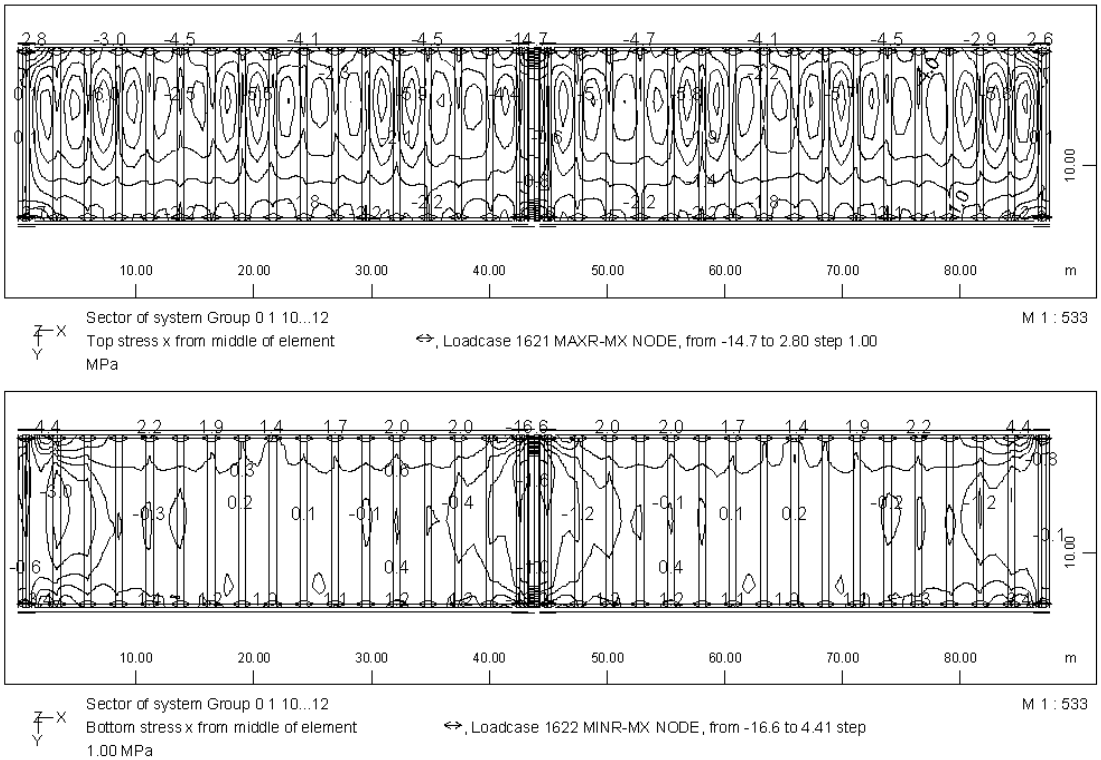

Figure 15.1: Maximum compressive stresses of the deck slab for SLS (characteristic) load combination

Σχήμα 15.1: Μέγιστη θλιπτική τάση στην πλάκα καταστρώματος για τους συνδυασμούς λειτουργικότητας (χαρακτηριστικός)

15.2 Maximum deformation of the deck

As mentioned in section 12.7 the deformation of the deck is calculated for the frequent load combination of both analyses. In Figure 15.2 the maximum deflection of the main and transverse beams is illustrated, arising at 72.6mm for the main beams (72.6mm<

L/300=42000/300=140mm) and 91.6mm-72.6mm=19.0mm for the transverse ones (19.0mm<L/300=14700mm/300=49mm).

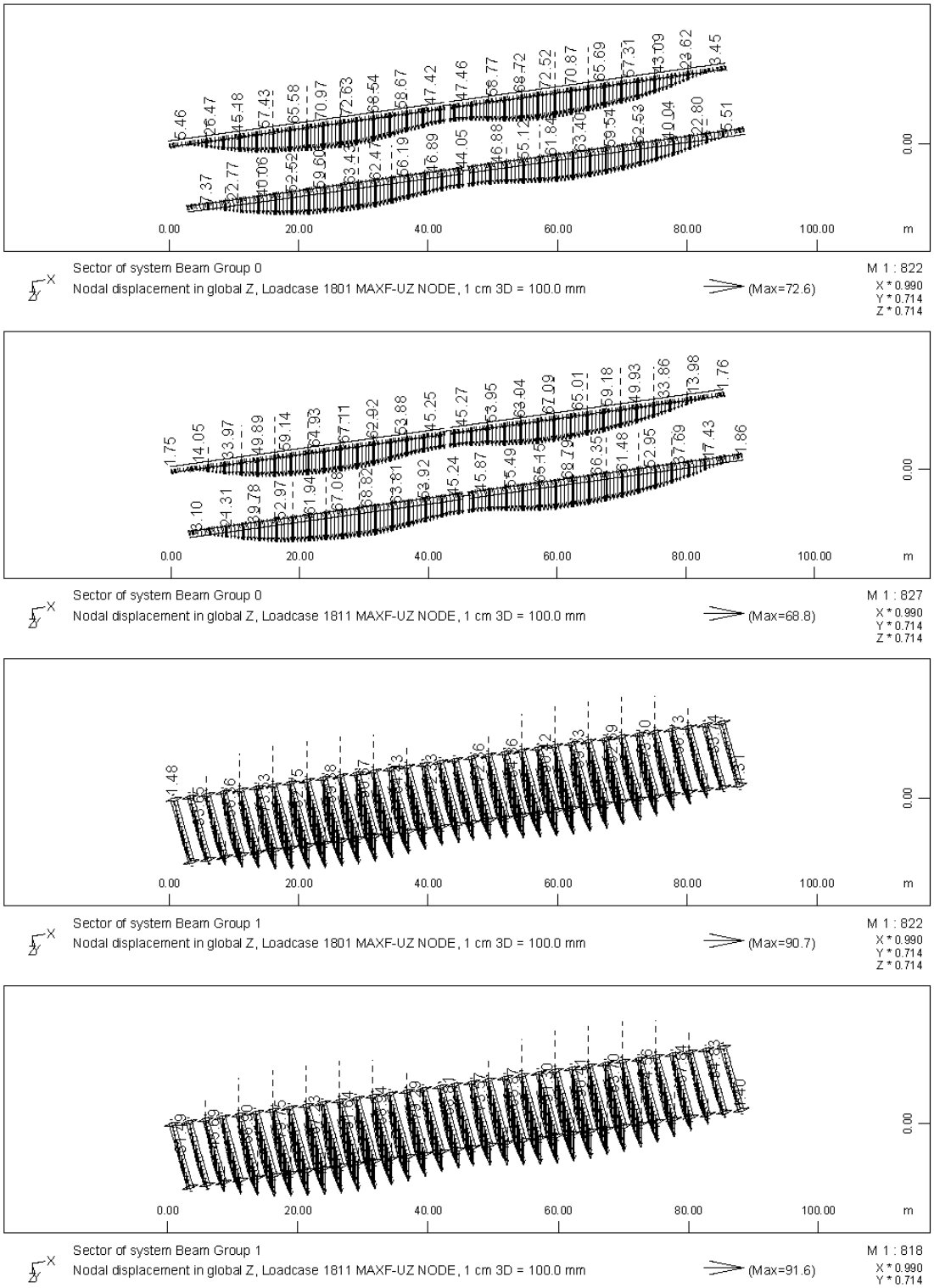

Figure 15.2: Deflection of the deck's beams for SLS (frequent) load combination

Σχήμα 15.2: Βέλος δοκών καταστρώματος για τους συνδυασμούς λειτουργικότητας (συχνός)

Chapter 16

CHECK OF BEARINGS AND EXPANSION JOINTS

16.1 Check of bearings for the case of no liquefaction

	parallel to axis:	x		y	
Dimensions:		80	x	80	cm^2
Number of elastomeric layers:				9	
Thickness of an indivicual elastomeric layer:				18	mm
Total thickness:				162	mm

Axial loads	most loaded bearing		
Permanent:	1351.00 kN		
Superimposed:	845.30 kN	: N_g =	2196.30 KN
Traffic load:	1438.40 kN	: N_p =	1438.40 KN
Earthquake z-z:	522.00 kN	$N_{max,st}$ =	3634.70 KN
	less loaded bearing		
Permanent:	1351.00 kN		
Superimposed:	845.00 kN	$N_{min,st}$ =	2196.00 KN
Earthquake z-z:	522.00 kN		

Displacements				
Braking load:	23.70 mm			
Shrinkage:	4.00 mm			
Uniform difference of temperature ΔT = -41°C:	18.00 mm			
Earthquake x-x:	190.90 mm			
Earthquake y-y:	174.20 mm			
Rotations				
permanent:	α_x =	0.212×10^{-3} rad	α_y =	0.000×10^{-3} rad
superimposed:	α_x =	0.554×10^{-3} rad	α_y =	0.413×10^{-3} rad
traffic load:	α_x =	2.891×10^{-3} rad	α_y =	0.110×10^{-3} rad

A. Check for static combinations (according to DIN 4141 / Part 14)

Total displacement d_{td} = 45.70 mm

Shear strain γ_{td} = 0.28 < $\gamma_{\varepsilon n}$ = 0.70 OK

Design pressure

$\sigma_{max}=N_{o\ddot{u}}/A=$	5.68 MPa	<	15,00 MPa		
$\sigma_{min}=N_g/A=$	3.43 MPa	<	5.00 MPa	ANCHORAGE IS REQUIRED	

Angular rotation about x	$\varphi_{td,x}$= 0.0037 rad	<	$\varphi_{\varepsilon n}=n\times\varphi_{1,\varepsilon n}$ = 0.0180 rad	OK	
Angular rotation about y	$\varphi_{td,y}$= 0.0005 rad	<	$\varphi_{\varepsilon n}=n\times\varphi_{1,\varepsilon n}$ = 0.0180 rad	OK	

B. Check for seismic combinations (according to EC8-2)

Apparent conventional shear modulus:	G_g=	900 kPa			
Shear modulus:	G_b=	1125 kPa			
Lower bound design properties:	$G_{b,min}$=	1125 kPa			
Upper bound design properties:	$G_{b,max}$=	1350 kPa			
Displacement +x:	d_{Edx} =	203.9 mm			
Displacement +y:	d_{Edy} =	52.3 mm			
Total displacement	d_{Ed} =	210.5 mm			
Design shear strain due to horizontal displacement	$\varepsilon_{q,d}$=	1.30	<2.0		OK
	S =	11.11			
	A_r =	4350.72 cm^2			
	N_{sd} =	2640.58 kN			
	σ_e =	6069.29 kPa			
Design strain due to compressive load	$\varepsilon_{c,d}$ =	0.73			
Design strain due to design angular rotation	$\varepsilon_{\alpha,d}$ =	0.20			
Maximum design strain	$\varepsilon_{t,d}$ =	2.22	<$\varepsilon_{u,k}$ /γ_m=	7.00	OK

C. Stability

One of the following criteria should be satisfied:

$b_{min}>4\Sigma t_i$	=>	80 cm	>	64.8 cm	OK
$\sigma_e<2b_{min}G_{b,min}S/3\Sigma t_i$	=>	6069.29 kPa	<	41152.26 kPa	OK

D. Anchorage

Minimum vertical design force:	N_{Ed} =	2039.40 KN		
Minimum design pressure:	σ_e =	4.69 N/mm^2	>3,00	
Stiffness:	K = $G_{b,max}$ x A / T =	5333.3 KN/m		
Maximum shear force:	V_{Ed} = K d_{Ed} =	1122.62 KN		
	V_{Ed} / N_{Ed} =	0.550		
	α =	0.100		
	β =	0.300		
	μ_e= $\alpha + \beta/\sigma_e$ =	0.164		

Check: V_{Ed} / N_{Ed} > $\alpha + \beta/\sigma_e$ ANCHORAGE IS REQUIRED

E. Uplift of the bearings

The minimum vertical load at the bearings due to the seismic load combinations is:

$minN_{Ed}$= 1674.00 kN COMPRESSIVE FORCE, OK

16.2 Check of expansion joints for the case of no liquefaction

Displacements:

Braking load:	23.70 mm
Shrinkage:	4.00 mm
Uniform difference of temperature $\Delta T = -41^{\circ}C$:	18.00 mm
Uniform difference of temperature $\Delta T = +59^{\circ}C$:	25.90 mm
Earthquake x-x:	190.90 mm
Earthquake y-y:	174.20 mm

Total displacement

Static combination		
Maximum negative	$d'_{Ed}=-d_G-1.50*d_{TR}-1.5*0.60*d_{t(-41)}=$	-55.75 mm
Maximum positive	$d'_{Ed}=-d_G+1.50*d_{TR}+1.50*0.6*d_{t(+59)}=$	54.86 mm
Seismic combination		
Maximum negative	$d'_{Ed}=-0.4*d_E-d_G-0.5*d_{t(-41)}=$	91.77 mm
Maximum positive	$d'_{Ed}=0.4*d_E-d_G+0.5*d_{t(+59)}=$	87.83 mm

Minimum displacements of the expansion joint

Static combination	112 mm
Seismic combination	184 mm

Minimum gap

$d'_{Ed}=d_E-d_G+0.5*dt_{(+59)}=$ 210 mm

An expansion joint of type Algaflex T330 or similar is chosen

16.3 Check of bearings for the case of liquefaction

parallel to axis:	x		y	
Dimensions:	80	x	80	cm^2
Number of elastomeric layers:			9	
Thickness of an indivicual elastomeric layer:			18	mm
Total thickness:			162	mm

Axial loads	most loaded bearing		
Permanent:	1351.00 kN		
Superimposed:	845.30 kN	: N_g =	2196.30 KN
Traffic load:	1438.40 kN	: N_p =	1438.40 KN
Earthquake z-z:	868.60 kN	$N_{max,st}$ =	3634.70 KN
	less loaded bearing		
Permanent:	1351.00 kN		
Superimposed:	845.00 kN	$N_{min,st}$ =	2196.00 KN
Earthquake z-z:	868.60 kN		

Displacements	
Braking load:	23.70 mm
Shrinkage:	4.00 mm
Uniform difference of temperature $\Delta T = -41^{\circ}C$:	18.00 mm
Earthquake x-x:	109.70 mm
Earthquake y-y:	99.90 mm
Longitudinal movement (Rx)	47.50 mm
Transverse movement (displacement Ry)	52.10 mm
Ex+0.30Rx	123.95 mm
Ey+0.30Ry	115.53 mm
0.30Ex+Rx	80.41 mm
0.30Ey+Ry	82.07 mm
maximum displacement x-x:	123.95 mm
maximum displacement y-y:	115.53 mm

Rotations				
permanent:	α_x =	0.212 x 10^{-3} rad	α_y =	0.000 x 10^{-3} rad
superimposed:	α_x =	0.551 x 10^{-3} rad	α_y =	0.413 x 10^{-3} rad
traffic load:	α_x =	2.891 x 10^{-3} rad	α_y =	0.216 x 10^{-3} rad

A. Check for static combinations (according to DIN 4141 / Part 14)

Total displacement		d_{td} =	45.70 mm		
Shear strain		γ_{td} = 0.28	<	$\gamma_{\varepsilon n}$ = 0.70	OK
Design pressure	$\sigma_{max}=N_{o/}/A=$	5.68 MPa	<	15,00 MPa	
	$\sigma_{min}=N_g/A=$	3.43 MPa	<	5.00 MPa	ANCHORAGE IS REQUIRED

Angular rotation about x	$\varphi_{td,x}$= 0.0037 rad	<	$\varphi_{\varepsilon n}=nx\varphi_{1,\varepsilon n}$ = 0.0180 rad		OK
Angular rotation about y	$\varphi_{td,y}$= 0.0006 rad	<	$\varphi_{\varepsilon n}=nx\varphi_{1,\varepsilon n}$ = 0.0180 rad		OK

B. Check for seismic combinations (according to EC8-2)

Apparent conventional shear modulus:	G_g=	900	kPa		
Shear modulus:	G_b=	1125	kPa		
Lower bound design properties:	$G_{b,min}$=	1125	kPa		
Upper bound design properties:	$G_{b,max}$=	1350	kPa		
Displacement +x:	d_{Edx} =	136.95	mm		
Displacement +y:	d_{Edy} =	34.7	mm		
Total displacement	d_{Ed} =	141.3	mm		
Design shear strain due to horizontal displacement	$\varepsilon_{q,d}$=	0.87	<2.0		OK
	S =	11.11			
	A_r =	5027.13	cm^2		
	N_{sd} =	2744.56	kN		
	σ_e =	5459.50	kPa		
Design strain due to compressive load	$\varepsilon_{c,d}$ =	0.66			
Design strain due to design angular rotation	$\varepsilon_{\alpha,d}$ =	0.20			
Maximum design strain	$\varepsilon_{t,d}$ =	1.72	<$\varepsilon_{u,k}$ /γ_m=	7.00	OK

C. Stability

One of the following criteria should be satisfied:

$b_{min}>4\Sigma t_i$	=>	80 cm	>	64.8 cm		OK
$\sigma_e<2b_{min}G_{b,min}S/3\Sigma t_i$	=>	5459.50 kPa	<	41152.26 kPa		OK

D. Anchorage

Minimum vertical design force:	N_{Ed} =	1935.42	KN	
Minimum design pressure:	σ_e =	3.85	N/mm^2	>3,00
Stiffness:	K = $G_{b,max}$ x A / T =	5333.3	KN/m	
Maximum shear force:	V_{Ed} = K d_{Ed} =	753.43	KN	
	V_{Ed} / N_{Ed} =	0.389		
	α =	0.100		
	β =	0.300		
	μ_e= $\alpha + \beta/\sigma_e$ =	0.178		

Check: V_{Ed} / N_{Ed} > $\alpha + \beta/\sigma_e$ ANCHORAGE IS REQUIRED

E. Uplift of the bearings

The minimum vertical load at the bearings due to the seismic load combinations is:

minN_{Ed}= 1327.40 kN COMPRESSIVE FORCE, OK

16.4 Check of expansion joints for the case of liquefaction

Displacements:

Braking load:	23.70 mm
Shrinkage:	4.00 mm
Uniform difference of temperature $\Delta T = -41^{\circ}C$:	18.00 mm
Uniform difference of temperature $\Delta T = +59^{\circ}C$:	25.90 mm
Earthquake x-x:	123.95 mm
Earthquake y-y:	115.53 mm

Total displacement

Static combination		
Maximum negative	$d'_{Ed}=-d_G-1.50*d_{TR}-1.5*0.60*d_{t(-41)}=$	-55.75 mm
Maximum positive	$d'_{Ed}=-d_G+1.50*d_{TR}+1.50*0.6*d_{t(+59)}=$	54.86 mm
Seismic combination		
Maximum negative	$d'_{Ed}=-0.4*d_E-d_G-0.5*d_{t(-41)}=$	64.10 mm
Maximum positive	$d'_{Ed}=0.4*d_E-d_G+0.5*d_{t(+59)}=$	60.15 mm

Minimum displacements of the expansion joint

Static combination	112 mm
Seismic combination	128 mm

Minimum gap

$d'_{Ed}=d_E-d_G+0.5*dt_{(+59)}=$ 141 mm

An expansion joint of type Algaflex T200 is required.

An expansion joint of type Algaflex T330 or similar is chosen

Chapter 17

SOIL STRESSES

17.1 Model of the bridge

In order to calculate the soil stresses at the pier's footing, a new model is set up, shown in Figure 17.1. In this model the superstructure remains the same as described in section 12.1, while the pier's footing is simulated with shell elements with a thickness of 2.00m. Elastic constants C and CT, normal and tangential to the surface, respcectively, are taken into consideration accounting for the soil-structure interaction. These constants are equal to the values listed in Table 12.4 divided by the area of the footing. Thus, the values of these elastic constants are given in Table 17.1.

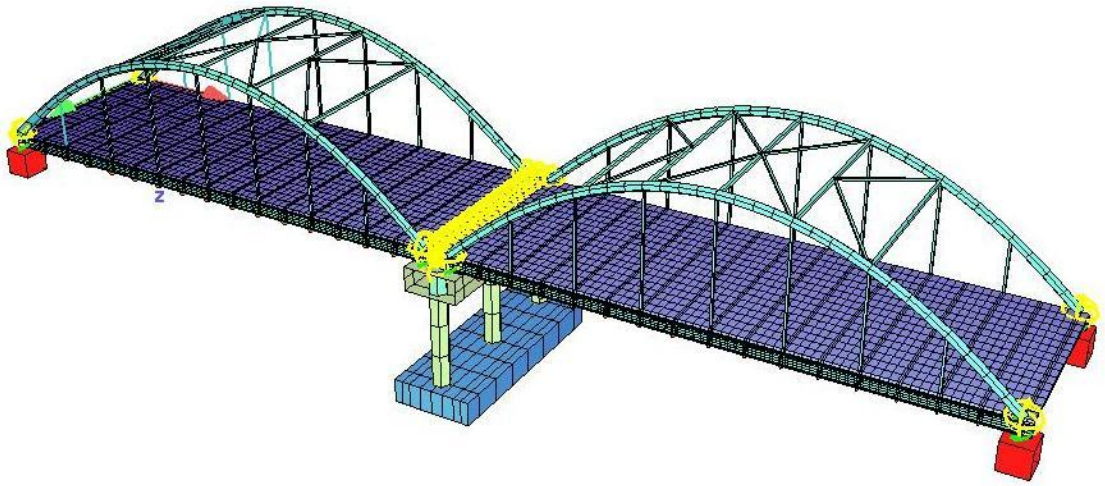

Figure 17.1: Model of the bridge for the calculation of the soil stresses
Σχήμα 17.1: Προσομοίωμα γέφυρας για τον υπολογισμό των τάσεων εδάφους

Table 17.1: Elastic constants for the pier's footing
Πίνακας 17.1: Ελαστικές σταθερές για το πέδιλο μεσοβάθρου

Direction	No liquefaction	With liquefaction
Horizontal (CT)	20322 kN/m^3	8181 kN/m^3
Vertical (C)	20150 kN/m^3	5274 kN/m^3

17.2 Load Cases

The earthquake effects are determined by applying a horizontal equivalent static force F given by the expression:

$$F=M\ S_d(T) \qquad (17\text{-}1)$$

where M is the effective mass of the structure, including 20% of the live load and $S_d(T)$ is the spectral acceleration of the design spectrum corresponding to the fundamental period T of the bridge, estimated as:

$$S_{d,x}(T)= a_g \cdot S \cdot n \cdot 2.5\left(\frac{T_C}{T_x}\right) \text{ (elastic spectral acceleration for x-earthquake)} \qquad (17\text{-}2)$$

$$S_{d,y}(T)= a_g \cdot S \cdot n \cdot 2.5\left(\frac{T_C}{T_y}\right) \text{ (elastic spectral acceleration for y-earthquake)} \qquad (17\text{-}3)$$

$$S_{d,v}(T)= a_{vg} \cdot S \cdot n \cdot 3.0 \text{ (vertical elastic spectral acceleration)} \qquad (17\text{-}4)$$

where $a_g=PGA_{b,h}$,, $a_{vg}=PGA_{b,v}$, S, n and T_C are given in section 11.2, while T_x and T_y are the eigenperiods of the bridge presented in section 12.3. The following Load Cases are created:

LC 7000: Earthquake X on permanent loads, including self weight, the weight of the slab and the superimposed.

LC 7001: Earthquake Y on permanent loads, including self weight, the weight of the slab and the superimposed.

LC 7002: Earthquake Z on permanent loads, including self weight, the weight of the slab and the superimposed.

LC 7010: Earthquake X on 20% of the live loads.

LC 7011: Earthquake Y on 20% of the live loads.

LC 7012: Earthquake Z on 20% of the live loads.

17.3 Load Combination

The following two Load Combinations are considered:

LC 10001: This combination includes the following load cases:

LC1	Self weight
+LC2	Superimposed
+LC3	Shrinkage
+LC600*0.2	Uniform traffic load
+(LC7000+LC7010)*1.0	Earthquake X
+(LC7001+ LC7011)*0.3	Earthquake Y
+(LC7002+ LC7012)*0.3	Earthquake Z

LC 10002: This combination includes the following load cases:

LC1 (1.00+0.3 $S_{d,v}$(T)/g)	Self weight
+LC2	Superimposed
+LC3	Shrinkage
+LC600*0.2	Uniform traffic load
+(LC7000+LC7010)*0.3	Earthquake X
+(LC7001+ LC7011)*1.0	Earthquake Y
+(LC7002+ LC7012)*0.3	Earthquake Z

17.4 Soil stresses

The diagrams of the soil stresses are plotted in Figure 17.2 for the case without liquefaction and in Figure 17.3, when liquefaction occurs.

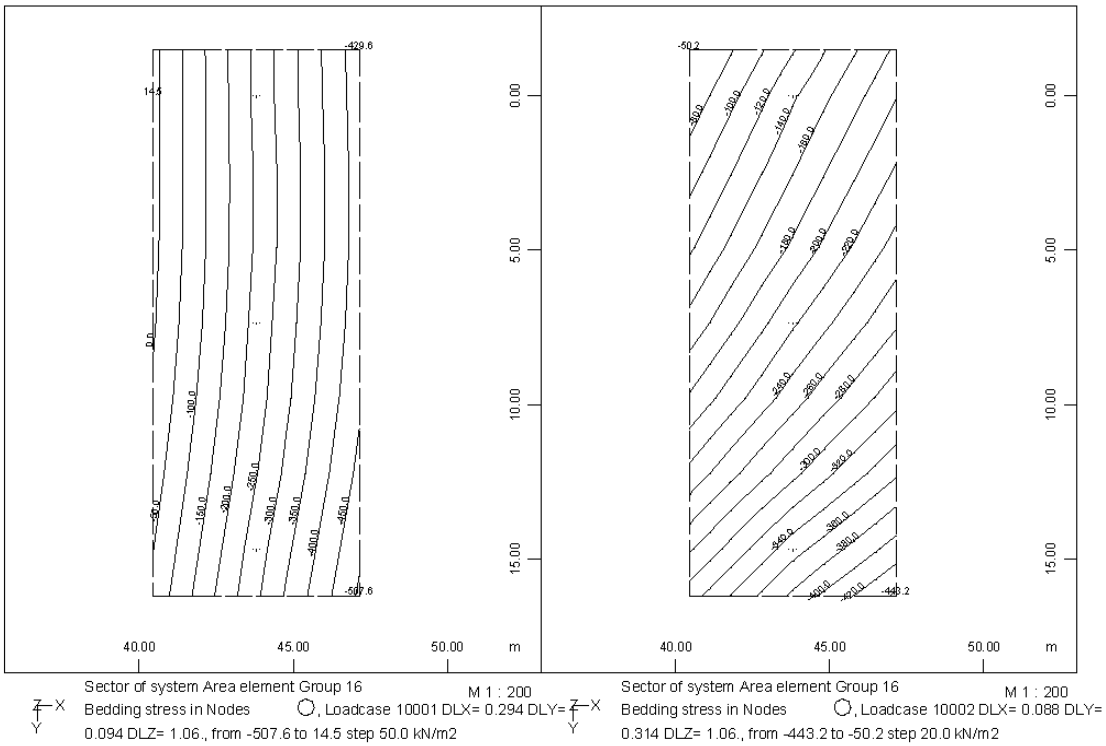

Figure 17.2: Soil stresses for the case without liquefaction

Σχήμα 17.2: Τάσεις εδάφους για την περίπτωση χωρίς ρευστοποίηση

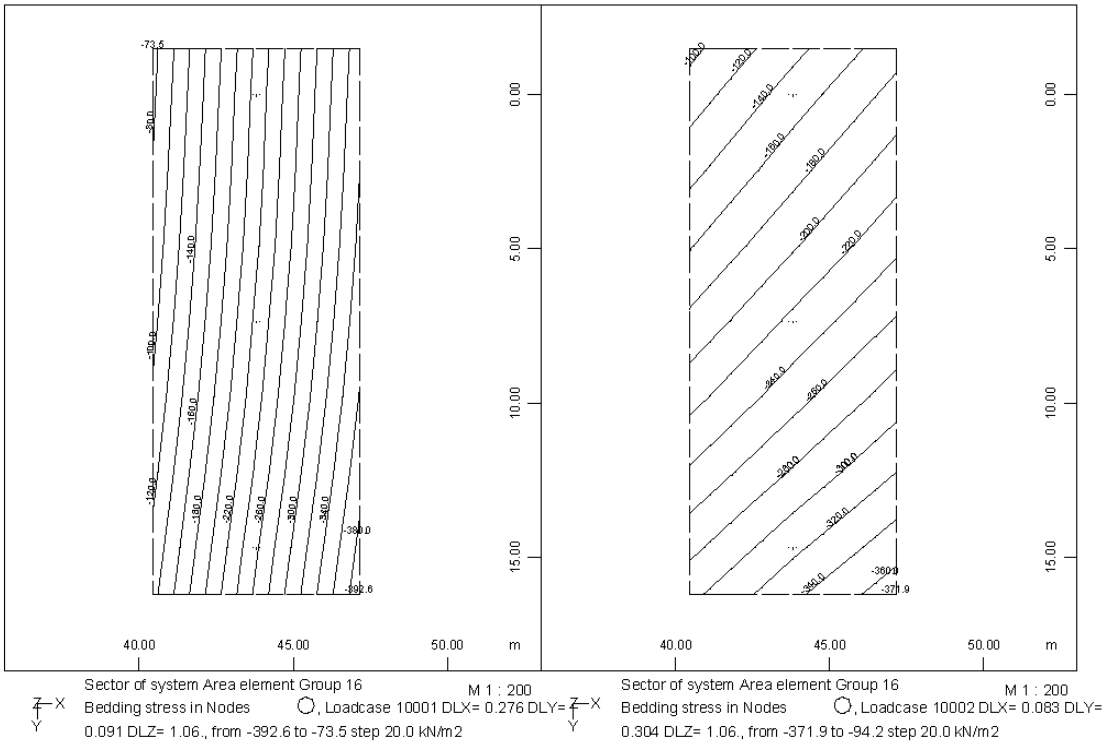

Figure 17.3: Soil stresses for the case with liquefaction

Σχήμα 17.3: Τάσεις εδάφους για την περίπτωση με ρευστοποίηση

PART III: COMPARATIVE EVALUATION

Chapter 18

COMPARISON OF THE RESULTS

18.1 Reinforcement of concrete members

The reinforcement of the pier's columns and the deck's slab are listed in Table 18.1 for both solutions. No significant differences are noted between the two solutions.

Table 18.1: Reinforcement requirements for concrete members

Πίνακας 18.1: Απαιτήσεις οπλισμών για στοιχεία από οπλισμένο σκυρόδεμα

Members	Results / Requirement	Conventional solution	Innovative solution	
			(no liquefaction)	(with liquefaction)
Pier	Longitudinal Reinforcement	186.70cm^2	187.10cm^2	94.30cm^2
	Stirrups	16.60cm^2	16.60cm^2	16.60cm^2
Deck slab	Longitudinal Reinforcement	47.9cm^2	41.2cm^2	46.8cm^2
	Transverse Reinforcemnt	33.6cm^2	20.3cm^2	27.6cm^2

18.2 Exploitation factor for steel members

The maximum exploitation factor is given in Table 18.2 for both solutions. Comparing the results, the Innovative Solution leads to larger exploitation factors and to larger steel section for the Diabonal bracing members.

Table 18.2: Maximum exploitation factors for the steel members

Πίνακας 18.2: Μέγιστοι συντελεστές εκμετάλλευσης για τα μεταλλικά στοιχεία

Members	Cross sections	Solution	
		Conventional	Innovative
Arches	CHS750/20	0.82	0.98
Transverse bracing	CHS244.5/8	0.46	0.49
Diagonal bracing	-	0.99 (CHS139.7/8)	0.96 (CHS168.3/12.5)
Hangers	CHS168.3/8	0.85	0.87
Transverse beams (during construction)	HEB900	0.94	0.94
Main beams	HEB900	0.52	0.60

Chapter 19

QUANTITIES AND BUDGET

19.1 Quantities

In order to compare the cost of the innovative solution with the one of the conventional solution, only the quantities of the different materials, sections or structural elements used for both solutions are measured, considering that the rest of the structure is the same for both solutions.

Conventional solution

- Pier's piles Φ120: 8×25.00m=200m
- Pier's pilecap: 6.00m×17.70m×2.00m=212.40m^3
- Reinforcement:31640kg+25488kg=57128kg

  Piles: 200m×1.13m^2×140kg/m^3=31640kg

  Pilecap: 6.00m×17.70m×2.00m×120kg/m^3=25488kg
- Expansion joints: 3×15.00m×480/60=360m
- Bearings: 8×70cm×80cm×27.5cm=1232000cm^3=1232lt
- Diagonal bracing members (CHS139.7/8): 16×8.45m×25.98kg/m=3512.50kg
- Gravel piles: 1412.21m

  $H_{total}=\alpha_s\cdot(L+2)(B+2)\cdot H_{impr}/(\pi D_{gr}^2/4)-n_{piles}\times H_{impr}$

  =9.36(L+2)(B+2)=9.36(17.70+2.00)(6.70+2.00)-8×24.00m=1412.21m

  where

  replacement ratio: α_s=0.196,

  diameter of gravel piles: $D_{gr.}$=0.80m,

  Thickness of improved zone H_{impr}=24m

Innovative solution

- Pier's footing: 6.70m×17.70m×2.00m=237.18m^3
- Reinforcement of footing: 6.70m×17.70m×2.00m×120kg/m^3=28462kg

- Expansion joints: 3×15.00m×330/60=247.50m
- Bearings: 8×80cm×80cm×28.2cm=1443840cm^3=1443.84lt
- Diagonal bracing members (CHS168.3/12.5): 16×8.45m×48.03kg/m=6493.66kg
- Gravel piles: 163.10m

  $H_{total}=\alpha_s \cdot V_{impr}/(\pi D_{gr}^2/4)=0.122\times672.00m^3/[\pi(0.80m)^2/4]=163.10m$

  where

  replacement ratio: $\alpha_s=0.122$ (Table 10.2),

  diameter of gravel piles: $D_{gr.}=0.80m$,

  Volume of improved ground $V_{impr}=672.00m^3$ (Table 10.2),

19.2 Budget comparison

The overall cost of the bridge is estimated as 1000÷1500€/m^2. Taking into account the dimensions of the bridge, with width 15.00m and length 87.60m, the total cost arises at 1314000.00÷1971000.00€. The itemized budget regarding the differences between the two solutions is presented in Table 19.1 for the conventional solution and in Table 19.2 for the innovative one. These budgets are based on nominal prices for construction of public works issued by the Ministry of Infrastructure for 2013. The difference between the two solutions is 171960€ with the cost of the innovative solution being smaller. This difference arises at 9%÷13% of the total cost of the bridge.

Table 19.1: Itemized budget for the conventional solution

Πίνακας 19.1: Αναλυτικός προϋπολογισμός για τη συμβατική λύση

Description	Quantity	Unit	Unit value (€)	Cost (€)
Piles Φ120	200	m	170.00	34000.00
Pier's pilecap	215	m^3	158.00	33970.00
Reinforcement	57200	kg	1.05	60060.00
Expansion joints	360	m	473.80	170280.00
Bearings	1250	lt	36.80	46000.00
Steel members	3520	kg	2.40	8448.00
Gravel piles	1450	m	58.00	84100.00
SUM				**436858.0**

Table 19.2: Itemized budget for the innovative solution

Πίνακας 19.2: Αναλυτικός προϋπολογισμός για την καινοτόμο λύση

Description	Quantity	Unit	Unit value (€)	Cost (€)
Pier's footing	240	m^3	158.00	37920.00
Reinforcement	28500	kg	1.05	29925.00
Expansion joints	250	m	473.80	118250.00
Bearings	1450	lt	36.80	53360.00
Steel members	6500	kg	2.40	15600.00
Gravel piles	165	m	58.00	9570.00
SUM				**264625.0**

In addition, the cost of the foundation of these two solutions is calculated in Table 19.3 for the conventional solution and in Table 19.4 for the innovative one. The difference between the two solutions is considerable, with the innovative foundation costing only 36% of the conventional one.

Table 19.3: Itemized budget for the foundation of the conventional solution

Πίνακας 19.3: Αναλυτικός προϋπολογισμός για τη θεμελίωση της συμβατικής λύσης

Description	Quantity	Unit	Unit value (€)	Cost (€)
Piles Φ120	200	m	170.00	34000.00
Pier's pilecap	215	m^3	158.00	33970.00
Reinforcement	57200	kg	1.05	60060.00
Gravel piles	1450	m	58.00	84100.00
SUM				**212130.0**

Table 19.4: Itemized budget for the foundation of the innovative solution

Πίνακας 19.4: Αναλυτικός προϋπολογισμός για τη θεμελίωση της καινοτόμου λύσης

Description	Quantity	Unit	Unit value (€)	Cost (€)
Pier's footing	240	m^3	158.00	37920.00
Reinforcement	28500	kg	1.05	29925.00
Gravel piles	165	m	58.00	9570.00
SUM				**77415.0**

Finally, as the benefit from reduced cost of the foundation in the innovative solution is significant, it appears meaningful to compare the overall cost per span. This comparison is more appropriate for multi-span bridges, in which the benefit from the cost of foundation of individual piers will have a stronger participation in the overall bridge cost. This benefit is estimated at approximately 20%, by considering in this example one half of the total bridge length, which can be viewed as "influence area" of the pier.

Chapter 20

SUMMARY AND CONCLUSIONS

20.1 Summary

The bridge under investigation is a steel arch road bridge with two simply supported spans, with total length 87.60m. The steel members of each span include two main beams, seventeen transverse beams, and two arches connected with transverse and diagonal bracing members. Each main beam is suspended from the corresponding arch with seven hangers. A composite deck is formed using trapezoidal profiles and a concrete slab. The concrete slab is connected with the transverse and main beams through steel shear connectors in order to ensure composite action. The pier consists of three circular reinforced concrete columns. They are connected at the top with a concrete beam, forming thus a frame in the transverse direction of the bridge. The bridge is founded on liquefaction susceptible soil. The subsoil conditions are well established by geotechnical surveys from an actual (existing or in the design stage) river bridge site, where extensive liquefaction is expected underneath one or more of the bridge piers after a major earthquake event.

First, the conventional foundation approach is considered, using pile groups with ground improvement between and around the piles, as deep foundation for the pier. The design of the bridge is performed under static and seismic conditions in Ultimate Limit State and Serviceability Limit State and the cost of this conventional solution is estimated. In this case the bridge model includes the superstructure, the pier, the pilecap and the piles, while horizontal and vertical springs at the piles simulate the soil-structure interaction.

Then, the static and seismic design of the same bridge is repeated in ULS and SLS, adopting the innovative foundation approach, in order to exploit the "natural" seismic isolation developing during liquefaction. In this case, a spead footing and partial improvement of the top part only of the liquefiable soil (crust) are considered for the foundation of the pier. The dimensions of the footing and the crust are appropriately chosen so that the degraded factor of safety, $F.S._{deg}$ is equal or larger than 1.10 for the seismic load combination. The model of the bridge includes the superstructure and the pier, while the footing and the soil-structure interaction are simulated with appropriate translational and rotational springs. Static and dynamic springs are assumed for static and seismic loads, respectively. Damping elements at the base of the pier are also activated in the dynamic analysis.

Two Seismic Scenarios are assumed for the innovative solution, defined in the Appendix C of Deliverable D4: Elastic Response Spectra for Liquefiable soils. In Seismic Scenario 1, an earthquake with return period T_{ret} = 225 years is taken into account, which does not cause liquefaction, while in Seismic Scenario 2, the earthquake, having a return period T_{ret} = 1000 years, causes liquefaction. The dynamic springs and the damping elements have different constant values for the two Scenarios, leading to stiffer springs for Seismic Scenario 1, in which no liquefaction occurs. The first Seismic Scenario leads to larger PGA, as in the second one the "natural seismic isolation" occurring due to liquefaction is assumed and exploited.

However, the second Seismic Scenario is associated with the evolution of large horizontal displacements of the pier's foundation, which occur during the earthquake event, as well as significant permanent settlement and rotations at the base of the pier after the earthquake event, which are included in the static load combinations describing operation of the bridge after the earthquake. The aim of the design is that the bridge with the shallow foundation can sustain both Seismic Scenarios.

20.2 Conclusions

The comparative advantages and limitations of the new design methodology, relative to the conventional one, are evaluated on the basis of technical, as well as cost criteria.

From the analyses it is concluded that in the innovative solution liquefaction indeed acts as seismic isolation for the bridge superstructure, resulting in relatively small action effects for Seismic Scenario 2. Hence, this scenario is not critical for member dimensioning, despite the fact that significant simultaneous horizontal displacements at the pier base are also taken into account in these load combinations. However, the price that has to be paid in this alternative is the fact that the static load combinations describing operation of the bridge after the earthquake that causes liquefaction become critical, as they incorporate the permanent settlements and rotations due to liquefaction. As a result, the steel members of the superstructure have slightly larger exploitation factors for the innovative foundation solution than for the traditional one, however, no increase of their cross-section is required, with the exception of diagonal bracing members between arches, bearings and expansion joints.

Moreover, as far as the pier is concerned, the beneficial action of liquefaction as natural seismic isolation as well as the footing's flexibility in comparison to the pile foundation, do not cause any difference in the columns' cross-section or reinforcement in comparison to the traditional solution. This is due to the fact that Seismic Scenario 1 is critical, as the absence of liquefaction leads to stronger seismic actions, and the required reinforcement for Seismic Scenario 1 is similar to the one of the traditional foundation solution.

The small increase of cross-section of some members of the superstructure results in slightly reduced financial benefit of the innovative solution in comparison to the traditional one. However the innovative solution still achieves considerable overall savings in the order of 9%÷13% of the total bridge cost, due to the substantially simpler foundation. It is noted that the benefit in terms of foundation cost only is quite substantial, as this cost for the innovative solution is approximately 36% of the corresponding for the conventional one. Furthermore, the savings for bridges with many piers, in which the foundation cost has a higher participation, can thus be approximated at 20%.

It is further noted that the reliable calculation of the transient soil displacements as well as the remaining settlements and rotations following an earthquake causing liquefaction, is deemed as very important, taking into account that these quantities are critical for the design of the bridge with the innovative foundation solution. As this calculation encounters considerable uncertainties, this is an issue to be solved for achieving increased application of the proposed concept. Alternatively, as well as in addition, the proposed innovative shallow foundation solution is certainly more suitable for structural systems of the bridge superstructure that are less sensitive to foundation settlements and rotations.

In addition to the above it is emphasized that, for this particular bridge, the members of the superstructure which require an increase due to the static load combinations after a potential liquefaction (bracing members between arches, bearings and expansion joints) are secondary and easily replaceable. It is therefore possible to adopt a design strategy of retaining these members at their initial size, removing them (if needed) after a possible liquefaction, so that the other members of the – otherwise structurally determinant – bridge shall return to stress-free state (with the exception of self-weight effects) and replacing them. Then, for the design of the superstructure, it is not necessary to include in the static load combinations after

liquefaction the residual settlements and rotations, as they will not induce stresses. Main advantage of this approach is not so much the – anyway negligible – cost benefits, but the downgrade of the importance of reliable prediction of liquefaction induced residual settlements and rotations.

In any case, an additional advantage of the proposed innovative solution is the fact that in this solution a "bonus safety" is incorporated, in case very high seismic actions are encountered, which exceed those expected for the project location, and considered for seismic design, even for seismic scenario 2. In this case, liquefaction will surely develop and the natural base isolation advantage will be explored, which will not be the case for the conventional solution.

ANNEXES

Annex I

COMPUTATION OF DYNAMIC SPRING AND DASHPOT COEFFICIENTS

Figure I.1 sketches a rigid rectangular footing of dimensions 6.70m × 17.70m in plan resting on a 2-layer soil profile consisting of an improved soil "crust", over a liquefiable loose sand layer of thickness h_2=14m. Embedment effects on footing stiffness are neglected, since material around the footing is assumed to be loose fill. The thickness of the surface layer under the footing is h_1=3.20m. Due to ground improvement, the weighted average value of shear wave velocity of the surface soil crust, V_{s1}, (considering also the correction for overburden pressure) is taken equal to ~212m/sec before liquefaction and ~203m/sec during liquefaction. The corresponding shear wave velocity of the liquefiable soil layer is assumed at ~136m/sec before liquefaction and ~26.5m/sec during liquefaction.

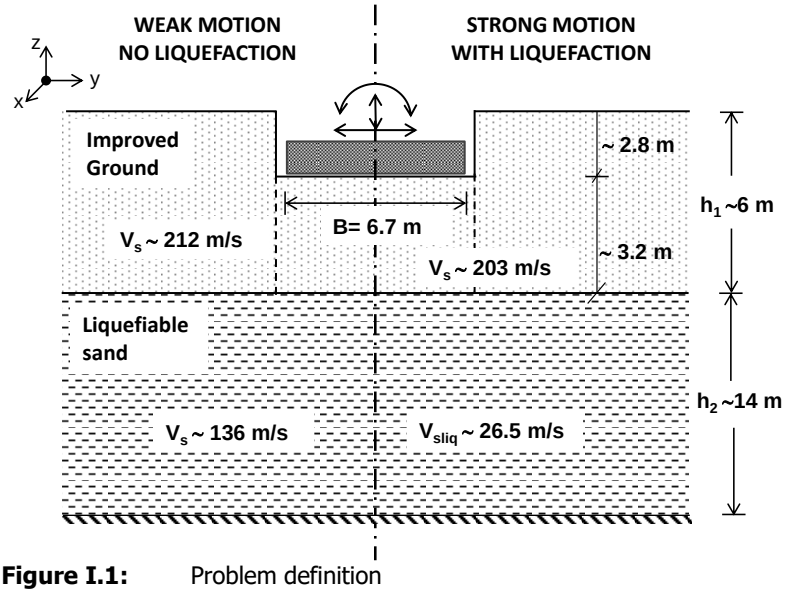

Figure I.1: Problem definition

Σχήμα I.1: Ορισμός του προβλήματος

Following the assumptions employed on the report entitled "Soil springs and dashpots for footings on liquefiable soil" of Work Package WP5, given the low aspect ratio of the footing (L/B < 4), the frequency dependence of the dynamic impedance of the rectangular footing can be well approximated by that of a square footing of dimensions B×B. To analyze a square footing with computer code CONAN, an equivalent circular radius should be determined. For translational degrees of freedom, this is equal to:

$$R = \frac{B}{\sqrt{\pi}} = \frac{6.7}{\sqrt{\pi}} = 3.8\ \text{m} \qquad \text{(I.1)}$$

while for rotational degrees of freedom

$$R = \frac{B}{\sqrt[4]{3\pi}} = \frac{6.7}{\sqrt[4]{3\pi}} = 3.82 \text{ m} \tag{I.2}$$

So in this case, one may assume the same radius for all modes, equal to 3.8m. The diameter of the equivalent footing is D=7.6m. The dimensionless ratios h_1/D and h_2/D are as follows:

$$h_1/D=3.2m/7.6m=0.4 \tag{I.3}$$

$$h_2/D=14.02m/7.6m=1.8 \tag{I.4}$$

$$\frac{V_{s1}}{V_{s2}} = \frac{212m/sec}{136m/sec} = 1.6 \left(\text{before liquefaction}\right) \tag{I.5}$$

$$\frac{V_{s1}}{V_{s2}} = \frac{203m/sec}{26.5m/sec} = 7.7 \left(\text{during liquefaction}\right) \tag{I.6}$$

From CONAN analysis, the dynamic impedance functions for a square footing of dimensions 6.70m $\times$ 6.70m are obtained. Given that the rectangular footing has an aspect ratio L/B=17.7m/6.7m $\sim$ 2.6 < 4, it is assumed that the dynamic impedance coefficients are approximately the same. Hence, the values of stiffness k_0 must be modified according to Table 5.1 and Eqs (5.1) to (5.6) given in the report "Soil springs and dashpots for footings on liquefiable soil". The values of stiffness k_0 can also be determined from Table 3.2 of the report "Soil springs and dashpots for footings on liquefiable soil" using the approximate ratios $h_1/D=0.5$, $h_2/D=2$ and linear interpolation for establishing the ratio V_{s1}/V_{s2}. The interpolation is necessary because the impedance contrast between the two first layers is a major parameter in the dynamic response of the footing.